Universidade de Lisboa

Faculdade de Farmácia

Biological effects of phytocannabinoids and endocannabinoids on oestrogen receptor-positive (ER^+) breast cancer cells

Fabien Marc Trouille

Dissertation Report supervised by Doctor Cristina Isabel Borges Dias Amaral and co-supervised by Professor Cecília M.P. Rodrigues.

Biopharmaceutical Sciences

2018

This dissertation was carried out at the UCIBIO.REQUIMTE - Laboratory of Biochemistry, Department of Biological Sciences of the Faculty of Pharmacy of the University of Porto, under the supervision of Doctor Cristina Isabel Borges Dias Amaral. It also had the co-supervision of Professor Cecília M.P. Rodrigues from the Faculty of Pharmacy of the University of Lisbon.

This project had the financial support from Fundação para a Ciência e Tecnologia (FCT), through the attribution of the Post-Doc grant to Cristina Amaral (SFRH/BPD/98304/2013) and by the project FCT/MEC (UID/MULTI/04378/2013 – POCI/01/0145/FEDER/007728), co-financed by FEDER and by national funds, under the Partnership Agreement PT2020.

Author's presentations

Trouille, F., Augusto, T., Correia-da-Silva, G., Rodrigues, C.M.P., Teixeira, N., Amaral, C., Biological effects of endo- and phytocannabinoids on ER^+ breast cancer cells, IJUP'18 – 11º Encontro de Investigação Jovem da Universidade do Porto, 7-9 February, 2018, Porto, Portugal – Poster communication.

Trouille, F., Augusto, T., Correia-da-Silva, G., Rodrigues, C.M.P., Teixeira, N., Amaral, C., Cannabidiol (CBD) and Δ^9-tetrahydrocannabinol (THC) inhibit aromatase and growth of ER^+ breast cancer cells, 3rd ASPIC International Congress, 10-11 May, 2018, Lisbon, Portugal – Poster communication.

Acknowledgements

I would like to extend my sincere thanks to all those who have helped me over the past two years and made my time here in Portugal more enjoyable.

To my wonderful supervisor Cristina Amaral, who has taught me so much this year, made me feel so at home in Porto, been there for me not matter what, always putting my project first, who has shown so much patience, has given so much advice, and has played such a big role in making my time in Porto as enjoyable as it was. Thank you, I really could not have hoped for a better supervisor.

To professora Cecília Rodrigues, who organised the liaison between the faculties in Lisbon and Porto, and as a result allowed me to experience both cities and meet even more amazing people, thank you for all your support during the course of the master's, and for this life-changing opportunity in which I have learnt so much.

To professora Natércia Teixeira, without whom none of this would have been possible, thank you for giving me this opportunity, not only to work in an exciting and inspiring area of science, but also to discover such a wonderful city in Porto and experience such an incredible year, learning valuable skills and making lifelong friendships along the way. Thank you for making me feel so welcome, for all your support inside and outside of the lab, for helping me along the way with my project, and for letting me know that I could always rely on you if need be.

To professora Georgina Correia-da-Silva, thank you for being there for me during the past year, for being so friendly and making sure everything was going well, for always showing an interest in my project, and for all of your knowledge that has helped in making it even better.

To Tiago Augusto, thank you for always being there to help me when needed, for being such a great team member and friend, for teaching me so many things and for making work so much more fun. It was a pleasure working with you.

I would also like to thank Cristina Almeida, for helping me with numerous experiments, especially in the early days of my project, but also during the busiest times, allowing me to gather even more results and helping to improve my project.

To my friends and colleagues from the lab, João Maia, Niloy Bhowmick, Luís Midão, Marta Almada, Déborah Gonçalves, Lia Costa, Bruno Fonseca, Sara Fernandes, Susana Rocha and Maria João Valente, thank you for making me feel so welcome and at home, whilst always providing help when needed and showing an interest in my project and results.

To Ana Paula Ribeiro & Susana Maia, for making sure I always had everything I needed in order to work! Thank you for giving me somewhere to escape to, and for showing an interest in my experiments and results.

To everyone from the biochemistry lab at FFUP, without a doubt my project would not have been so successful without your help and support, but neither would my experience of Porto and working in the lab have been so memorable. One final big thank you for this.

To my friends and course mates both in Lisbon and in Porto, thank you for making me feel right at home in your wonderful country, and for helping me improve my Portuguese language skills along the way. This whole experience wouldn't have been the same without you and I know that many of you will be friends for life.

To the Gonçalves family, in particular Filomena, Catarina and Eduardo, who were with me from the very beginning, thank you for being there for me, and for letting me know that there was always someone whom I could rely on, no matter what the situation.

Muito obrigado a todos os meus amigos portugueses, e boa sorte para os vossos futuros. Nunca vos esquecerei!

I would also like to thank my friends and family in England, for showing continued support and interest in my project, it meant more to me than you might think!

And finally, to my amazing parents, whose support, encouragement and backing from the very beginning has made this whole experience possible. You have always believed in me and been there for me, during the good and the not so good times, shown patience and sacrificed so much, and I am immensely grateful for this. Thank you for everything.

Abstract

Breast cancer is one of the most common forms of cancer worldwide and the second leading cause of cancer-related death. Oestrogen receptor positive (ER^+) breast cancer makes up the majority of breast cancer cases, where oestrogens play a key role in promoting cancer cell growth and tumour progression. Besides the therapeutic success of the endocrine therapies and their clinical effectiveness in the treatment of this type of tumours, the side effects associated with these therapies, along with the development of endocrine resistance, emphasise the importance and the need to find new and improved therapies. In recent years, several studies on different cancer cell models, including breast cancer, have demonstrated and enhanced the anticancer properties of cannabinoids. Considering this, in this study, the *in vitro* effects of the phytocannabinoids, cannabidiol (**CBD**) and Δ9-tetrahydrocannabinol (**THC**), as well as of the endocannabinoid anandamide (**AEA**), were investigated on an ER^+ breast cancer cell line that overexpresses the enzyme aromatase (MCF-7aro) and on a resistant ER^+ breast cancer cell line (LTEDaro), which mimics the late-stage of resistance to endocrine therapy. A non-tumour fibroblastic cell line (HFF-1) was also used to explore whether these compounds are toxic towards non-cancerous cells. Our results demonstrate that **AEA**, **CBD** and **THC** are non-toxic towards the non-cancerous cells, and have the ability to reduce MCF-7aro cell viability and inhibit and decrease the levels of aromatase, as well as ERα, in these cells. Moreover, in MCF-7aro cells, these compounds also caused cell cycle arrest and induced apoptotic cell death in, through the mitochondrial pathway. Curiously, **AEA** and **CBD** also caused an up-regulation of ERβ levels in these cells, which along with aromatase inhibition may be a therapeutic advantage for this type of tumour. Contrary to **CBD**, the effects induced by **THC** on these cells were dependent on cannabinoid receptors CB_1 and CB_2, while for **AEA** were only CB_2-dependent. In addition, it was also shown that **CBD** induced autophagy in MCF-7aro cells as a promoter mechanism of apoptosis. Interestingly, the resistant LTEDaro cells were sensitive to cannabinoid treatment. In conclusion, these cannabinoids show promising anti-tumour properties regarding ER^+ breast cancer treatment, and even in cases of late-stage resistance. Thus, the results from this study will provide relevant information for future research involving cannabinoids and cancer, which may lead to their potential use in the clinic for the treatment of this disease.

Keywords: Hormone-dependent/Oestrogen receptor-positive (ER^+) breast cancer, cannabinoids, cannabidiol, Δ^9-tetrahydrocannabinol, anandamide.

Resumo

O cancro de mama é uma das formas mais comuns de cancro em todo o mundo e a segunda principal causa de morte relacionada com cancro. A maioria dos casos de cancro de mama são recetor de estrogénio positivo (ER^+), onde os estrogénios desempenham um papel fundamental na promoção do crescimento e progressão do tumor. No entanto, apesar do sucesso terapêutico e da eficácia clínica das terapias endócrinas utilizadas neste tipo de tumores, os efeitos adversos associados a estas terapias, juntamente com o desenvolvimento de resistência endócrina, realçam a importância e a necessidade da procura de novas terapias mais eficazes. Nos últimos anos, vários estudos em diferentes modelos celulares, incluindo cancro de mama, demonstraram a possível relevância das propriedades anticancerígenas dos canabinóides. Tendo isto em consideração, neste trabalho foram estudados os efeitos *in vitro* dos fitocanabinóides, canabidiol (**CBD**) e Δ^9-tetrahidrocanabinol (**THC**), assim como do endocanabinóide anandamida (**AEA**), numa linha celular de cancro de mama ER^+ que sobreexpressa a enzima aromatase (MCF-7aro) e numa linha celular resistente de cancro de mama ER^+ (LTEDaro), que mimetiza a fase tardia da resistência à terapia endócrina. Uma linha celular de fibroblastos não-tumoral (HFF-1) foi também utilizada, de forma a explorar se estes compostos são tóxicos para células não-cancerígenas. Os nossos resultados demonstram que **AEA**, **CBD** e **THC** não são tóxicos para as células não-cancerígenas, contudo têm a capacidade de reduzir a viabilidade das células MCF-7aro e inibir e diminuir os níveis da aromatase, bem como do ERα. Além disso, em células MCF-7aro, estes compostos causaram uma paragem do ciclo celular e induziram a morte celular por apoptose, através da via mitocondrial. Curiosamente, **AEA** e **CBD** também causaram um aumento dos níveis do ERβ nessas células, o que, juntamente com a inibição da aromatase, poderá ser uma vantagem terapêutica para esse tipo de tumores. Ao contrário do **CBD**, os efeitos induzidos pelo **THC** nestas células foram dependentes dos recetores canabinóides CB_1 e CB_2, enquanto que para a **AEA** foram apenas dependentes do CB_2. Para além disso, foi demonstrado também que o **CBD** induziu autofagia nas células MCF-7aro como um mecanismo promotor da apoptose. Curiosamente, as células resistentes LTEDaro foram sensíveis ao tratamento com os canabinóides. Em conclusão, estes canabinóides apresentaram propriedades anti-tumorais promissoras para o tratamento do cancro de mama ER^+, até mesmo em casos de uma resistência tardia. Assim, os resultados deste estudo poderão fornecer informações relevantes para pesquisas futuras envolvendo canabinóides e cancro, o que poderá conduzir ao seu potencial uso na clínica para o tratamento desta doença.

Palavras-chave: Cancro de mama dependente de hormonas/recetor de estrogénio positivo (ER^+), canabinóides, canabidiol, Δ^9-tetrahidrocanabinol, anandamida.

Table of contents

Index of figures

Index of tables

Abbreviations list

17β-HSD 17β-hydroxysteroid dehydrogenase
2-AG 2-arachidonoylglycerol
3-MA 3-methyladenine
3β-HSD 3β-hydroxysteroid dehydrogenase
4T1 mouse triple-negative breast cancer cell line
5-HT 5-hydroxytryptamine
AA arachidonic acid
ABHD alpha/beta domain hydrolase
AC adenylate cyclase
AEA anandamide
AF-1 activation function 1
AF-2 activation function 2
AI aromatase inhibitor
ALS amyotrophic lateral sclerosis
AKT protein kinase B
ANOVA analysis of variance
AP-1 activator protein 1
AR androgen receptor
AVO acid vesicular organelle
BRCA1 breast cancer susceptibility gene 1
BRCA2 breast cancer susceptibility gene 2
cAMP cyclic AMP
CAPS capsaicin
CARM1 coactivator-associated arginine methyltransferase 1
CB_1 cannabinoid receptor 1
CB_2 cannabinoid receptor 2
CBD cannabidiol
CBN cannabinol
CCCP chlorophenylhydrazone
CDK cyclin-dependent kinase
CDK2 cyclin-dependent kinase 2
CDK7 cyclin-dependent kinase 7
CFBS charcoal heat-inactivated foetal bovine serum
cGMP cyclic GMP
CK2 casein kinase 2
COX-2 cyclooxygenase-2
CREB cAMP response element-binding protein
CYP11A1 cholesterol side-chain cleavage enzyme
CYP17 17α-monooxygenase
CYP450 cytochrome P450
DAG diacylglycerol
DAGL diacylglycerol lipase
DBD DNA-binding domain
DCF 2′7′-dichlorofluorescein
$DCFH_2$ 2′7′-dichlorodihydrofluorescein
$DCFH_2$-DA 2′7′-dichlorodihydrofluorescein diacetate
DHEA dehydroepiandrosterone
$DiOC_6(3)$ 3,3′-dihexyloxacarbocyanine iodide
DMEM Dulbecco's modified Eagle's medium
DMSO dimethylsulphoxide
E_1 oestrone
E_1S oestrone sulphate
E_2 oestradiol
E_2S oestradiol sulphate
EDTA ethylenediaminetetraacetic acid
EFM-19 human hormone-dependent breast cancer cell line
EGF epidermal growth factor
EGFR epidermal growth factor receptor

EMT endocannabinoid membrane transporter
ER oestrogen receptor
ER$^+$ oestrogen receptor-positive
ERE oestrogen response element
ERK extracellular signal-regulated kinase
ERα oestrogen receptor α
ERβ oestrogen receptor β
$EtNH_2$ ethanolamine
EVSA-T human oestrogen receptor-negative, progesterone receptor-positive breast cancer cell line
Exe exemestane
F Fos
FAAH fatty acid amide hydrolase
FAK focal adhesion kinase
FAN factor associated with neutral sphingomyelinase action
FBS foetal bovine serum
FDA Food and Drug Administration
FGFR1 fibroblast growth factor receptor 1
FoxA forkhead box A
FSH follicle stimulating hormone
GATA3 GATA-binding protein 3
GFR growth factor receptor
GPR30 G protein-coupled receptor 30
GPR55 G protein-coupled receptor 55
GSK3 glycogen synthase kinase 3
HER2 human epidermal growth factor receptor 2
HFF-1 human foreskin fibroblast 1 cell line
HSP heat shock protein
HTB-126 human triple-negative breast cancer cell line
ICI fulvestrant/ICI 182 780
IGF1R insulin-like growth factor 1 receptor
IKKα inhibitor of kappa kinase α
J Jun
JNK c-Jun N-terminal kinase
LBD ligand-binding domain
LC3 microtubule-associated protein 1A/1B-light chain 3
LDH lactate dehydrogenase
LH luteinising hormone
LTEDaro long-term oestrogen deprivation human oestrogen receptor-positive breast cancer cell line overexpressing aromatase enzyme
MAGL monoacylglycerol lipase
MAPK mitogen activated protein kinase
MCF-10A non-tumoural human breast epithelial cell line
MCF-7 human oestrogen receptor-positive breast cancer cell line
MCF-7aro human oestrogen receptor-positive breast cancer cell line overexpressing aromatase enzyme
MDA-MB-231 human triple-negative breast cancer cell line
MDA-MB-436 human triple-negative breast cancer cell line
MDA-MB-468 human triple-negative breast cancer cell line
MEM Eagle's minimum essential medium
MFI mean fluorescence intensity
MTA1 metastasis-associated protein 1
mTOR mammalian target of rapamycin
MTT 3-(4,5-dimethylthiazol-2-yl)-2,5 diphenyltetrazolium bromide
NAAA *N*-acylethanolamine-hydrolysing acid amidase
NADH nicotinamide adenine dinucleotide
NADPH nicotinamide adenine dinucleotide phosphate

NAPE *N*-arachidonoyl phosphatidylethanolamine
NAPE-PLD NAPE-associated phospholipase D
NAT *N*-acyltransferase
NCOR1 nuclear receptor corepressor 1
NCOR2 nuclear receptor corepressor 2
NF-κB nuclear factor κB
NLS nuclear localisation signal
PARP poly ADP ribose polymerase
PBS phosphate-buffered saline
PCR polymerase chain reaction
PG-EA prostaglandin-ethanolamide
PI propidium iodide
PI3K phosphatidylinositol-3-kinase
PIP2 phosphatidylinositol bisphosphate
PKA protein kinase A
PLA phospholipase A
PLC phospholipase C
PPAR-γ or **PPARG** peroxisome proliferator-activated receptor gamma
PRMT1 protein arginine methyltransferase 1
RLU relative luminescence units
ROS reactive oxygen species
SEM standard error of the mean
SERD selective oestrogen receptor down-grader
SERM selective oestrogen receptor modulator
SkBr3 human human epidermal growth factor receptor 2-positive breast cancer cell line
SM sphingomyelin
SMase sphingomyelinase
SP-1 specificity protein 1
SRC1 nuclear receptor coactivator 1
SRC2 nuclear receptor coactivator 2
STAT signal transducer and activator of transcription
STS staurosporine
T testosterone
T-47D human hormone-dependent breast cancer cell line
TBS tris-buffered saline
TCA trichloroacetic acid
THC Δ^9-tetrahydrocannabinol
TNTE tris-NaCl-Triton X-100-EDTA
TRPV1 transient receptor potential vanilloid 1
TSA-E1 mouse oestrogen receptor-positive breast cancer cell line
VEGF vascular endothelial growth factor
$\Delta\psi_m$ mitochondrial transmembrane potential

1. Introduction

1.1. Hormone-dependent breast cancer

After cardiovascular diseases, cancer is the principle cause of death worldwide (1, 2). There are over one hundred different types of cancer, which are essentially caused by genetic errors that lead to an overtranscription of genes, uncontrolled cell growth, and/or a decrease in programmed cell death. In recent years, improvements have been made to the early detection and treatments of cancer, thus increasing the chance of disease-free survival, however, the rise in the world's population and in life expectancy, along with continued exposure to environmental risk factors, as well as less healthy lifestyle choices, has significantly increased the risk of developing this disease.

Despite around 99% of all breast cancer cases occurring in women (3), this type of cancer is still one of the most common forms worldwide, whilst being the second leading cause of cancer-related death (4). Overall, it causes around half a million deaths each year, with more than one million new diagnoses (4). There are three different types of breast cancer: hormone-dependent, where the cells express the oestrogen receptor (ER) and/or the progesterone receptor, HER2-positive, which express the human epidermal growth factor receptor 2 (HER2), and triple-negative, where neither of the three receptors are expressed and is often the most difficult to treat (5). Hormone-dependent, or oestrogen receptor-positive (ER^+), breast cancer is the most common form, totalling around 60% of cases in premenopausal women, and 75% in postmenopausal women (6, 7). ER^+ breast cancer cells overexpress the ER, specifically oestrogen receptor alpha (ERα), which is primarily activated upon oestrogen binding. Activation of ERα then leads to gene transcription, cell proliferation and thus tumour progression (7).

Obesity, lack of exercise, poor diet, alcohol, smoking, hormone replacement therapy, oral contraception, age and family history, as well as exposure to various common chemicals and radiation, are all considered risk factors that are related to an increase in cancer risk in general (8-10). Moreover, mutations in the BRCA1 and BRCA2 tumour suppressor genes are linked to a higher risk of developing breast cancer (9, 11), whilst an increased lifetime exposure to oestrogens, as a result of early menarche and late menopause, or a late age of first pregnancy, fewer total pregnancies, and a lack of breast feeding, is also linked to an increased risk (9, 11-13). Therefore, more developed countries in general have higher incidence rates of breast cancer (4, 9), in part due to the average number of births per woman, and the average age of the first pregnancy. For example, in 2014, in both Portugal and the UK, breast cancer was responsible for around 17% of female cancer deaths, whereas in the less developed countries of the Gambia and Mozambique, it accounted for less than 10% (14). It must be noted,

however, that less developed countries often have higher mortality rates than the richer countries, due to poorer health systems and less access to improved therapies (Figure 1) (4).

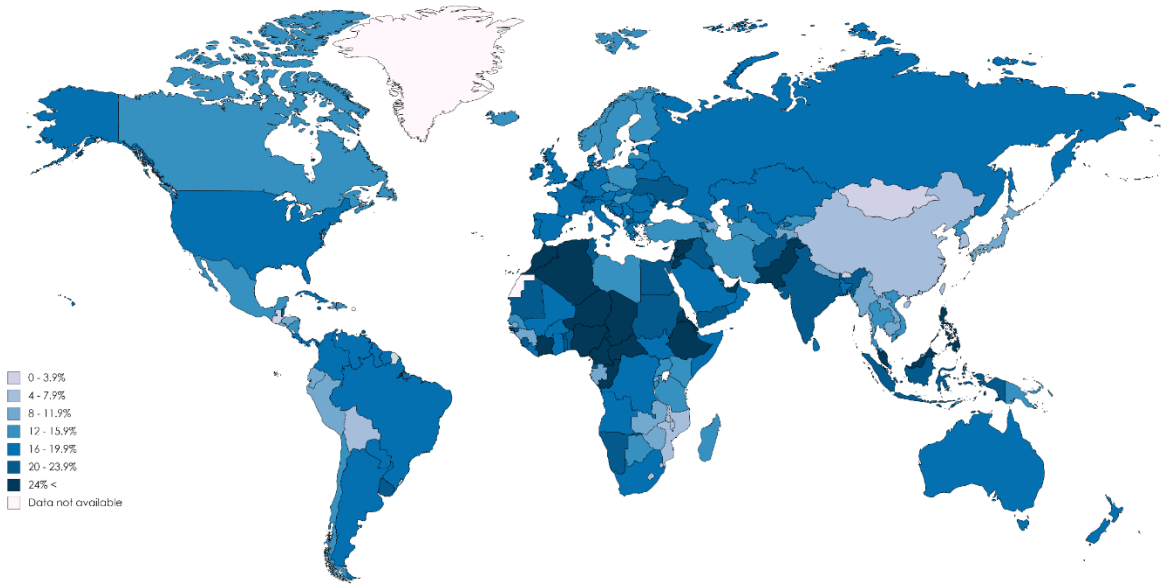

Figure 1: Worldwide death rates of breast cancer per country in 2014. Death rate is expressed as a percentage of total female cancer deaths, with darker colours showing that a higher percentage of those deaths were due to breast cancer. Data for map was obtained from (14).

Although major advances with regards to the treatment of breast cancer have been made in recent times, it still remains a principle concern. The issue of acquired resistance to the current therapies used in the clinic, and the possible recurrence of disease, as well as the fact that incidence is rising and is projected to continue to do so (9), means that drastic action is required if we are to continue to improve in terms of treatments, and increase the chance of survival for people who are diagnosed with this disease.

1.2. Oestrogens and aromatase

Oestrogens, such as oestrone (E_1) and oestradiol (E_2) (Figure 2), are steroid hormones produced in the body that, depending on the cell type, can regulate a range of different biological processes. These processes include the control of reproductive functions and sexual behaviour, the modulation of brain, heart and inflammatory functions, skeletal homeostasis, metabolism, and cell growth, differentiation and survival (15-18). Furthermore, not only do oestrogens play an important role in the development of the breast, but they are also involved in the development and progression of many ER^+ breast cancers (19, 20). In premenopausal women, the ovaries are the primary source of oestrogens, and are also

responsible for regulating their release during the menstrual cycle. During pregnancy, the placenta will also produce a significant amount, whereas in postmenopausal women and in men, the production of oestrogens takes place in peripheral tissues, where it is required for non-reproductive purposes. This occurs in cells such as mesenchymal cells of adipose tissue, osteoblasts, chondrocytes, aortic smooth muscle and vascular endothelial cells, as well as in various parts of the brain (17). In men, the testes are also a source of oestrogen production (18, 20).

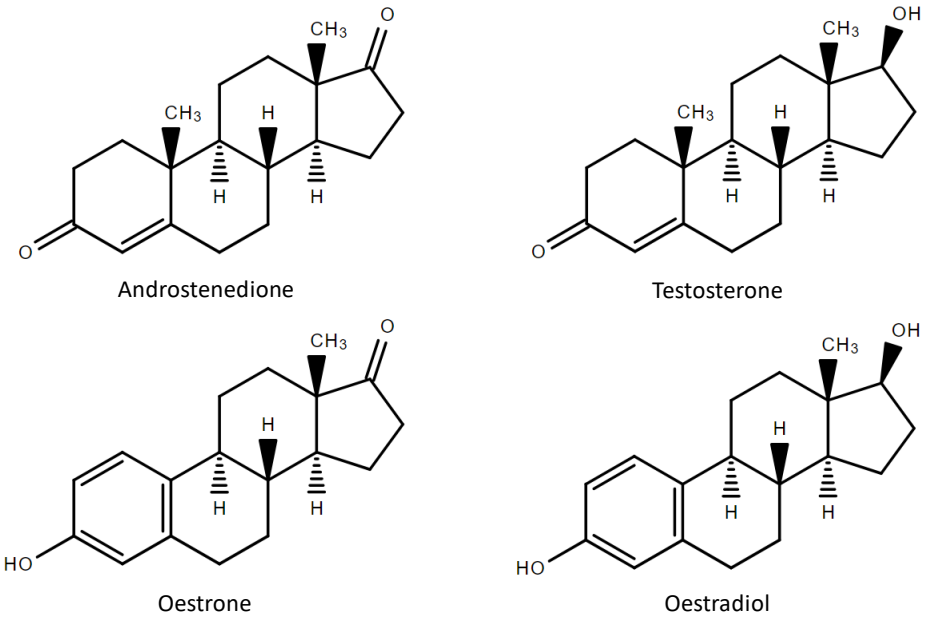

Figure 2: Chemical structures of the oestrogens, oestrone (E_1) and oestradiol (E_2), as well as the androgens, androstenedione and testosterone.

Several mechanisms involved in oestrogen-mediated carcinogenesis have already been proposed, with the induction of DNA damage and the increase in cell proliferation being the most elucidated. Sustained exposure to oestrogens leads to genomic instability, which can favour tumour development and progression, and has in fact already been observed in early breast cancer cases. This occurs because oestrogen's oxidative metabolites can lead to the formation of DNA adducts, double-strand breaks and/or oxidative DNA damage (11, 21). Moreover, excessive cell proliferation as a result of increased oestrogen signalling induces excessive cell division, which increases the probability of errors during DNA replication, thus leading to DNA damage and an accumulation of mutations (11, 22). DNA damage is not uncommon and is usually repaired via the activation of DNA damage response mechanisms. Nevertheless, these mechanisms can fail, thus causing the cell to undergo apoptosis, however, if the cell is unable to do so, mutations will continue to arise and may eventually

contribute to the development of a cancer (21). Furthermore, oestrogens have been found to regulate several DNA damage response proteins, such as BRCA1, BRCA2 and p53, as well as interacting directly with DNA repair machinery (11). Thus, deregulation of these proteins, and suppression of DNA damage response and DNA repair mechanisms, leads to the accumulation of genomic alterations promoting carcinogenesis. Therefore, through these different interactions, oestrogens have the ability to positively or negatively regulate a cell's response to DNA damage, thus contributing to tumour development and progression.

Oestrogen production occurs from androgens such as testosterone and androstenedione (Figure 2), which themselves are produced from cholesterol (23). In premenopausal women, the production of androgens occurs in the ovaries and adrenal glands, however, in postmenopausal women, the adrenal glands are the only source (24). Aromatase, a member of the cytochrome P450 (CYP450) family, is the only enzyme in vertebrates that catalyses the synthesis of oestrogens (25).

The aromatase enzyme, which is located in the endoplasmic reticulum of oestrogen-producing cells (26), is encoded by the *CYP19A1* gene, located on chromosome 15 (25, 26). Its expression is primarily mediated by follicle stimulating hormone (FSH), cyclic AMP (cAMP) and protein kinase A (PKA). The *CYP19A1* gene has a total of ten promotor regions. Directly upstream of its coding region, which contains a total of nine exons and is 30 kb in length, is the promotor region PII (27). Further upstream from the PII promotor are the other nine promotors: I.1, I.2, I.2a, I.3, I.4, I.5, I.6, I.7 and I.f. These promotors are all tissue-specific and therefore, along with their transcription factors, regulate the expression of this enzyme at different rates, depending on the cell type. Promotors I.3, I.7 and PII, for example, have been found to be expressed in breast cancer, whilst promotor I.4 is expressed in normal breast adipose tissue (26, 27). Although its expression is regulated by various promotor regions, they all code for a single gene, which is translated into one protein (Figure 3), made up of a total of 503 amino acids (28).

Figure 3: Tertiary structure of the aromatase enzyme isolated from human placenta. The N-terminus, which begins at amino acid 45, is shown in dark blue, whilst the C-terminus, which ends at amino acid 496, is shown in red. The α-helices are labelled from A to L whereas the β-sheets are numbered 1 to 10. The haem group, as well as the androstenedione molecule bound at the active site, are shown. Figure adapted from (28).

The biosynthesis of oestrogens (Figure 4) involves various biochemical reactions carried out by different CYP450 enzymes, beginning with the conversion of cytosolic cholesterol into the precursor molecule pregnenolone (23, 27). This occurs via two hydroxylation reactions before the cleavage of the cholesterol side chain, by cholesterol side-chain cleavage enzyme, also known as CYP11A1 (29). Pregnenolone, a precursor for the majority of human steroid hormones, can then be converted either into progesterone, via 3β-hydroxysteroid dehydrogenase (3β-HSD), or into 17-OH pregnenolone by steroid 17α-monooxygenase (CYP17). CYP17 then catalyses the reaction of 17-OH pregnenolone into dehydroepiandrosterone (DHEA), which is converted into androstenedione by 3β-HSD (27, 29). Progesterone, on the other hand, is converted into 17-OH progesterone by CYP17, a reaction that can also be catalysed by 3β-HSD from 17-OH pregnenolone. 17-OH progesterone is then further catalysed, by CYP17, into androstenedione (27). This series of reactions that results in the conversion of cholesterol into androgens, can take place in both the adrenal cortex and the ovaries, due to the presence of the required enzymes. As breast

tissue does not possess these enzymes, the synthesis of oestrogens must therefore rely on circulating androgens from the blood.

Androstenedione is converted by aromatase into E_1, whereas testosterone, which is produced from androstenedione via 17β-hydroxysteroid dehydrogenase (17β-HSD), is converted by aromatase into E_2. Moreover, 17β-HSD is also able to convert E_1 into E_2, in a reaction which is reversible (23, 27), and largely depends on the cofactors present, e.g. NADPH or NADH (29). Aromatase, similarly to the other enzymes involved in this chain of reactions, requires an H^+, an O_2, and the presence of a reductase enzyme, in order to aid in the transfer of electrons. NAPDH-cytochrome P450 reductase is the specific reductase enzyme that catalyses the electron transfer from NAPDH to aromatase, contributing to the aromatisation of the A-ring of the androgen (25, 26). The catalytic portion of aromatase contains a haem group that also contributes to the transfer of electrons, as well as a steroidal binding site (26, 27), thus making aromatase an enzymatic complex that catalyses the rate limiting and final step of oestrogen biosynthesis. The aromatisation of the steroidal A-ring occurs via three oxidative reactions, each requiring one molecule of O_2 and one of NADPH (28).

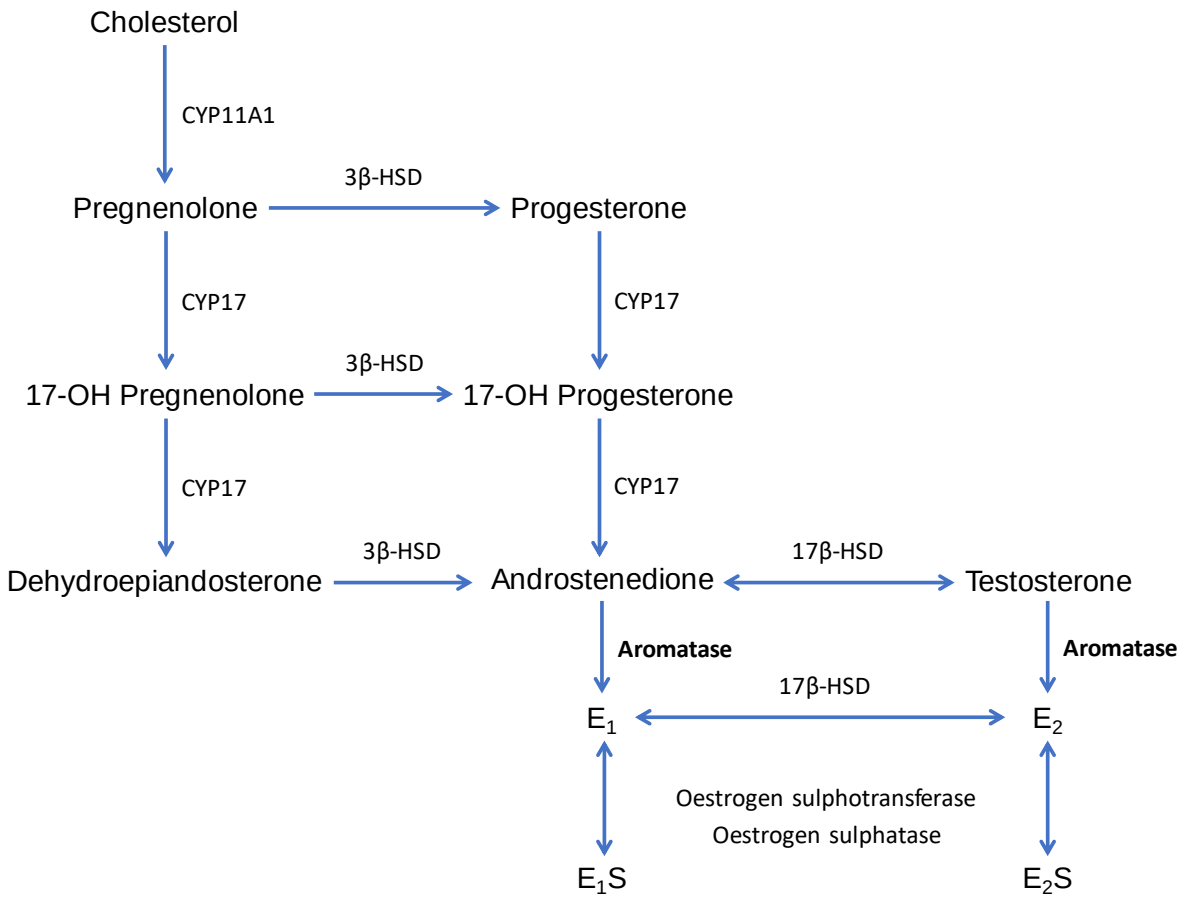

Figure 4: Pathway for the synthesis of oestrogens. Oestrogen synthesis begins with a cholesterol precursor that is converted into pregnenolone or progesterone, by cholesterol side-chain cleavage enzyme (CYP11A1), or by CYP11A1 then 3β-hydroxysteroid dehydrogenase (3β-HSD), respectively. These molecules are then converted into androstenedione via a series of reactions. Androstenedione can be converted into testosterone by 17β-hydroxysteroid dehydrogenase (17β-HSD), and these two androgens are further converted into oestrone (E_1) and oestradiol (E_2), respectively, by the enzyme aromatase. E_1 and E_2 can also be converted into oestrone sulphate (E_1S) and oestradiol sulphate (E_2S), respectively, by the enzyme oestrogen sulphotransferase, in a reaction that is reversed by oestrogen sulphatase.

E_1 and E_2 can be converted into the biologically inactive oestrone sulphate (E_1S) and oestradiol sulphate (E_2S), respectively, via oestrogen sulphotransferase. This often occurs as an oestrogen storage mechanism, as these compounds can be converted back into oestrogens via the enzyme oestrogen sulphatase (27), and has therefore been described to play a role in oestrogen-sensitive, but not insensitive, breast cancer cases (30).

1.3. Oestrogen receptors (ER)

ER is a member of the nuclear receptor superfamily, that is activated by circulating oestrogens. There are two isoforms, ERα and ERβ, which possess different functions and are

expressed in different parts of the body. ERα is present in the breast, ovarian theca cells, uterus, prostate stroma, testes and liver, whereas ERβ exists in the ovarian granulosa cells, prostate epithelium, testes, breast, bone marrow and brain (18). Both isoforms are encoded by different genes, share a 59% overall homology (7), and have a similar affinity for oestrogens (31). ERα is encoded by the *ESR1* gene on chromosome 6, is composed of 595 amino acids and has a molecular mass of 66 kDa, whereas ERβ is encoded by the *ESR2* gene on chromosome 14, is composed of 530 amino acids and has a molecular mass of 59 kDa (18, 32). ERα and ERβ differ greatly in the N-terminus (also known as the A/B domain) with a sequence homology of approximately 18% (33). This domain is associated with the recruitment of coregulator proteins, that assist in gene transcription (32), via one of two activation functions, named ligand-independent transcriptional activation domain (activation function 1; AF-1). On the other hand, a 97% homology between the two receptor isoforms can be seen in the DNA-binding domain (DBD; also known as the C domain) (16, 33-35), which is responsible for the binding of ER to the DNA in the promotor region of specific target genes, whilst the hinge region (or D domain), contains a nuclear localisation signal (NLS) that is necessary for translocation of ER to the nucleus upon receptor activation (35). The ligand-binding domain (LBD; also known as the E domain), which is located in the C-terminus (36), is responsible for ligand-binding and receptor dimerisation, and shares a 47% homology between ERα and ERβ (33). The E conserved domain also contains an NLS, as well as a ligand-dependent transcriptional activation domain (activation function 2; AF-2), that is responsible for ligand-dependent activation of ER (35). The F domain of ER, for which a role in ERβ is yet to be found, shares a sequence homology of just 18% between the two isoforms, and in ERα is associated with its interaction with coregulators, receptor dimerisation, gene transcription and overall stability of the protein (Figure 5) (32).

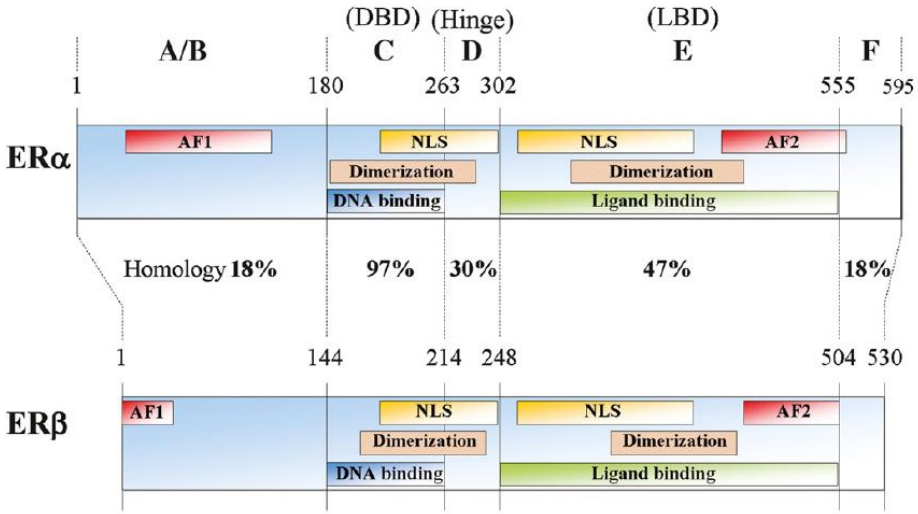

Figure 5: Representation of the structure of human ERα and ERβ. Both ERα and ERβ have an A/B domain at the N-terminus, a C domain that represents the DNA-binding domain (DBD), a D domain/hinge region, an E domain that harbours the ligand-binding domain (LBD) and an F domain at the C-terminus. Numbers refer to amino acid numbers, while percentages represent the amino acid homology between each domain of ERα and ERβ. Figure adapted from (33).

In breast tissue, the binding of oestrogens to ERα, which is upregulated in ER^+ breast cancer cases, is associated with cell growth and proliferation, with it being a tumour promotor (36, 37). ERβ, on the other hand, is reported to act as a tumour suppressor, preventing the growth of cells by causing cell cycle arrest, explaining why its expression is diminished as the tumour progresses (37). Nevertheless, in normal breast tissue, both ER isoforms are expressed at similarly low levels, whilst in breast cancer tissue the expression of ERα is increased. This has already been shown in several studies, suggesting that a balance between ERα and ERβ may interfere with the progression of tumours (38, 39).

Activation of ER in the cytosol occurs after binding of E_2 to AF-2, located in the LBD of ER, which causes the dissociation of the receptor from specific chaperone proteins, like heat shock proteins 56, 70 and 90 (HSP56, HSP70 and HSP90, respectively). These chaperone proteins are bound to the LBD of ER and, in the absence of E_2, ensure that the receptor remains inactive, thus preventing its degradation (18, 36, 40). Conformational changes then follow this dissociation, including homo- or heterodimerisation of ER, which leads to its translocation to the nucleus, where the receptor binds to specific oestrogen response elements (EREs) in the promotor region of ER-regulated genes. This mechanism is what is known as the classical oestrogen signalling pathway (Figure 6) (20). A heterodimer will have a similar affinity for DNA as an ERα homodimer, however its level of transcriptional activity will be lower (26). Moreover, as both ER isoforms share such a high sequence homology within the DBD it seems that,

when activated by this pathway, ERα and ERβ may target similar genes in order to regulate their transcription. After binding to EREs, ER recruits specific coactivators, such as cAMP response element-binding protein (CREB), coactivator-associated arginine methyltransferase 1 (CARM1), protein arginine methyltransferase 1 (PRMT1), and nuclear receptor coactivator 1 (SRC1) and 2 (SRC2), or corepressors, such as nuclear receptor corepressors 1 (NCOR1) and 2 (NCOR2), and metastasis-associated protein 1 (MTA1) (17), that aid in inducing the activation or suppression of gene transcription (7, 15, 16, 41).

Besides binding to EREs in specific ER-regulated genes, ER can also regulate transcription via other genomic mechanisms. One of these involves protein-protein interaction with other transcription factors, such as activator protein 1 (AP-1), specificity protein 1 (SP-1), nuclear factor-κB (NF-κB), forkhead box A (FoxA), transacting T-cell-specific transcription factor (GATA-3) and various members of the signal transducer and activator of transcription (STAT) family of proteins (17, 42, 43). Here, the activated ER will bind indirectly to these alternative non-EREs, in order to activate the transcription of different target genes (7), a mechanism that is known as the non-classical oestrogen signalling pathway (Figure 6). The expression levels of around one third of all oestrogen responsive genes are regulated through this manner (17), including cyclin D1, which is associated with cell cycle progression (16).

Thus, the mechanisms of oestrogen action can be performed via either the classical or non-classical genomic pathway, however, another mechanism of ER signalling exists, which is ligand-independent and relies on the phosphorylation of one of several serine or tyrosine residues found in AF-1 of ER. This phosphorylation can happen as a result of the activation of a range of different signalling pathways, including: p38/mitogen activated protein kinase (p38/MAPK), phosphatidylinositol-3-kinase/protein kinase B (PI3K/AKT), cyclin dependent kinase 2/cyclin A (CDK2/cyclin A), PKA, glycogen synthase kinase 3 (GSK3), cyclin dependent kinase 7 (CDK7), casein kinase 2 (CK2) and inhibitor of kappa kinase α (IKKα) (7, 15, 16, 34, 36). Phosphorylation of serine residues via these specific signalling pathways facilitates the recruitment of coregulator proteins (34, 36). Thus, activated ER can also lead to gene transcription via a non-genomic pathway (Figure 6), causing a more rapid response. The activation of this non-genomic pathway can occur through various membrane receptors, including growth factor receptors such as HER2, epidermal growth factor receptor (EGFR), fibroblast growth factor receptor 1 (FGFR1) and insulin-like growth factor 1 receptor (IGF1R), as well as G-protein coupled receptors (GPR30) (7), leading to signal transduction and the activation of downstream cytosolic ER. The release of second messengers such as cAMP, cGMP and Ca^{2+}, following ER-activation of non-genomic pathways, has also been reported (7, 17). Moreover, it has also been documented that the membrane receptor GPR30 can also act as an ER and be itself activated by oestrogens, leading to activation of these signalling pathways without the need for ER (26, 44, 45).

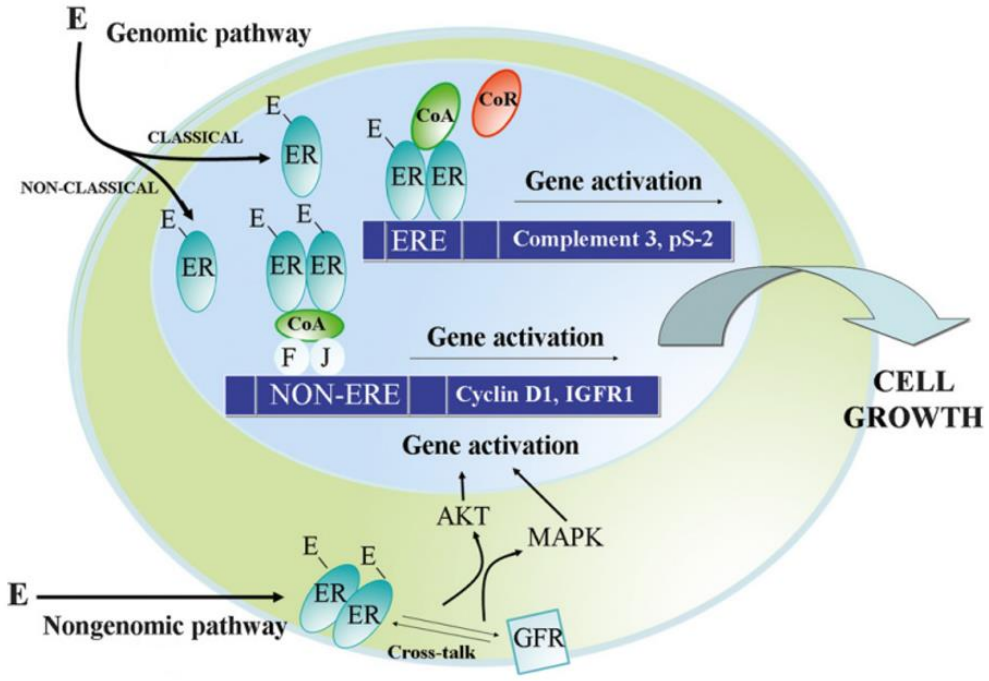

Figure 6: Genomic and non-genomic oestrogen signalling pathways. Classical and non-classical genomic signalling pathways are shown, where activated oestrogen receptor (ER) induces gene transcription through dimerisation, followed by either direct binding to oestrogen response elements (EREs) in the DNA, or indirect binding to non-EREs through interactions with transcription factors, such as Fos (F) and Jun (J), which together form activator protein 1 (AP-1). Non-genomic pathway is also shown, where membrane-bound growth factor receptors (GFRs) activate ER through the activation of signalling pathways such as MAPK and AKT, which further leads to the activation of gene transcription. Figure adapted from (33).

There are therefore several oestrogen signalling pathways, the genomic and the non-genomic, the ligand-dependent and the ligand-independent, by which ER is able to regulate gene transcription. In ER^+ breast cancer, deregulation of the various signalling pathways involving the activation or suppression of ER has already been reported (31, 46). The vast number of genes that can have their expression regulated by oestrogens and ER underlines the complications that exist with regards to the treatment of this type of cancer.

1.4. Hormone therapy for ER^+ breast cancer

In recent years, adjuvant endocrine therapy following the removal of a primary tumour, also known as adjuvant hormone therapy, has been the preferred form of treatment for postmenopausal women with ER^+ breast cancer (7, 12). In premenopausal women, which account for around 11% of diagnoses (47), the combination of endocrine therapy with or without suppressed ovarian function, via surgery or the use of an LH-releasing hormone agonist, has been suggested to be used in the clinic (7, 48). The main aim of endocrine therapy

is to control the effects of circulating hormones, that will ultimately play a key role in the growth and progression of a tumour. Thus, in order to prevent oestrogen-mediated cell proliferation, and consequently tumour progression in ER^+ breast cancer, endocrine therapy can currently be performed via three different classes of drug: selective oestrogen receptor modulators (SERMs), selective oestrogen receptor down-regulators (SERDs) and aromatase inhibitors (AIs). The chosen form of treatment will depend on various factors, including the stage and size of the tumour, the menopausal status, receptor expression and the overall condition of the patient. Therefore, the type of treatment will differ from patient to patient, in order to be as effective as possible in treating the cancer, whilst causing as few changes as possible to their short-term and long-term lifestyle.

Tamoxifen (Figure 7) is the most commonly used SERM in the clinic. This drug acts by binding reversibly to ER, altering its structure and preventing oestrogens from binding (49). Moreover, it has been suggested that tamoxifen also triggers the recruitment of corepressors to ER (43), in order to prevent gene transcription. SERDs, on the other hand, bind irreversibly to ER, destabilising it and leading to its degradation, with fulvestrant/ICI 182 780 (Figure 7) being the first of these to be developed (50). Although this particular drug was found to be effective in the treatment of ER^+ breast cancer, its poor solubility means that it is inefficient when taken orally, so it must be administered via intramuscular injection (7), thus limiting its availability for regular use in the clinic. A SERD with high oral bioavailability that is effective in the treatment of ER^+ breast cancer would therefore be ideal, though until now is yet to reach the market. There are, however, studies and clinical trials ongoing in this area (50). Furthermore, due to their positive results in clinical trials, it has been proposed that SERDs could be used in the clinic in order to treat breast cancer patients that have shown to be resistant to the other forms of therapy (50).

Beyond their use in ER^+ breast cancer treatment, SERMs are also prescribed to women who are at a high risk of developing this disease. In 1998, following various clinical trials, tamoxifen was approved by the FDA for the chemoprevention of breast cancer for both pre- and postmenopausal women who fall into this category. Furthermore, in 2007, the SERM raloxifene was also approved for chemoprevention, although it was not deemed suitable for premenopausal women (51). Moreover, although SERDs have also been suggested for the prevention of ER^+ breast cancer in women at high risk, they are often only preferred for women with advanced stages of disease (50).

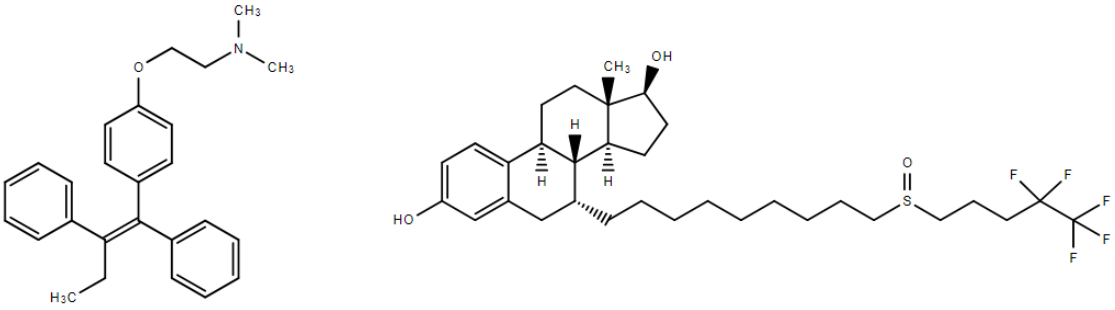

Tamoxifen Fulvestrant/ICI 182 780

Figure 7: Skeletal structures of tamoxifen and fulvestrant/ICI 182 780.

Ever since its approval for the treatment of ER^+ breast cancer by the FDA in 1977, tamoxifen was considered the first-line treatment option for both pre- and postmenopausal women with ER^+ breast cancer (12, 52), until the discovery of the third-generation AIs in the 1990s. Although the first- and second-generation AIs were effective in the treatment of this cancer, they caused considerable side effects, had lower specificity for aromatase, and interfered with other hormones such as cortisol and aldosterone (53). Therefore, tamoxifen was often regarded as a better option. Nevertheless, according to recent guidelines, the third-generation of AIs are now recognised as the first-line therapeutic option in postmenopausal women with ER^+ breast cancer, in early and metastatic stages, and their introduction in premenopausal women with suppressed ovarian function is being considered (54). In the latter case, however, tamoxifen still remains the preferred therapy.

The third-generation of AIs, which consists of the steroidal (or type I) inhibitor exemestane, and the non-steroidal (or type II) inhibitors, anastrozole and letrozole, act by inhibiting the aromatase enzyme, and thus decrease the levels of oestrogens available to stimulate ER^+ breast cancer cell growth (12, 23). The non-steroidal AIs, anastrozole and letrozole (Figure 8), bind non-covalently and reversibly to the haem group of aromatase (23), saturating its active site and thus preventing androgens from binding. The steroidal AI exemestane (Figure 8), on the other hand, has a chemical structure similar to androstenedione, the natural substrate of aromatase, and acts by binding covalently and irreversibly to the active site of aromatase. This causes inactivation and degradation of aromatase via the proteasome, with exemestane also being known as a suicide inhibitor (55).

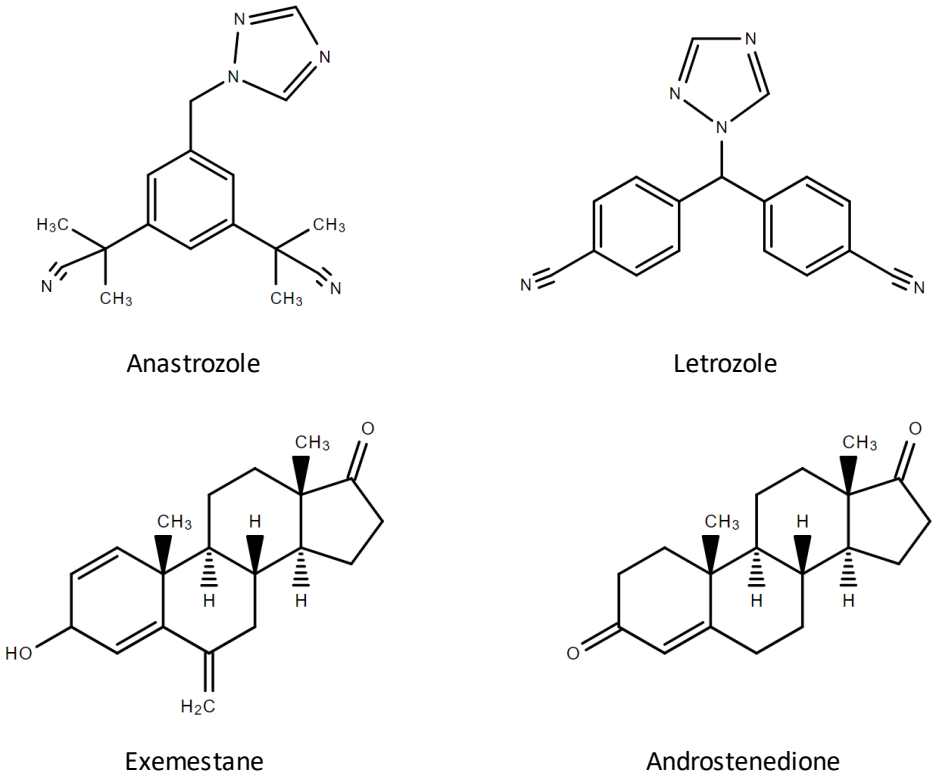

Figure 8: Skeletal structures of the third-generation AIs: anastrozole, letrozole and exemestane, and a comparison between the structures of exemestane and androstenedione.

Not only do these third-generation AIs have a high oral bioavailability (48), thus facilitating their clinical use, but they also present fewer side effects than tamoxifen. Moreover, according to the different clinical trials, these AIs are often more effective, and provide a prolonged disease-free survival and time-to-recurrence than tamoxifen and fulvestrant (7, 55). Because of their higher efficacy in the treatment of ER^+ breast cancer in the adjuvant setting, AIs have also been suggested for use as chemoprevention to reduce the risk of developing cancer.

Nevertheless, some adverse effects are associated with AIs, such as musculoskeletal pain, arthralgia, fibromyalgia, hot flashes, sexual dysfunction, cardiovascular events and loss of bone mineral density (7, 12, 48). In some cases, these side effects, which are a result of oestrogen deprivation (56), can lead to an interruption in the therapy, in part due to the increase in the likelihood of bone fractures and osteoporosis, a consequence of a loss in bone density (7, 55). This remains the major issue with regards to this form of treatment, however, it has been reported that these negative effects on bone density can be reduced when an AI is taken in combination with bisphosphonates (48). Even so, the side effects pointed to AI treatment are generally less severe than those associated with SERMs. For example, endometrial cancer and venous thromboembolic disease are two of the most serious side

effects that can occur with tamoxifen treatment, however they are not associated with AI treatment (7, 48, 55).

Recent clinical trials suggest that changing to AI treatment after two or three years of taking tamoxifen could be more effective and improve the breast cancer therapy, as cancerous cells are subject to two forms of therapy that each function via different mechanisms. In addition, this may also potentially reduce the likelihood of acquiring resistance to endocrine therapy (54). Moreover, this could also help to reduce the risk of fractures and osteoporosis, when compared to treatment only with AIs, due to tamoxifen's oestrogenic properties in osteoblasts, which actually causes an increase in bone density in postmenopausal women, as opposed to the third-generation of AIs (48).

Due to advances in treatments and diagnoses, as well as in knowledge about hormone-dependent breast cancer, more cases can be detected at an earlier stage, with these patients now having an increased chance of survival when compared to the past (57). The five-year survival rate for postmenopausal women with ER^+ metastatic breast cancer taking endocrine therapy is now one in four, with the average survival time being between two and three years, which is a great improvement when compared to the past (7). Unfortunately, however, even before treatment has begun some patients are already resistant, and will not respond to endocrine therapy. This is what is known as *de novo* resistance (6). Furthermore, with prolonged treatment there is also the possibility of developing acquired resistance, which remains the major obstacle when it comes to endocrine therapy. Around one third of patients will develop this type of resistance (7), where breast cancer cells have the ability to adapt to oestrogen deprivation, and continue to grow even in the presence of an anticancer drug. Consequently, this type of resistance leads to tumour relapse and re-growth (7). In addition to knowing that the two forms of resistance may occur, the clinical differences between them are not completely defined. In some cases it is possible to switch from one form of treatment to another, as resistance to SERMs, for example, does not necessarily mean that the cancer will be resistant to AIs. Moreover, it has also been found that acquired resistance to an AI will not always mean cross-resistance between both steroidal and non-steroidal AIs (6), potentially due to the different mechanisms of interaction between the drug and aromatase. Cross-resistance to multiple drugs can, however, also occur.

Various different mechanisms of resistance both *in vitro* and *in vivo* could occur independently or in combination, to allow the cell to grow. In fact, over the last ten years, several mechanisms have been proposed (7, 33, 58-60), however, the exact mechanism for each therapy is not yet fully elucidated. Moreover, the mechanism of resistance that has been observed *in vitro* may not be the same as the one that occurs in patients, further complicating this topic of research.

As endocrine therapy primarily targets oestrogen signalling, either through the inhibition of ER or by the prevention of oestrogen production, the mechanisms of resistance that have so far been described are linked to alterations in ER expression and/or function. Some tumours may adapt to progress without the need for ERα expression and activation, using other receptors such as HER2, in order to drive proliferation (7, 61). In other cases, however, where tumours are still dependent on ERα activation in order to grow, a hypersensitivity to oestrogens, due to low oestrogen levels, has been documented (62), though the exact mechanism is still unknown. It has also been described that ER can be activated independently of oestrogens (7, 36, 63), as a result of specific mutations in the LDB of this receptor, which could cause resistance to endocrine therapy.

Aside from the mutations that cause oestrogen-independent activation of ERα, the overexpression and hyperactivation of signalling pathways, such as MAPK and PI3K, are also mechanisms that are linked to acquired resistance to AIs. Deregulation of these signalling pathways can lead to an oestrogen-independent activation of ER, an upregulation in the expression levels of ERα, a deregulation in the expression levels of the coactivators, corepressors and transcription factors used by ER to regulate transcription, as well as a deregulation of anti- or proapoptotic proteins or proteins involved in the cell cycle (7, 58, 59). In fact, an overexpression of cyclins, cyclin-dependent kinases (CDKs), and other proteins associated with cell cycle progression has been reported in patients resistant to endocrine therapy, whereas a downregulation or inactivation of all negative cell cycle regulators, has also been described (7, 58-60).

Another mechanism that has also been reported to be involved in endocrine resistance is the overexpression of androgen receptor (AR), as a response to a decrease in ER levels (7, 58, 59). AR is expressed in the majority of ER^+ breast cancers and, it is known that, in resistant cases, it can cooperate with ER in order to activate transcription, via PI3K signalling, which ultimately promotes breast cancer cell growth (7).

Autophagy, a biological process whereby a cell begins to break down internal components in response to nutrient deprivation or increased stress levels, can function as either a mechanism of cell survival or of programmed cell death. In various cancer models, autophagy has already been reported as a cell survival mechanism, with its role in endocrine resistance also being proposed (7, 64, 65). In fact, Amaral, *et al*. recently demonstrated that autophagy is involved in exemestane-acquired resistance, as a mechanism of cell survival, and that the inhibition of autophagy re-sensitises resistant breast cancer cells to exemestane (66).

Taking all of this into account, the major drawbacks with endocrine therapy are therefore the development of resistance, and the occurrence of adverse effects, such as bone loss with AIs or endometrial cancer and thromboembolic events with tamoxifen. Even though, in many cases, endocrine therapy has proved to be effective in treating ER^+ breast cancer,

nevertheless, these drawbacks highlight the urgent need for research in order to find new and improved treatments, with fewer adverse effects, and that can increase the disease-free survival and the quality of life of cancer patients.

1.5. Cannabinoids and cannabinoid receptors

Cannabinoids are a large class of chemical compounds that is divided into subcategories based on occurrence in nature. Phytocannabinoids, such as cannabidiol (CBD) and Δ^9-tetrahydrocannabinol (THC), exist naturally in plants, primarily in those of the *Cannabis* genus, however other compounds with similar structures and functions have also been found elsewhere (67). Endocannabinoids, such as anandamide (AEA) and 2-arachidonoylglycerol (2-AG), are synthesised naturally by the body, and are in fact vital components of a variety of different biochemical processes (68). Synthetic cannabinoids, such as nabilone, WIN-55,212-2 and JWH-015 (69), have been designed and synthesised in order to mimic the beneficial health or medical effects of phyto- and endocannabinoids, often binding receptors with higher affinity than their natural counterparts. Cannabinoids are known to exert their effects through their binding to the specific G protein-coupled cannabinoid receptors, CB_1 and CB_2. Moreover, it has also been described that some cannabinoids can interact with other receptors such as the orphan G protein-coupled receptor 55 (GPR55), the transient receptor potential vanilloid 1 (TRPV1) receptor and the peroxisome proliferator-activated receptor gamma (PPAR-γ or PPARG) (68, 70-72).

CB_1 and CB_2 are two of the most abundant G protein-coupled receptors in our body (69, 71), however they each have specific distribution patterns and are not expressed ubiquitously. CB_1 receptors are expressed primarily in the central nervous system, in particular in the cortex, hippocampus, cerebellum and basal ganglia (68, 70), whereas they can also be found in smaller amounts in some peripheral tissues, such as adipocytes, the liver, pancreas, skeletal muscle and some reproductive tissues (68, 71). CB_2 receptors, on the other hand, are expressed at much lower levels in the central nervous system, and instead are mainly restricted to certain peripheral tissues, being predominantly expressed in cells of the immune system (68, 71). Both cannabinoid receptors are primarily located in the outer membrane of the cells in which they are expressed, however, CB_1 has also been found to be present inside the cell in the membrane of lysosomes, in the endoplasmic reticulum and in mitochondria (68, 73).

CB_1 was first cloned in 1990, and was the first cannabinoid receptor to be discovered (74). It is encoded by the *CNR1* gene on chromosome 6 and is composed of 472 amino acids (73). The discovery of the second cannabinoid receptor, CB_2, came shortly after, in 1993 (74). This receptor is encoded by the *CNR2* gene on chromosome 1, consists of 360 amino acids and shares a sequence homology of 44% with CB_1 (68, 73). The fact that these two receptors

share such a low sequence homology may explain the differences between their functions, and their affinity for different ligands. As with the other members of the G protein-coupled receptor superfamily, CB_1 and CB_2 consist of seven transmembrane domains, the intra- and extracellular loops that connect them, an extracellular N-terminus and an intracellular C-terminus. The binding of a ligand to the extracellular binding domain, which share 68% of homology between CB_1 and CB_2, causes intracellular conformational changes that lead to activation of the receptor. The activation of CB_1 can lead to the inhibition of adenylate cyclase and of P/Q-type calcium channels, as well as activation of potassium channels. In contract, CB_2 activation does not modulate the ion channel function. The stimulation of these receptors may induce the activation of various intracellular signalling pathways, such as extracellular signal-regulated kinase (ERK), c-jun N-terminal kinase (JNK), focal adhesion kinase (FAK) and p38 MAPK, as well as the production and accumulation of ceramide (Figure 9) (68, 70, 71, 75). Through these mechanisms, cannabinoid receptors are able to regulate a series of cellular functions including neuronal development, programmed cell death, gene transcription and cell proliferation. Thus, cell fate may depend on the activated transduction pathway (73, 75, 76).

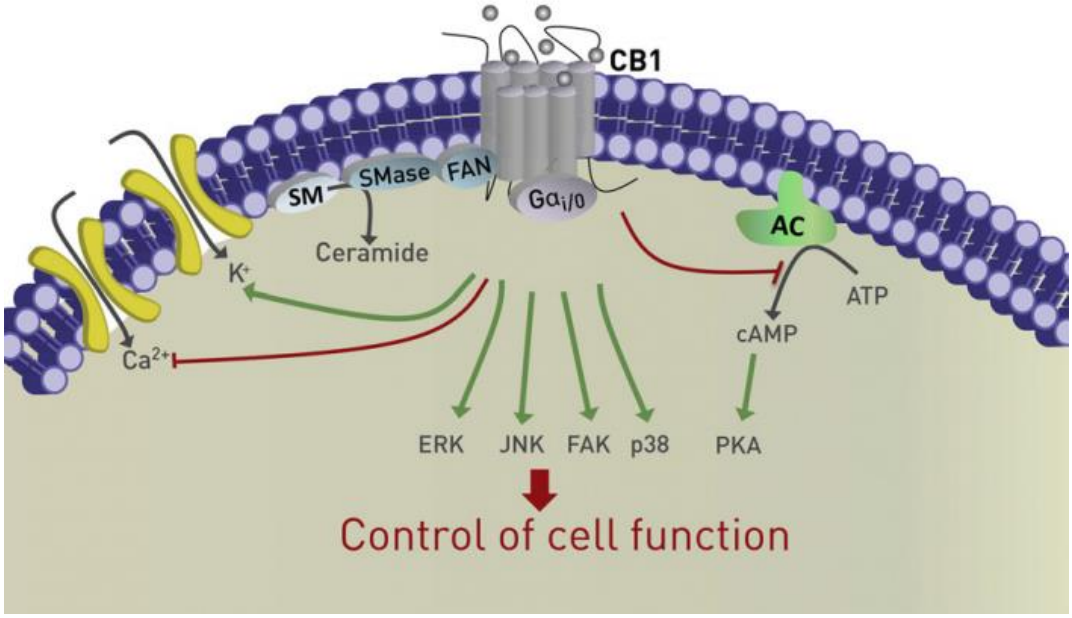

Figure 9: Cannabinoid receptor signalling inside a cell. Cannabinoid receptor activation can lead to a series of alterations to intracellular functions, thus changing the outcome of a cell. This can include the mediation of K^+ and Ca^{2+} membrane ion channels, inhibition of adenylate cyclase (AC), or activation of various signalling pathways such as extracellular signal-related kinase (ERK), c-Jun N-terminal kinase (JNK), focal adhesion kinase (FAK) and p38 MAPK. Furthermore, cannabinoid receptor activation can also lead to the regulation of ceramide accumulation, via the modulation of factor associated with neutral sphingomyelinase activation (FAN) protein, that activates the enzyme sphingomyelinase (SMase), which hydrolyses sphingomyelin (SM), and in turn causes an increase in ceramide levels. Figure adapted from (68).

1.5.1. Endocannabinoids

In 1992, the search for an endogenous ligand for CB_1 was concluded, when AEA became the first endocannabinoid to be discovered. The discovery of the second endocannabinoid, 2-AG, which is also a ligand for CB_1, came shortly after (77). In fact, both AEA and 2-AG (Figure 10) show affinity for both cannabinoid receptors (77), and, whilst other peptides and molecules that possess endocannabinoid-like functions do exist, to date, AEA and 2-AG remain the two most well-studied endocannabinoids (73, 78). Both molecules exert their biological effects through both cannabinoids receptors, although AEA has lower affinity and efficacy for CB_2 compared with CB_1, while 2-AG has higher affinity and efficacy than AEA for both cannabinoid receptors (68).

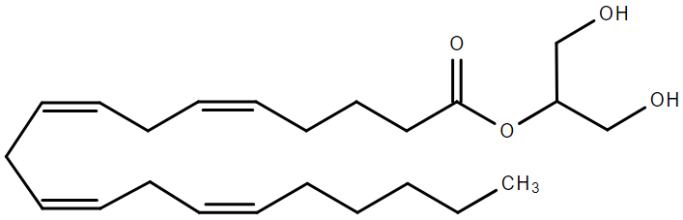

2-arachidonoylglycerol

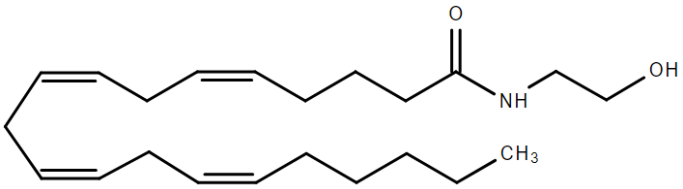

Anandamide

Figure 10: Skeletal structures of two most abundant endocannabinoids, 2-arachidonoylglycerol (2-AG) and anandamide (AEA).

Unlike many other neurotransmitters, endocannabinoids, which consist of arachidonic acid linked to a polar head group, are only synthesised on demand, in response to an increase in intracellular Ca^{2+} levels (71, 73). This production happens from membrane phospholipid precursors (75, 79), and takes place rapidly via a range of different enzymes (70). The synthesis of AEA, for example, can occur via different mechanisms, often involving the same *N*-arachidonoyl phosphatidylethanolamine (NAPE) precursor, and various different phospholipases, phosphodiesterases and phosphatases (70, 80-82). The main route of synthesis of this endocannabinoid begins with a transacylation by a Ca^{2+}-dependent *N*-

acyltransferase (NAT), to produce the NAPE precursor, which is subsequently converted into AEA, through a NAPE-specific phospholipase D (NAPE-PLD) (Figure 11) (68). 2-AG synthesis, on the other hand, requires a hydrolysis step on an arachidonoyl-containing phosphatidylinositol bisphosphate (PIP2) by a phospholipase C (PLC) enzyme, to generate 1,2-diacylglycerol (DAG), which is further hydrolysed into 2-AG by a diacylglycerol lipase (DAGL) (Figure 11) (68). Moreover, another synthesis pathway for AEA that has been documented involves cleavage by a phospholipase A (PLA) before hydrolysis by a lyso-phospholipase C (68, 70, 78). After being synthesised, these molecules are released into the extracellular space, by cell membrane diffusion or by a selective transport via the putative endocannabinoid membrane transporter (EMT). In the extracellular space, cannabinoids either interact with cannabinoid receptors or are internalised and degraded (68).

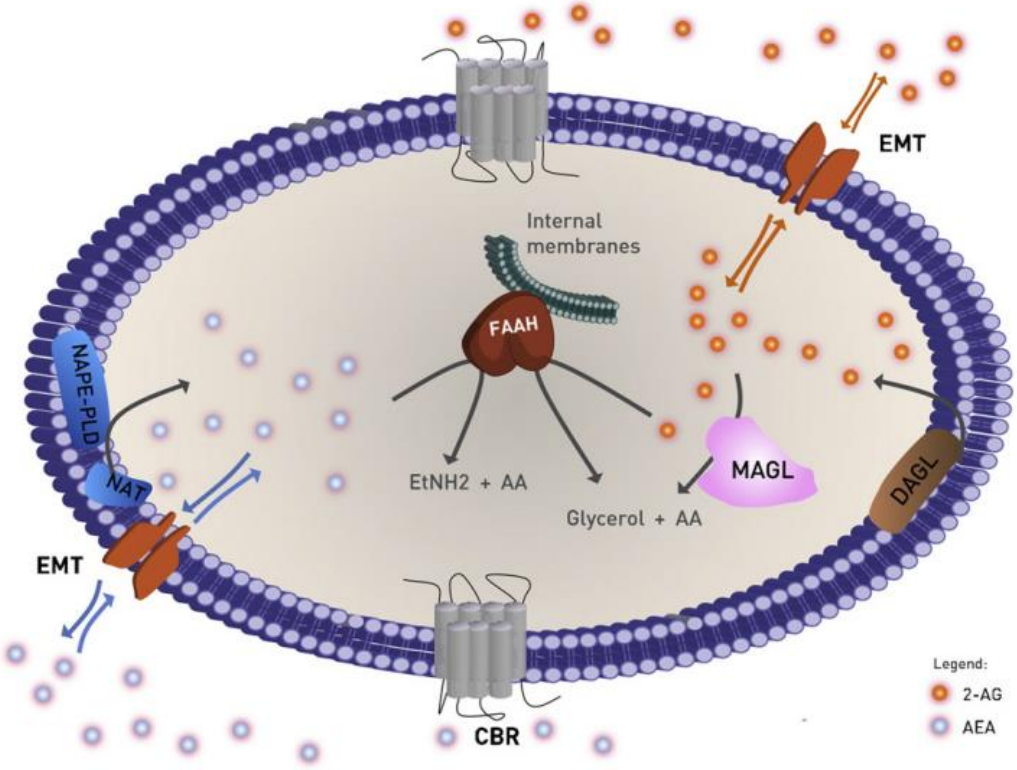

Figure 11: Biosynthesis of anandamide (AEA) and 2-arachidonoylglycerol (2-AG). Biosynthesis of AEA occurs through transacylation by *N*-acyltransferase (NAT) into *N*-arachidonoyl-phosphatidylethanolamine (NAPE), which is converted into AEA by a NAPE-specific phospholipase D (NAPE-PLD). 2-AG, on the other hand, is produced by diacylglycerol lipase (DAGL). Upon synthesis, endocannabinoids are transported into the extracellular space by the putative endocannabinoid membrane transporter (EMT), where they bind cannabinoid receptors (CBRs). Moreover, internalisation of endocannabinoids for degradation also occurs through EMT. AEA is hydrolysed by fatty acid amide hydrolase (FAAH) into ethanolamine ($EtNH_2$) and arachidonic acid (AA), whereas 2-AG, on the other hand, is hydrolysed by monoacylglycerol lipase (MAGL) or FAAH into glycerol and AA. Figure adapted from (68).

After re-uptake, AEA and 2-AG are primarily degraded by fatty acid amide hydrolase (FAAH) and monoacylglycerol lipase (MAGL), respectively, although their metabolism is not limited to these two enzymes (70, 83). FAAH hydrolyses AEA into arachidonic acid (AA) and ethanolamine ($EtNH_2$), while MAGL, as well as FAAH, transform 2-AG into AA and glycerol (Figure 11) (68). Quite unsurprisingly, an inhibition of these enzymes was found to cause an increase in the expression levels of each respective substrate cannabinoid (84, 85). Furthermore, cyclooxygenase-2 (COX-2) can also biotransform AEA through an oxidative mechanism, generating prostaglandin-ethanolamides (PG-EAs), as well as deoxygenating 2-AG to produce prostaglandin-glyceryl esters, before 2-AG is hydrolysed by FAAH (Figure 11) (68). With regards to AEA degradation, *N*-acylethanolamine-hydrolysing acid amidase (NAAA) can also be responsible, albeit at a lower rate than FAAH and COX-2. Moreover, 2-AG can also be metabolised by alpha/beta domain hydrolases 6 and 12 (ABHD6 and ABHD12, respectively) (70, 78).

The cannabinoid receptors, along with their endogenous ligands, the enzymes responsible for their synthesis and degradation and the membrane transporters, form the endocannabinoid system (Figure 11) (68). The endocannabinoid system modulates a range of physiological functions including appetite, pain and analgesia, learning, memory and cognitive behaviour, metabolism, insulin sensitivity, fertility, stress and anxiety, as well as a variety of immunological processes including inflammation, bone remodelling and tumour progression (76-78, 83, 86). A deregulation in the endocannabinoid system could therefore have large consequences, and thus has already been linked to numerous diseases and conditions. These include various neurodegenerative disorders, such as amyotrophic sclerosis (ALS), Alzheimer's, Parkinson's and Huntington's diseases, as well as cancer, multiple sclerosis, musculoskeletal disorders, epilepsy, glaucoma, cardiovascular and liver disorders, inflammation, obesity, stroke, and mental health disorders such as depression, anxiety, insomnia, schizophrenia, addiction and eating disorders (73, 76).

1.5.2. Phytocannabinoids

Phytocannabinoids are known to have been used for their medical purposes as long as 5 000 years ago, with the first known record of their use being in China during the reign of Emperor Chen Nung (73, 77). Although in general these compounds are structurally different to endocannabinoids, they also act by binding both cannabinoid receptors. Despite having been used for thousands of years, it was not until the early 1930s that the first cannabinoid structure was elucidated, and only around ten years later that this cannabinoid, named cannabinol (CBN), was successfully synthesised. In the year 1940 came the discovery of a second cannabinoid, CBD, with the discovery of THC coming two years later in 1942. It wasn't

until 1963 and 1964, however, that the elucidation of the structures of both CBD and THC (Figure 12), respectively, occurred, with the synthesis of both coming a year later, in 1965 (74). Altogether, over 120 different phytocannabinoids have been identified in cannabis, with the majority of them sharing the same dibenzopyran ring and hydrophobic alkyl chain (72). Although many of the phytocannabinoids have already been shown to have potential therapeutic benefits, the majority of them are only present in low concentrations in the cannabis plant (87), and thus, to date, CBD and THC remain the two most well-studied. In fact, a plethora of studies have already been published highlighting some of the medical benefits of these compounds, namely in appetite stimulation, anti-anxiety, anti-inflammatory, analgesic, anti-glaucoma, anti-emetic and anti-tumour effects (72).

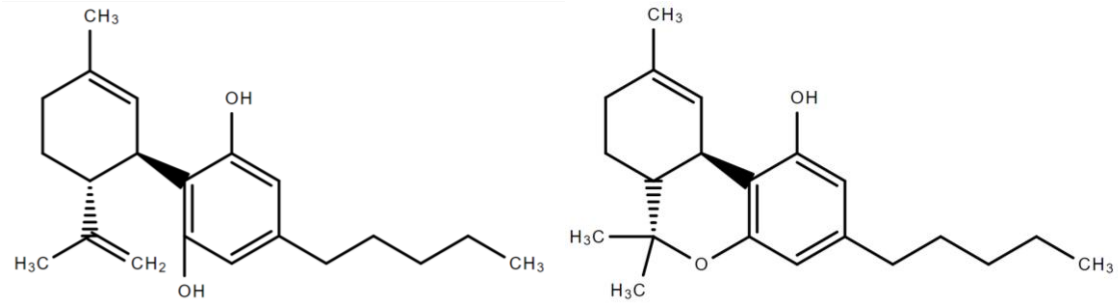

Cannabidiol Δ^9-tetrahydrocannabinol

Figure 12: Skeletal structures of the two most abundant phytocannabinoids found in the cannabis plant, cannabidiol (CBD) and Δ^9-tetrahydrocannabinol (THC).

THC is a partial agonist for both CB_1 and CB_2 (72, 75), whilst CBD has been found to exert its effects in other ways, via activation of TRPV1 or through receptor-independent mechanisms (72). The psychoactive effects induced by THC are most likely as a result of its binding to CB_1 receptors, since they are primarily located in various parts of the brain, whilst this could also explain the neuroprotective effects that have been seen to be triggered following the activation of this receptor. Contrary to THC, CBD does not present any psychoactive effects (73).

1.6. Cannabinoids in cancer

Cannabinoids in general have been linked to the treatment of many different diseases (73), and their anticancer properties have already been shown in a wide range of different cancer cell models, including cancers of the lung, skin, prostate, breast, uterus, thyroid and pancreas, as well as glioma, lymphoma and neuroblastoma (76). In certain cases, cannabinoids have been shown to inhibit cancer cell proliferation by inducing cell cycle arrest and programmed

cell death in cancer cells, as well as impairing cancer metastasis (88, 89). Moreover, cannabinoids also inhibit angiogenesis by down-regulating vascular endothelial growth factor (VEGF) receptors, inducing apoptosis of vascular endothelial cells, and impairing migration and invasion of cancer cells (Figure 13) (89, 90). Furthermore, cannabinoids can also be taken by patients for their analgesic effects, whilst relieving other side effects such as nausea, vomiting and lack of appetite (73, 76, 88, 91). In addition to this, various studies have demonstrated that cannabinoids have the ability to improve the efficacy of other forms of therapies, like chemotherapy or radiation (92). This, if successful, could prove to be a ground breaking advance in terms of cancer treatment, as patients would require a smaller dose of a potentially harmful drug, with more positive results and fewer undesired side effects.

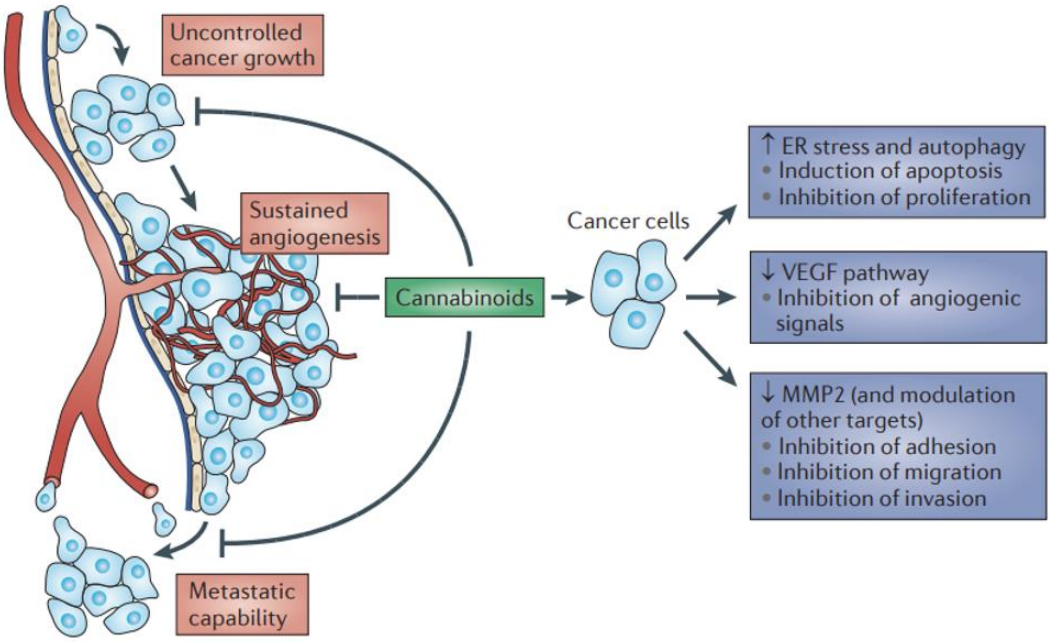

Figure 13: General anticancer mechanisms of cannabinoids. Cannabinoids are able to induce cancer cell death and suppress the growth of a tumour through several different mechanisms. This can be via apoptosis, autophagy or the inhibition of cell proliferation, or by preventing angiogenesis, and cell adhesion, migration and invasion. Figure adapted from (90).

Interestingly, cannabinoid receptors have been found to be upregulated in many cancer cell lines and tissues (76, 93), when compared with healthy tissues. The fact that cannabinoid receptors are often upregulated in cancer cases, may explain why treatment with cannabinoids generally does not present such toxic side effects, as are seen with chemotherapy. Moreover, an upregulation in the enzymes responsible for the degradation of endocannabinoids, thus leading to a downregulation in their expression, has also been described in some cancer models, with the inhibition of these enzymes resulting in cancer cell death (76).

Although the majority of cannabinoid-related cancer studies have been performed on glioma models, a considerable amount of research has also been carried out in other forms of cancer, including breast cancer. One particular study on breast cancer patients found that at least one of the two cannabinoid receptors was upregulated in the majority of cases, and that cannabinoids can prevent cancer progression in any of the three breast cancer subtypes (94). Furthermore, the anticancer properties of cannabinoids have already been demonstrated in numerous breast cancer cell lines, such as MCF-7, EFM-19, T-47D, MDA-MB-231, MDA-MB-468, MDA-MB-436, 4T1, TSA-E1, EVSA-T, SkBr3 and HTB-126 (75, 95).

Cannabinoids can function via numerous mechanisms in order to reduce cell proliferation and even induce cell death in breast cancer cells. Generally, apoptosis is the mechanism by which these molecules induce cell death in breast cancer cells, although autophagy has also been reported in some cases (90, 93, 96, 97). Programmed cell death in cancerous cells following cannabinoid treatment can be a result of an increase in intracellular ROS production leading to oxidative stress (92), a disruption in the mitochondrial membrane (93), endoplasmic reticulum stress (92), or cell cycle arrest (98-100). It has also been reported that a dysregulation of vital cellular functions induced by cannabinoids, including cell growth, repair and survival, and consequently inhibition of tumour growth, are associated with the inhibition of various cell signalling pathways such as AKT, mammalian target of rapamycin (mTOR) and MAPK (76, 90, 92, 95). Furthermore, in ER^+ breast cancer, THC has been suggested to inhibit ERα signalling, perhaps via interaction with upstream signalling pathways, whilst upregulating the expression of ERβ (101). Moreover, CBD in particular has proven to reduce viability of both ER^+ and ER^- cell lines by inducing apoptosis and autophagy, whilst causing a much smaller reduction in the non-cancerous human breast epithelial cell line, MCF-10A (96).

Cannabinoids are known to have anti-angiogenic properties both *in vitro* and *in vivo*, due to their ability to inhibit epidermal growth factor (EGF) signalling (90, 98, 102, 103). Angiogenesis is the formation of new blood vessels, which is crucial for tumour progression and cancer metastasis. In fact, CBD has been found to downregulate the expression of Id-1, a protein that is involved in the development of lung metastasis in breast cancer patients. It is thought that inhibition of Id-1 occurs through suppression of MAPK and an increase in intracellular ROS production (76, 86, 88, 98).

Cannabinoids therefore have the ability to function in various different ways in order to induce cancer cell death. The fact that they are largely non-toxic towards non-cancerous cells is promising, however conflicting results from different reports using different cell models, cancer types, cannabinoids and respective concentrations, show that this form of medication is not quite ready to be prescribed to cancer patients. Although cannabinoid-derived medicines have been available on the market for their palliative effects for some 30 years, cannabinoids are still not available in the clinic for the treatment of cancer. Early clinical trials have been

performed with success, whilst others are currently ongoing, however few have progressed past phase I (89). The anticancer properties of cannabinoids are undeniable, although much more research on the many different types of cancer is required before there is sufficient evidence for them to be transferred to the clinic.

Aims of the study

With the discovery of the third-generation AIs, this form of endocrine therapy has overtaken tamoxifen as the first-line therapy for the treatment of postmenopausal women with ER^+ breast cancer. Despite proving effective and successful in improving disease-free survival and time-to-recurrence when compared to other forms of treatment, endocrine resistance can occur, causing tumour relapse and thus re-growth. Acquired resistance to endocrine therapy is considered the major concern in breast cancer treatment, adding importance to the research for new drug therapies for this type of cancer.

The anti-tumour properties of cannabinoids have already been demonstrated in numerous cancer cell models, including breast. Moreover, they can be prescribed to some cancer patients due to their ability to alleviate various side effects including pain, nausea, vomiting and lack of appetite. Therefore, cannabinoids could be an attractive form of therapy, for ER^+ breast cancer, if they can prove to be effective in preventing tumour growth, whilst causing limited adverse effects. Taking this into account, the aim of this study was to investigate the anti-tumour properties of the phytocannabinoids, cannabidiol **(CBD)** and Δ^9-tetrahydrocannabinol **(THC)**, as well as the endocannabinoid anandamide **(AEA)** on an ER^+ breast cancer cell line that overexpresses aromatase (MCF-7aro) and is considered a good cell model to study this type of cancer, as well as on a resistant ER^+ breast cancer cell line (LTEDaro). In order to do so, the expression of cannabinoid and vanilloid receptors on these cell models, as well as the *in vitro* effects of these cannabinoids on a non-tumour human foreskin fibroblast cell line (HFF-1), will be explored. Furthermore, as ER^+ breast cancer cells depend on oestrogens in order to grow, the ability of cannabinoids to inhibit the aromatase enzyme and to modulate the expression levels of aromatase, ERα and ERβ, will be investigated. In addition, as the anti-tumour efficacy may be due to suppression of cell proliferation and/or induction of programmed cell death, in MCF-7aro cells, the effects of cannabinoids on cell cycle progression and on the occurrence of apoptosis or autophagy will also be explored. Moreover, the effects of these molecules on the viability of LTEDaro cells will be studied, in order to understand whether cannabinoids could also be suitable for patients who have become resistant to the current therapies used in the clinic.

2. Materials and Methods

2.1. Materials

MCF-7aro and LTEDaro cells were kindly provided by Dr. Shiuan Chen (Beckman Research Institute, City of Hope, Duarte, CA, USA). HFF-1 cells were obtained from ATCC (Manassas, VA, USA). Eagle's minimum essential medium (MEM), Dulbecco's Modified Eagle's Medium (DMEM), foetal bovine serum (FBS), sodium pyruvate, penicillin-streptomycin-amphotericin B (10 000 units/mL penicillin G sodium, 10 000 mg/mL streptomycin sulphate and 25 mg/mL amphotericin B), Geneticin (G418), L-glutamine, trypsin, 3,3′-dihexyloxacarbocyanine iodide ($DiOC_6(3)$) and the antibody for mouse monoclonal ERβ were supplied by Gibco Invitrogen Co. (Paisley, Scotland, UK). Testosterone (T), oestradiol (E_2), ethylenediaminetetraacetic acid (EDTA), charcoal, dimethylsulphoxide (DMSO), Trypan blue, ICI 182780 (**ICI**), 3-(4,5-dimethylthiazol-2-yl)-2,5-diphenyltetrazolium bromide (MTT), 3-Methyladenine (3-MA), progesterone, DNase-free RNase A, Triton X-100, Propidium iodide (PI), DPX mounting medium, Hoechst 33258, fluoroshield mounting medium, 2′7′-dichlorodihydrofluorescein diacetate ($DCFH_2$-DA), Chlorophenylhydrazone (CCCP), staurosporine (STS), Z-VAD-FMK, acridine orange (AO) and protease inhibitor cocktail were supplied by Sigma-Aldrich Co. (Saint Louis, USA). Anandamide (**AEA**), cannabidiol (**CBD**), AM630 and capsaicin (CAPS) were obtained from Tocris Bioscience (Biogen Cientifica, S.L., Spain). Δ^9-tetrahydrocannabinol (**THC**) was supplied by Lipomed AG (Switzerland). AM281, and the antibodies for goat polyclonal CB_1, rabbit polyclonal CB_2, goat polyclonal TRPV1, mouse monoclonal aromatase, mouse monoclonal c-PARP, rabbit polyclonal ERα and mouse polyclonal β-tubulin were obtained from Santa Cruz Biotechnology (Dallas, TX, USA). The antibody for rabbit polyclonal LC3 was purchased from Cell Signalling (Danvers, MA, USA). Isopropanol and H_2O_2 were supplied by VWR Chemicals (Radnor, Pennsylvania, EUA). Cyto-Tox 96 nonradioactive cytotoxicity assay kit, as well as, Caspase-Glo® 3/7 and Caspase-Glo® 9 luminometric assays were supplied by Promega Corporation (Madison, USA). Exemestane (**Exe**) was obtained from Sequoia Research Products Ltd. (Pangbourne, UK). [1β-^{3}H] androstenedione was purchased from Perkin-Elmer (Boston, MA, USA). Scintillation cocktail was supplied by ICN Radiochemicals (Irvine, CA, USA). Bradford reagent was supplied by BioRad (Laboratories Melville, NY, USA). Giemsa solution was purchased from Merck (Kenilworth, NJ, USA). WesternBright™ ECL chemiluminescent substrate was purchased from Advansta Inc. (Menlo Park, CA, USA).

2.2. Compounds under study

In this study, the *in vitro* effects of anandamide (**AEA**), cannabidiol (**CBD**) and Δ^9-tetrahydrocannabinol (**THC**) were tested on an ER^+ human breast cancer cell line that

overexpresses the enzyme aromatase, MCF-7aro. In order to do so, MCF-7aro cells were stimulated cells with the proliferating agents, testosterone (T) or oestradiol (E_2). Exemestane (**Exe**) was used as a reference aromatase inhibitor (AI). The effects of cannabinoids were also tested in combination with the selective oestrogen receptor down-regulator (SERD), ICI 182780 (**ICI**). Moreover, the effects of **AEA**, **CBD** and **THC** were also tested on an ER^+ human breast cancer cell line that mimics the late-stage of resistance to the AIs used in clinic, LTEDaro. Stock solutions of T and E_2, as well as **AEA** and **THC**, were prepared in absolute ethanol, while stock solutions of **CBD**, **Exe** and **ICI** were prepared in 100% DMSO.

In order to understand if the effects induced by cannabinoids on MCF-7aro cells were mediated by cannabinoid and/or vanilloid receptors, antagonists for the CB_1, CB_2 and TRPV1 receptors were used. AM281 and AM630, antagonists for the CB_1 and CB_2 receptors, respectively, were prepared in 100% DMSO. Capsaicin (CAPS), the antagonist for the TRPV1 receptor, was prepared in absolute ethanol.

All compounds were stored at -20°C and diluted samples were prepared using fresh medium before beginning each experiment. Final concentrations of DMSO and ethanol in culture medium were less than 0.05% and 0.01%, respectively.

2.3. Cell Culture

ER^+ breast cancer cells from the MCF-7aro cell line were acquired by performing a stable transfection of MCF-7 cells with the human placental aromatase gene and Geneticin (G418) selection, as previously described (104). As these cells overexpress the enzyme aromatase, they are considered the best cell model for the study of AIs and ER^+ breast cancer (105, 106). MCF-7aro cells were cultured in Eagle's minimum essential medium (MEM) containing phenol-red with Earle's salts, 10% heat-inactivated foetal bovine serum (FBS), 1 mmol/L sodium pyruvate, 1% penicillin-streptomycin-amphotericin B and 100 µg/mL Geneticin, with medium being refreshed every three days. Three days before beginning an experiment, MCF-7aro cells were cultured in an oestrogen-free MEM without phenol-red, and containing Earle's salts, 5% pre-treated charcoal heat-inactivated foetal bovine serum (CFBS), 1 mmol/L sodium pyruvate, 2 mmol/L L-glutamine and 1% penicillin-streptomycin-amphotericin B. Phenol-red is a pH indicator, but has weak oestrogen-like properties that can interfere with the growth of the cells (105). It is therefore important that phenol-red is not present in the culture medium during assays with MCF-7aro cells as it may affect the final outcome. During assays, CFBS was used, in order to remove any hormones present in serum that may interfere with cell growth.

During one-, two-, three- and six-day assays, MCF-7aro cells were stimulated using testosterone (T) at 1 nM as a substrate for aromatase. T is converted into oestradiol (E_2) which induces cell proliferation. It has already been shown that, in the absence of T, MCF-7aro cells do not grow (106). Androstenedione was used to measure aromatase inhibition as it binds to

aromatase with higher affinity than T, although T induces proliferation at a faster rate and was thus used in all other assays with MCF-7aro cells. E_2 at 1 nM, the aromatase product, was added in some assays in order to determine whether or not the effects of the cannabinoids were dependent on aromatase inhibition (106).

A non-tumoural human foreskin fibroblast cell line (HFF-1) was used in order to test the cytotoxicity of each cannabinoid. The endocannabinoid system has already been characterised in these cells by Fonseca *et al*. (107), making HFF-1 an ideal cell line to determine the effects of cannabinoids on non-cancerous cells. HFF-1 cells were cultured in Dulbecco's Modified Eagle Medium (DMEM), with 10% heat-inactivated FBS, 1 mmol/L sodium pyruvate and 1% penicillin-streptomycin-amphotericin B. Assays were carried out using the same medium.

LTEDaro cells, a long-term oestrogen-deprived ER^+ breast cancer cell line, were derived from prolonged exposure of parental MCF-7aro cells in steroid-depleted medium, as previously described (108). LTEDaro cells are considered the best *in vitro* cell model to study acquired resistance to AIs, as they mimic the resistance to all the AIs used in the clinic (66, 108). LTEDaro cells were cultured in an oestrogen-free MEM without phenol-red, containing Earle's salts, 10% pre-treated CFBS, 1 mmol/L sodium pyruvate, 2 mmol/L L-glutamine, 1% penicillin-streptomycin-amphotericin and 100 µg/mL Geneticin. Assays were carried out using the same medium.

After cells had reached 80% confluency in culture flasks, they were washed with PBS and 0.25% trypsin was added in order to detach cells. Trypsin solution was prepared using 10% trypsin at 2.5%, 10% EDTA at 10 mM and 80% PBS. After two to three minutes of incubation with trypsin solution, medium was added in order to inactivate the trypsin. This enzyme allows adherent cells to detach from culture flasks or wells. After trypsinisation, cells were collected, centrifuged (300 *x* g for 5 minutes at 4ºC) and resuspended in 10 mL of medium. To know the cellular density of the cell suspension, cells were diluted 1:1 in Trypan blue solution, before being counted in a Neubauer chamber. Cells were plated at the required cellular density for each assay, and after 24 hours of cell adhesion they were treated with the different cannabinoids. All cells were grown in medium and kept at 37°C in 5% CO_2, with medium and compounds being refreshed after three days.

2.4. Cell viability assays

Cell viability was measured using a 3-(4,5-dimethylthiazol-2-yl)-2,5-diphenyltetrazolium bromide (MTT) assay. MTT is converted into formazan by mitochondrial reductases present in viable cells, and is therefore a good indicator of the number of viable cells. Cells were plated in 96-well plates for one, two, three or six days and treated with different concentrations of **AEA**, **CBD** and **THC** at 1, 5, 10 or 20 µM. Cells without cannabinoid treatment were considered

as control. HFF-1 cells were plated at a cellular density of 7.5 x 10^3 cells/mL (6 days), MCF-7aro cells were plated at a cellular density of 2 x 10^4 cells/mL (1, 2 or 3 days) or 1 x 10^4 cells/mL (6 days) and LTEDaro cells were plated at a cellular density of 2.5 x 10^4 cells/mL (3 days) or 1 x 10^4 cells/mL (6 days). After each time of incubation, 20 µL MTT (5 mg/mL) was added to each well, and cells were incubated at 37°C and 5% CO_2 for a further two and a half hours. The formazan product, a purple-coloured salt, was then dissolved in 200 µL DMSO-isopropanol (3:1) solution. After 15 minutes of agitation, absorbance at 540 nm was measured by a Biotek Synergy HTX Multi-Mode Microplate Reader (Biotek Instruments, Vermont, USA). The absorbance value is proportional to the number of viable cells and was therefore expressed as a percentage when compared with the control group (100%).

This type of assay was also performed in order to understand if the anti-proliferative effects induced by these cannabinoids on MCF-7aro cells are dependent on aromatase. In order to do this, E_2 at 1 nM was used on MCF-7aro cells instead of T. Since E_2 is the product synthesised from T by the aromatase enzyme, replacing it with E_2 indicates if the treated cells rely on aromatase in order to proliferate.

We also aimed to determine whether the effects on cell viability were dependent on cannabinoid receptors or the vanilloid receptor. In order to do this, before the compounds were added, MCF-7aro cells stimulated with T (1 nM) were incubated for 30 minutes with an antagonist for either of the two cannabinoid receptors: AM281 at 1 µM (CB_1 receptor) and AM630 at 1 µM (CB_2 receptor), or for the vanilloid receptor: CAPS at 100 nM (TRPV1 receptor). Cells treated only with antagonists were considered as control.

In order to test whether or not the effects of the cannabinoids on MCF-7aro cell viability are dependent on the ER, **ICI**, a SERD that causes degradation of the ER, in particular ERα, was used. Cells stimulated with T (1 nM) were treated with **AEA**, **CBD** and **THC** at 1, 5, and 10 µM in combination with **ICI** at 100 nM. Cells treated only with **ICI** were considered as control.

3-Methyladenine (3-MA), an inhibitor of autophagy, was used at 1 mM in combination with **CBD** at 1, 5, 10 and 20 µM in MCF-7aro cells stimulated with T (1 nM). As this compound prevents cells from undergoing autophagy (66, 105), it was used to determine if the mechanism of cell death induced by **CBD** on MCF-7aro cells was linked to autophagy. Cells treated only with 3-MA were considered as control.

A lactate dehydrogenase (LDH) release assay was also carried out, in order to test the toxicity of the compounds. LDH is an enzyme that is present in the cytosol, and is released into the extracellular space upon membrane rupturing. High levels of LDH release are generally linked to necrotic processes (109). This enzyme converts a tetrazolium salt into formazan, which can then be measured spectrophotometrically. LDH release was measured using a CytoTox 96 nonradioactive cytotoxicity assay kit, according to the manufacturer's protocol (Promega Corporation, Madison, WI, USA). Cells plated in a 96-well plate were

treated with **AEA**, **CBD** and **THC** at 1, 5, 10 or 20 µM and incubated for three days at 37°C and 5% CO_2. Cells without cannabinoid treatment were considered as control. After incubation, 20 µL culture medium was removed from each well, transferred to a separate 96-well plate, and the equivalent amount of LDH substrate solution was added. After incubating for 30 minutes at room temperature, 20 µL stop solution was added. Absorbance was then read at 450 nm in a Biotek Synergy HTX Multi-Mode Microplate Reader (Biotek Instruments, Vermont, USA). Results were expressed as an absolute value of the control group (value of 1).

2.5. In-cell aromatase assay

Aromatase inhibitory activity for each cannabinoid in MCF-7aro cells was determined using the method of Thompson and Siiteri (110) and Zhou, Pompon and Chen (104), with modifications (106). Cells were cultured in 24-well plates at a cellular density of 1 x 10^6 cells/mL in MEM with phenol-red. After 80% of confluency, cells were incubated with 50 nM [1β-^{3}H]-androstenedione, 500 nM progesterone and 10 µM of each cannabinoid in a serum-free MEM with phenol-red. **Exe** at 10 µM was used as a reference AI. [1β-^{3}H]-androstenedione was added as a substrate for aromatase, and was converted into oestrone + tritiated water (^3H_2O). The latter was then quantified using a scintillation counter, as the tritiated water released from [1β-^{3}H]-androstenedione during the aromatisation reaction, can be used as an index of oestrogen formation. Progesterone was added in order to suppress 5α-reductase activity, an enzyme that also uses androgens as substrate (106). After one hour at 37°C and 5% CO_2, the aromatase reaction was terminated using 20% trichloroacetic acid (TCA), and samples were transferred to charcoal/dextran-containing microcentrifuge tubes, to remove any steroid molecules. Samples were then homogenised and incubated at room temperature during one hour. After incubation, samples were centrifuged (14,000 x g for 10 minutes) and the supernatant was transferred to new microcentrifuge tubes containing fresh charcoal/dextran. The contents were then homogenised and incubated for 10 minutes at room temperature. After this incubation, the samples were centrifuged once more, and 300 µL of the supernatant was transferred to a separate scintillation tube, containing 3 mL liquid scintillation cocktail. Levels of tritiated water were measured using a scintillation counter (LS6500, Beckman Instruments, CA, USA).

After measuring the levels of tritiated water in each sample, it was important to normalise the results, so that they could be compared with the control (cells without cannabinoids or **Exe** treatment). A Bradford assay was performed to determine the protein content of each sample, and the value for aromatase activity was normalised to the protein content, in order to calculate the % of aromatase inhibitory activity for each cannabinoid in comparison to control. To

determine the protein content, cells were lysed with 1 mL of 0.5 M NaOH, overnight at room temperature under constant agitation, and a Bradford assay was performed using the Bio-Rad Protein Assay.

2.6. Cell cycle analysis

In order to investigate if cannabinoids treatment impairs MCF-7aro cell cycle progression, the effects of each cannabinoid on DNA content was analysed by flow cytometry. Cells were plated in a 6-well plate at a cellular density of 7 x 10^5 cells/mL and treated with T (1 nM) plus each cannabinoid at 5 or 10 µM, during three days. Cells treated only with T were considered as control. After incubation, cells were washed with PBS, trypsinised and transferred to 15 mL Falcon tubes, to be centrifuged at 300 x g, at 4°C for 5 minutes. The supernatant was then removed, and the cells were washed and resuspended in PBS. Cells were further centrifuged, and the pellet was resuspended in 500 µL PBS, before adding 4.5 mL cold 70% ethanol in order to fix the cells. Contents were once more homogenised, and samples were stored at 4°C for a minimum of 48 hours.

After fixation with ethanol, samples were centrifuged, the supernatant was removed, and the cells were washed at least two times and resuspended in 500 µL of a PBS staining solution containing 200 µg/mL RNAase A, 0.1% Triton X-100 and 5 µg/mL propidium iodide (PI). RNAase is important to ensure that only DNA is analysed, Triton permealises the membrane to allow the PI to cross, and the PI binds to nucleic acids, and therefore stains the DNA.

DNA content was further analysed using a BD Accuri™ C6 cytometer with BD Accuri™ C6 analysis software® (San Jose, CA, USA). Detectors for the three fluorescence channels (FL-1, FL-2, and FL-3), as well as for the forward and side light scatter (FSC and SSC, respectively), were all set on a linear scale. Cell debris, doublets and aggregates were gated out using a two-parameter plot of FL-2-Area to FL-2-Width of PI fluorescence. Data were analysed using BD Accuri™ C6 analysis software®, and the anti-proliferative effects of each cannabinoid were presented in terms of the percentage of cells in the G_0/G_1, S, and G_2/M phases of the cell cycle.

2.7. Morphological studies

MCF-7aro cells were cultured in a 24-well plate containing coverslips at a cellular density of 2 x 10^5 cells/mL. Giemsa and Hoechst staining were carried out in order to measure any changes in cell morphology after treatment with cannabinoids. Giemsa is a dye made up of methylene-blue, eosin and Azure B, components that allow for the staining of the cytoplasm and nucleus of cells. Hoechst stains the nucleus and allows for the identification of any changes in nuclear morphology. Before being fixed, MCF-7aro cells stimulated with T (1 nM)

were treated with each cannabinoid at 5 or 10 µM, during three days. Cells treated only with T were considered as control. For Giemsa staining, cells were washed with PBS, then fixed with 500 µL methanol at 4°C for 30 minutes. Cells were rewashed twice with PBS, before being incubated in 600 µL of a Giemsa solution (1:10) for 30 minutes, at room temperature. Cells were then washed twice with tap water, left to dry and mounted using DPX mounting medium, before being observed under a bright field microscope (Eclipse E400, Nikon, Japan) equipped with image analysis software Nikon NIS Elements v4.0 image software® (Nikon Instruments, Melville, NY, USA).

For Hoechst staining, cells were washed with PBS, then fixed with 500 µL 4% paraformaldehyde at 4°C for 20 minutes. Cells were rewashed twice with PBS, then incubated in 600 µL Hoechst 33258 (0.5 µg/mL in PBS) for 20 minutes at room temperature. Cells were then washed with PBS, left to dry and mounted with fluoroshield mounting medium, before being observed under a fluorescence microscope (Eclipse E400, Nikon, Japan) equipped with excitation filter with maximum transmission at 360/400 nm. Hoechst-stained images were then processed by Nikon NIS Elements v4.0 image software® (Nikon Instruments, Melville, NY, USA).

2.8. Intracellular reactive oxygen species (ROS) measurement

Intracellular ROS levels were measured in order to determine whether cannabinoid treatment could affect the production of ROS in MCF-7aro cells. Cells were cultured in black 96-well plates at a cellular density of 2×10^4 cells/mL, and were treated with each cannabinoid at 5 and 10 µM, for three days. MCF-7aro cells treated with H_2O_2 (200 µM) were used as a positive control and cells treated only with T were considered as control.

$DCFH_2$-DA with a final concentration of 50 µM was used as a probe, and the plate was covered and incubated for one hour at 37°C and 5% CO_2. This probe is non-fluorescent, but can cross the cell membrane where it deacetylates into $DCFH_2$. Inside the cell, $DCFH_2$ reacts with ROS to produce DCF, which gives a fluorescent signal (111). A larger increase in ROS will therefore cause a higher fluorescence signal. After incubation with the probe during a set time (30 minutes, one hour, two hours, six hours, one day, two days or three days), the plate was read in a Biotek Synergy HTX Multi-Mode Microplate Reader (Biotek Instruments, Vermont, USA).

2.9. Analysis of apoptosis

In order to explore the ability of each cannabinoid to induce apoptosis, changes in mitochondrial transmembrane potential ($\Delta\psi_m$) and activation of caspases -9 and -7 were measured. MCF-7aro cells were cultured in black and white 96-well plates for $\Delta\psi_m$ and

caspase activity assays, respectively, at a cellular density of 2 x 10^4 cells/mL. Cells were treated with each cannabinoid at 1, 5 and 10 μM for two and three days for $\Delta\psi_m$ assays, and for one, two and three days for caspase activity assays. Cells treated only with T were considered as control. MCF-7aro cells stimulated with T and treated with carbonyl cyanide 3-chlorophenylhydrazone (CCCP) and staurosporine (STS), both at 10 μM, were used as positive controls for $\Delta\psi_m$ and caspase activity assays, respectively. Z-VAD-FMK (50 μM), a pan-caspase inhibitor, was used as a negative control for Caspase-Glo® 3/7 assays.

For $\Delta\psi_m$ assays, after treatment with each cannabinoid, medium was removed and the probe 3,3′-dihexyloxacarbocyanine iodide ($DiOC_6(3)$) was added. $DiOC_6(3)$ was diluted in sucrose buffer (100 mM) to a final concentration of 50 nM. When used at low concentrations, this probe stains the mitochondria inside viable cells and produces a fluorescence signal. Depolarisation of the mitochondrial membrane, which is associated with cells undergoing apoptosis, causes a reduction in the accumulation of $DiOC_6(3)$, resulting in a weaker fluorescence signal. A decrease in ΔΨm is a result of a lower accumulation of $DiOC_6(3)$ (112). After adding the probe, the plate was covered with foil and left to incubate, for 30 minutes at 37 °C and 5% CO_2. After incubation, the probe was removed and replaced with sucrose buffer (100 mM), before being read in a Biotek Synergy HTX Multi-Mode Microplate Reader (Biotek Instruments, Vermont, USA).

Caspase activity was measured by a luminescence assay using Caspase-Glo® 3/7 and Caspase-Glo® 9 assay kits, according to the manufacturer's instructions (Promega Corporation, Madison, USA). This kit contains a luminogenic substrate that, once cleaved by caspases, causes a luminescent signal, with luminescence therefore being proportional to the amount of active caspase present. Activation of caspases occurs during the process of apoptosis, so a higher signal is associated with a larger number of cells undergoing apoptosis. After treatment with each cannabinoid, 20 μL substrate solution was added to each well. The plate was covered with foil and left on agitation for 30 minutes at room temperature. The plate was then read in a Biotek Synergy HTX Multi-Mode Microplate Reader (Biotek Instruments, Vermont, USA). As MCF-7aro cells do not contain caspase-3, the Caspase-Glo® 3/7 kit only evaluated the activity of caspase-7 in these assays (105).

2.10. Detection of acid vesicular organelles (AVOs)

During autophagy, the autophagosomes fuse with lysosomes, thus forming autolysosomes which, along with autophagosomes, are classed as acid vesicular organelles (AVOs). The production of AVOs is therefore a typical biochemical feature of cells undergoing autophagy (105, 113). In order to determine and observe their presence inside MCF-7aro cells, acridine orange (AO) staining was used, and the cells were observed under a fluorescence microscope. AO is a fluorescent dye that is cell permeable and accumulates inside low-pH

vesicles. Once protonated, it emits a yellow/orange/red fluorescence, and is therefore a good indicator for acidic organelles within a cell, which are typical features of autophagy (105, 113, 114).

MCF-7aro cells were cultured at a cellular density of 2 x 10^5 cells/mL, in 24-well plates containing coverslips. Cells were then treated with **CBD** for one, two or three days at 10 µM with and without 3-MA at 1 mM. **Exe** was used as a reference AI since it is known to induce autophagy in MCF-7aro cells (105) and was administered at 10 µM for 6 days. Cells treated only with T were used at control. Cells were then stained with AO at 0.1 µg/mL for 15 minutes, at 37°C in 5% CO_2. Following incubation, the medium containing AO was removed, and the cells were washed with PBS. PBS was removed, and the cells were mounted onto microscope slides using PBS. The slides were then observed using a fluorescence microscope (Eclipse E400, Nikon, Japan) equipped with Nikon NIS Elements v4.0 imaging software® (Nikon Instruments, Melville, NY, USA).

2.11. Western-blot analysis

Western-blots were carried out in order to evaluate the protein expression of target proteins. The expression of cannabinoid receptors (CB_1 and CB_2), as well as the transient receptor potential cation channel subfamily V member 1 (TRPV1) was determined in order to establish whether or not these receptors are present in MCF-7aro and LTEDaro cells. Changes in the expression of aromatase, ERα, ERβ, cleaved PARP and LC3 in MCF-7aro cells after treatment with cannabinoids were also analysed.

MCF-7aro cells were cultured in 6-well plates at a cellular density of 7 x 10^5 cells/mL, and treated with T (1 nM) plus each cannabinoid at 10 µM during three days for the study of ERα, ERβ and cleaved PARP. To study LC3 expression, cells were treated with cannabinoids during one day, and for the study of aromatase they were treated for just eight hours. Cells treated only with T were used as a control. For aromatase assays, **Exe** at 10 µM was used as a positive control, as it is known to induce aromatase degradation (115). For LC3 assays, 3-MA was added at 1 mM with and without **CBD**, during one day. Samples of MCF-7aro and LTEDaro cells that had not received cannabinoid treatment were used in order to determine CB_1, CB_2 and TRPV1 expression. After each different treatment, medium was removed and cells were washed with PBS. PBS was then removed and the cells were lysed using TNTE buffer (50 mM Tris pH 7.4, 150 mM NaCl, 1 mM EDTA and 0.5% Triton X-100) with a cocktail of protease inhibitors at a ratio of 1:100. In general, samples were centrifuged at 14 000 x g for 5 minutes at 4°C, except in the case of LC3 assays, where cells were centrifuged at 10 000 x g. The supernatants were transferred to new Eppendorfs, and the samples were stored at -80 °C until use. The pellets containing cell membranes and organelles were discarded. Protein concentration in each sample was determined by carrying out a Bradford assay.

Before electrophoresis, samples were diluted in sample buffer containing bromophenol blue, and boiled at 100 °C, or at 65°C in the case of LC3 assays, during three minutes in order to denature the proteins. A 50 µg protein sample was loaded per well into a 10% polyacrylamide gel before being transferred to a nitrocellulose membrane using a transfer buffer solution (48 mM Tris-Base, 39 mM glycine and 20% methanol at pH 9.2). Due to its large molecular weight, an 8% polyacrylamide gel was used for PARP assays, while in the case of LC3 assays a 4 – 20% gradient gel was used and 100 µg of protein sample was added. After the transfer, membranes were blocked in 5% milk in TBS with 0.1% TWEEN for one hour, and incubated with a primary antibody overnight at 4°C. Membranes were then washed twice with TBS with 0.1% TWEEN, and incubated for one hour, at room temperature, with the secondary antibody. See Table 1 for a list of all primary and secondary antibodies for each protein. Primary and secondary antibodies were prepared in blocking solution.

After incubation with secondary antibody, membranes were washed twice with TBS with 0.1% TWEEN, then twice with TBS. WesternBright ECL chemiluminescent substrate was added to the membranes, and they were visualised using a Chemidoc Touch Imaging System (BioRad Laboratories, Melville, NY, USA). Membranes were then stripped using stripping solution (200 mM Glycine, 3.5 Mm Sodium Dodecyl Sulphate, 1% TWEEN, pH 2.2), washed twice with PBS and further two times with TBS with 0.1% TWEEN. The membranes were the incubated overnight with the primary antibody for β-tubulin. β-tubulin was used as a loading control, as it is present in all cells and therefore allows the normalisation of results for comparison between samples.

Table 1: Description of the antibodies and conditions used to study the target proteins.

Protein	Primary antibody	Secondary antibody	Company
CB_1	Goat polyclonal 1:100	Mouse anti-goat 1:2000	Santa Cruz
CB_2	Rabbit polyclonal 1:100	Goat anti-rabbit 1:2000	Santa Cruz
TRPV1	Goat polyclonal 1:100	Mouse anti-goat 1:2000	Santa Cruz
Aromatase	Mouse monoclonal 1:200	Goat anti-mouse 1:2000	Santa Cruz
c-PARP	Mouse monoclonal 1:100	Goat anti-mouse 1:2000	Santa Cruz
ERα	Rabbit polyclonal 1:200	Goat anti-rabbit 1:2000	Santa Cruz
ERβ	Mouse monoclonal 1:200	Goat anti-mouse 1:2000	Invitrogen
LC3	Rabbit polyclonal 1:200	Goat anti-rabbit 1:2000	Cell Signalling
β-tubulin	Mouse polyclonal 1:500	Goat anti-mouse 1:4000	Santa Cruz

2.12. Statistical analysis

Statistical analysis of data was performed using GraphPad Prism 6® software and by the analysis of variance (ANOVA) using Bonferroni and Tukey post-hoc tests for multiple comparisons (Two-way and One-way ANOVA, respectively). Values of $p < 0.05$ were considered as statistically significant. Data presented are expressed as the mean ± SEM. All the assays were performed in triplicate in at least three independent experiments.

3. Results

3.1. Effects of cannabinoids on viability of HFF-1 cells

For an anticancer drug to be successfully used in the clinic, it should not cause any effect on non-cancerous cells. To address this issue and study the effects of each cannabinoid, an MTT assay was carried out on a non-tumour human foreskin fibroblastic cell line (HFF-1). Cells were treated with each cannabinoid (1-20 µM) during six days, and cells without cannabinoid treatment were used as a control (100% cell viability). Results show that none of the three cannabinoids tested caused a significant increase or decrease in HFF-1 cell viability (Figure 14), even at high concentrations (20 µM).

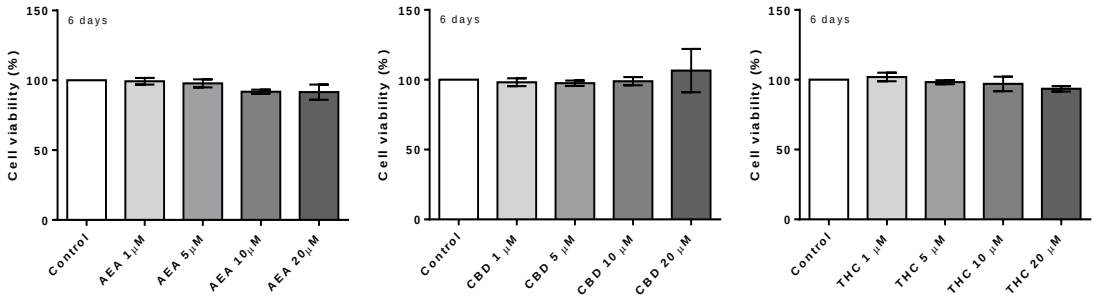

Figure 14: Effects of each cannabinoid on viability of non-tumour HFF-1 cells. Cells were treated with **AEA** (A), **CBD** (B), and **THC** (C) during six days. Cells receiving no cannabinoid treatment were used as control (100% cell viability). Results are presented as a mean ± SEM of at least three separate experiments, all performed in triplicate.

3.2. Cannabinoid receptor expression in ER^+ breast cancer cells

Cannabinoids can act on cells via mechanisms dependent and independent on cannabinoid receptors (89, 95, 107). The expression of cannabinoid receptors CB_1 and CB_2, as well as the vanilloid receptor TRPV1, was determined by Western-blot, in order to investigate whether the study of cannabinoids would be suitable in MCF-7aro and LTEDaro cell lines. As presented in Figure 15, the results confirm that both CB_1 and CB_2 receptors are present in both cell lines. However, the TRPV1 receptor was not detected under our conditions. Thus, further studies must be performed to confirm this result.

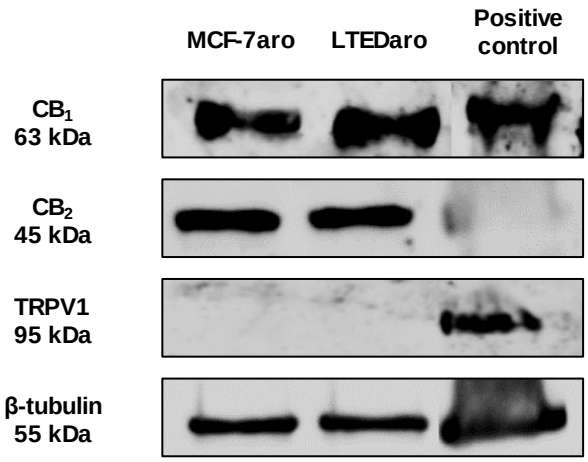

Figure 15: CB_1, CB_2 and TRPV1 receptor expression in MCF-7aro and LTEDaro cells. Cells were cultured during three days, lysed and the expression of each receptor was evaluated by Western-blot. β-tubulin was used as a loading control, and an extract of rat brain tissue was used as a positive control. Western-blot is a representative of one example of at least three different experiments.

3.3. Effects on viability of MCF-7aro cells

To investigate the effects of each cannabinoid on MCF-7aro cell viability, an MTT assay was carried out. Cells were treated with different concentrations of each cannabinoid (1 - 20 µM) during two, three and six days. Testosterone (T, 1 nM), which is converted into oestradiol (E_2) by aromatase, was used as a substrate in order to stimulate cell proliferation, and to better mimic the ER^+ breast cancer tumour microenvironment (106). Cells treated only with T were used as a control (100% cell viability). As **CBD** caused a pronounced decrease in cell viability, assays were also carried out over one day for this particular cannabinoid.

As presented in Figure 16, all cannabinoids reduced significantly ($p < 0.05$; $p < 0.01$; $p < 0.001$) MCF-7aro cell viability in a dose-dependent manner, whilst **CBD** and **THC** also reduced in a time-dependent manner. **CBD** caused by far the largest reduction in cell viability, with only 19.8% of cells remaining viable after three days of treatment at 20 µM ($p < 0.001$).

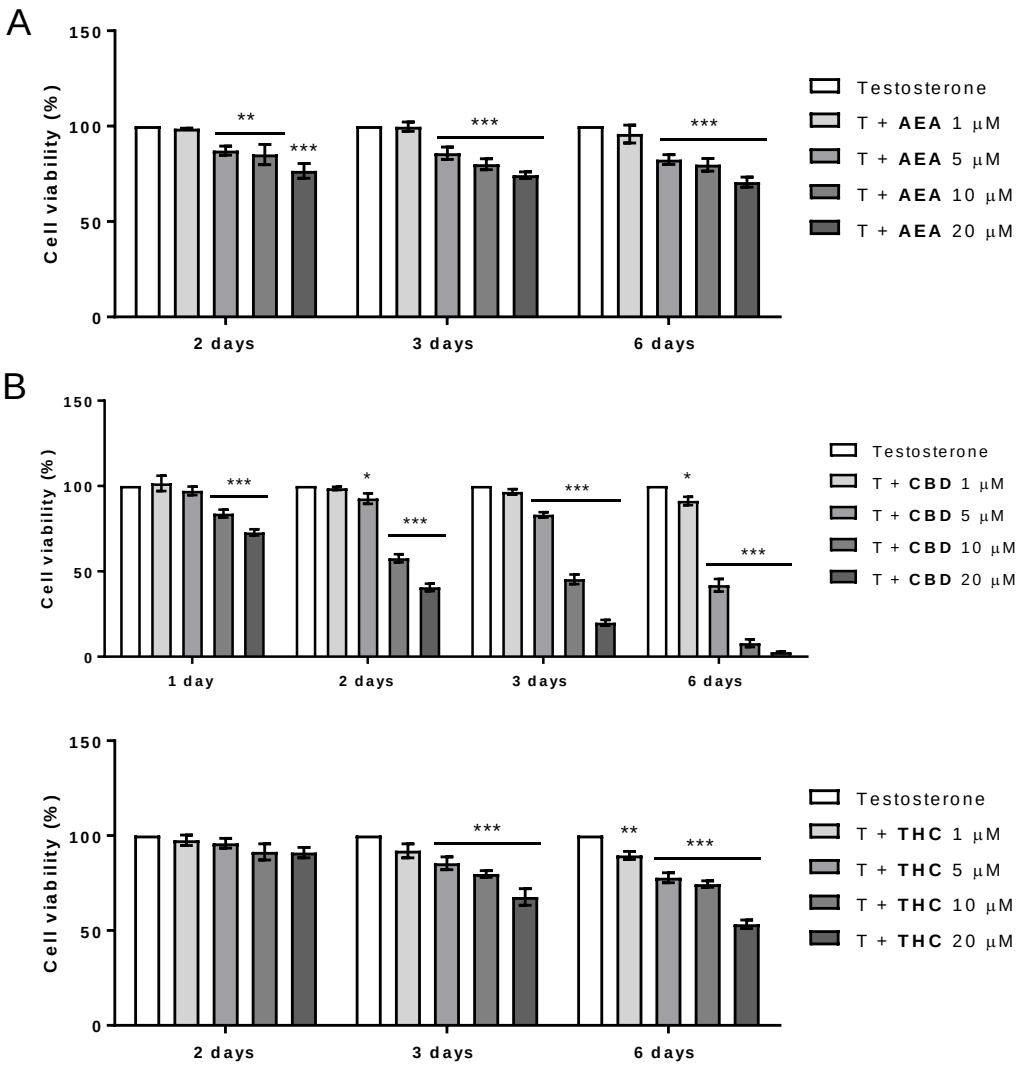

Figure 16: Effects of each cannabinoid on MCF-7aro cell viability. Cells stimulated with T (1 nM) were treated with different concentrations (1, 5, 10 and 20 µM) of **AEA** (A), **CBD** (B) and **THC** (C), during two, three and six days, as well as one day for CBD. Cells treated only with T were used as control (100% of cell viability). Results are expressed as a mean ± SEM of at least three independent experiments, each performed in triplicate. Significant differences between cannabinoid-treated cells and the control are shown by * ($p < 0.05$), ** ($p < 0.01$) and *** ($p < 0.001$).

In order to evaluate the potential cytotoxicity of each cannabinoid in MCF-7aro cells, LDH-release assays were also performed. Levels of released LDH enzyme were measured in cells after three days of treatment with each cannabinoid plus T (1 nM), at the same concentrations as for the MTT assay (1, 5, 10 and 20 µM). Cells treated only with T were used as a control. Results demonstrate that all the cannabinoids caused no LDH release at all concentrations (Figure 17), suggesting that, in our conditions, the cannabinoids did not affect MCF-7aro cell membrane integrity, and consequently, are not cytotoxic.

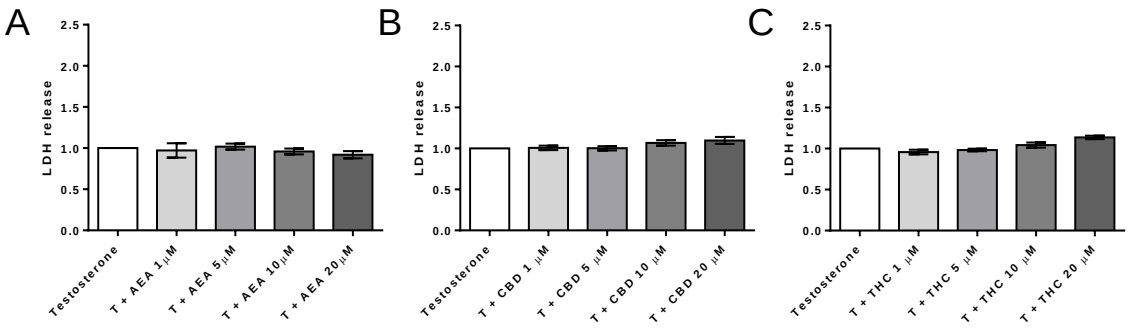

Figure 17: Effects of each cannabinoid on LDH release in MCF-7aro cells. Cells stimulated with T (1 nM) were treated with **AEA** (A), **CBD** (B) and **THC** (C) at 1, 5, 10 and 20 µM, during three days. Cells treated only with T were used as control (1 unit of LDH release). Results are presented as a mean ± SEM of at least three independent experiments, all performed in triplicate.

3.4. Cell viability effects in MCF-7aro cells with cannabinoid receptor antagonists

To determine whether or not the effects induced by cannabinoids on MCF-7aro cells may be dependent on cannabinoid or vanilloid receptor-binding, an MTT assay was carried out, using a combination of each cannabinoid with the different cannabinoid or vanilloid receptor antagonists. Cells were incubated for half an hour with antagonists for the CB_1 and CB_2 receptors (AM281 and AM630, respectively, both at 1 µM), and for the TVPV1 receptor (CAPS at 100 nM), before being subject to treatment with **AEA**, **CBD** and **THC** at 5 and 10 µM. It should be noted that, at the concentrations used in these assays, the cannabinoid and vanilloid receptor antagonists *per se* caused no effects on MCF-7aro cell viability. As previously mentioned, MCF-7aro cells do not appear to express TRPV1, however the results from the Western-blot only suggest this and do not confirm it, explaining why the involvement of this receptor was also explored.

As presented in Figure 18, significant differences were observed between **AEA** and the combination of **AEA** with AM630 ($p < 0.01$, $p < 0.001$ for **AEA** at 5 and 10 µM, respectively), suggesting that the effects induced by this cannabinoid on cells may be dependent on CB_2 receptor. Curiously, none of the antagonists reverted the reduction in cell viability induced by **CBD**, although the combination of AM281 with **THC** at 10 µM ($p < 0.01$), and AM630 with **THC** at 5 and 10 µM ($p < 0.001$ and $p < 0.01$, respectively), partially prevented the reduction in cell viability induced by **THC** (Figure 18). These results suggest that the effects induced by **THC** on cells may be dependent on CB_1 and CB_2 receptors. In addition, and as expected, none of the cannabinoids appeared to cause an effect dependent on TRPV1 receptor, suggesting that this receptor may not be present in this cell model.

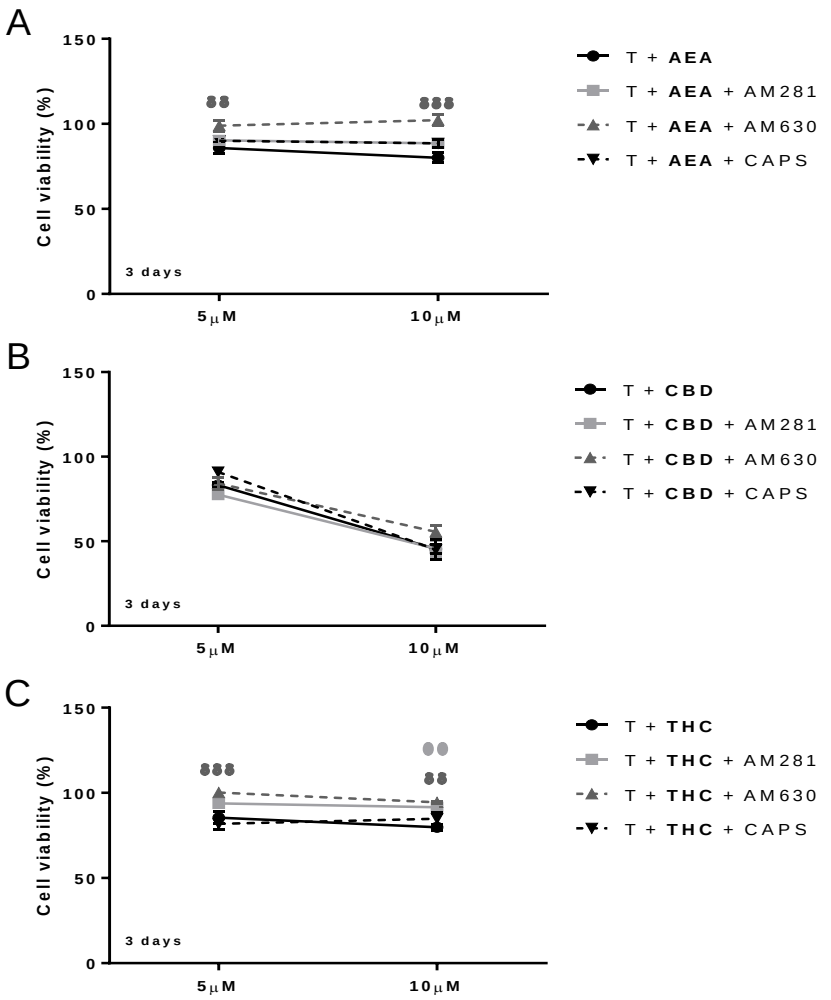

Figure 18: Effects on viability of MCF-7aro cells treated with cannabinoids in combination with cannabinoid and vanilloid receptor antagonists. Cells stimulated with T (1 nM) were treated with 5 and 10 µM **AEA** (A), **CBD** (B) and **THC** (C), and with each cannabinoid or vanilloid receptor antagonist (AM281 at 1µM, AM630 at 1µM and CAPS at 100 nM). Cells receiving no cannabinoid treatment were used as control (100% cell viability). Results for cannabinoid + antagonist-treated cells are expressed as a percentage of the cells that were treated only with antagonists. Results are the mean ± SEM of at least three independent experiments, each performed in triplicate. Significant differences between cannabinoid-treated cells and cells treated with cannabinoid + AM281 were indicated by ɵɵ ($p < 0.01$), whereas significant differences between cannabinoid-treated cells and cells treated with cannabinoid + AM630 were indicated by δδ ($p < 0.01$) or δ δ δ ($p < 0.001$).

3.5. The involvement of aromatase in the effects induced by cannabinoids on MCF-7aro cells

To investigate if the effects induced by each cannabinoid on MCF-7aro cells were dependent on aromatase inhibition, an MTT assay using E_2, the product of aromatase, was performed. Aromatase converts T into E_2, which is necessary for ER^+ breast cancer cell proliferation, thus, the inhibition of this enzyme can contribute to ER^+ breast cancer cell death. Cells were stimulated with E_2 (1 nM) and treated with **AEA**, **CBD** and **THC** at 1, 5 and 10 µM,

for three and six days. Results were then compared with those of the cells treated with cannabinoid plus T (1 nM). As shown in Figure 19A, the effect of **AEA** on MCF-7aro cell viability was not affected when T was substituted by E_2, suggesting an effect independent of aromatase. After 6 days of treatment, **CBD** at 5 and 10 µM showed significant ($p < 0.001$) differences between T- and E_2-treatments, with the reduction in cell viability being more pronounced in the presence of T than E_2 (Figure 19B), thus suggesting that this is an aromatase-dependent effect. In the case of **THC**, results demonstrate a small yet significant ($p < 0.05$) difference after six days of treatment at 1 µM (Figure 19C). Nevertheless, and in general, the behaviour of cells treated with **THC** plus T or E_2 is similar, suggesting that the mechanism of action of this cannabinoid is independent of aromatase inhibition.

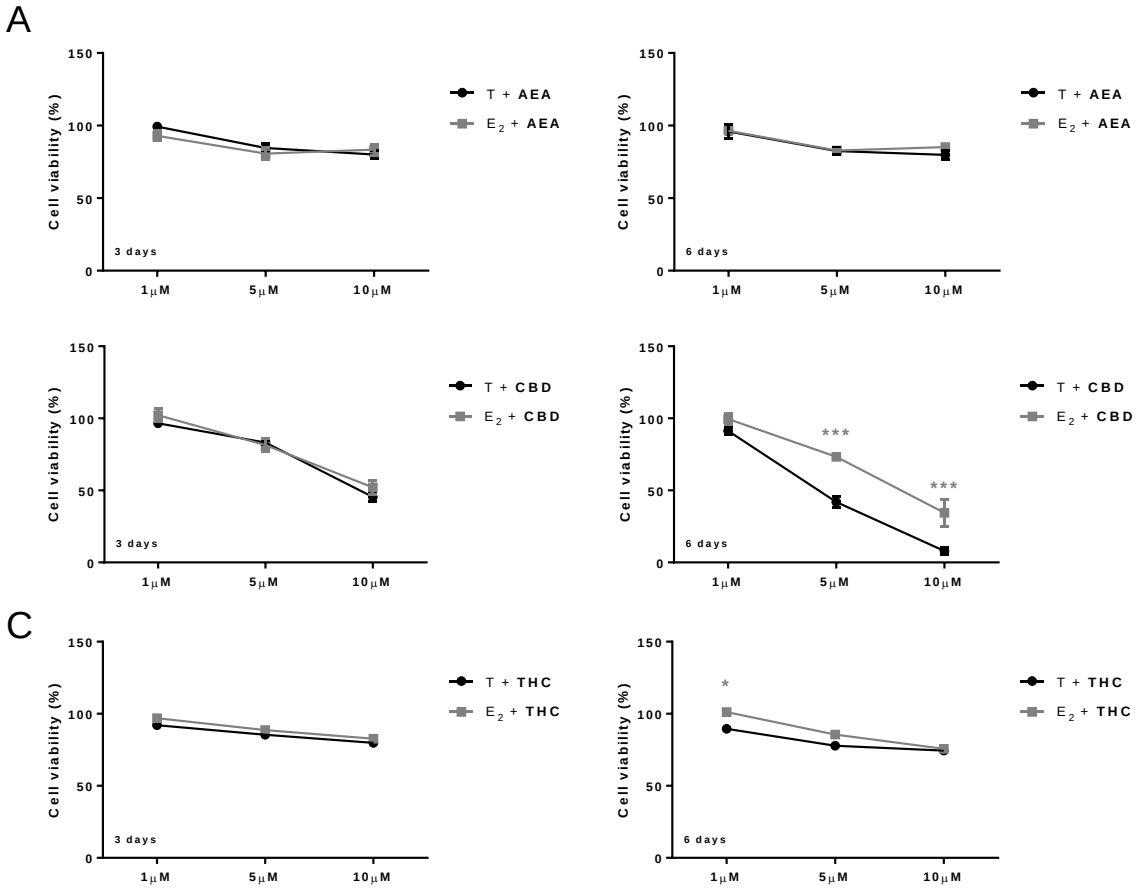

Figure 19: Effects of cannabinoids on MCF-7aro cell viability treated with E_2 or T. Cells were treated with **AEA** (A), **CBD** (B) and **THC** (C) at 1, 5 and 10 µM, during three and six days (left and right, respectively). Cells were also treated with either T as a substrate for aromatase, or E_2 as a product of the aromatase reaction, in order to determine whether or not the effects of each cannabinoid on these cells were due to aromatase inhibition. Cells receiving no cannabinoid treatment were used as control (100% cell viability). Results are the mean ± SEM of at least three independent experiments, each performed in triplicated. Significant differences between T-treated and E_2-treated cells are shown by * ($p < 0.05$) and *** ($p < 0.001$).

As aromatase seems to be involved in the effects induced by cannabinoids on MCF-7aro cells, the ability of each cannabinoid to inhibit the aromatase enzyme was further explored. Cells were incubated with radioactively-labelled androstenedione, and treated with each cannabinoid at 10 µM during one hour. The amount of tritiated water as a product of the aromatase reaction was then measured. Exemestane (**Exe**) was used as a reference AI, and gave an inhibition of 99.6%, as previously described (106, 116). Of the three cannabinoids tested, **AEA** and **CBD** presented considerable aromatase inhibition, 64.5% and 73.5%, respectively, whereas **THC** presented low anti-aromatase activity (13.9%) (Figure 20).

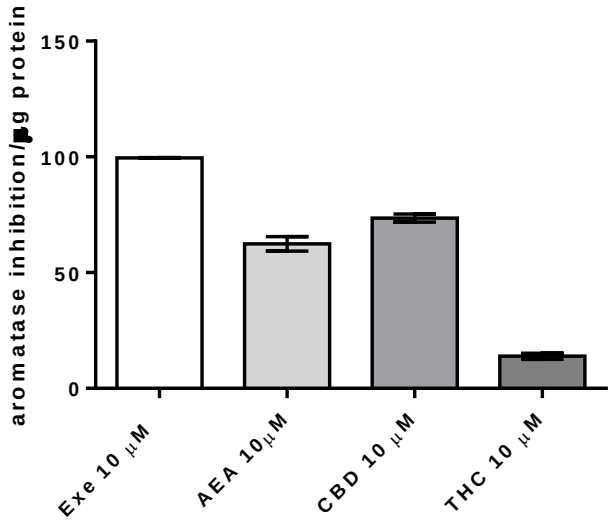

Figure 20: Anti-Aromatase activity of each cannabinoid in MCF-7aro cells. MCF-7aro cells were treated with **AEA**, **CBD** and **THC** at 10 µM, during one hour. **Exe** at 10 µM was used as a reference AI. Data are presented as a percentage/µg protein of aromatase inhibition and was obtained by comparing with the aromatase activity of a control group of cells that received no cannabinoid treatment. All assays were performed in triplicate and correspond to at least three independent experiments.

As it was observed that cannabinoids present anti-aromatase activity, and that **CBD** has an aromatase-dependent effect on cells, as well as the fact that **Exe** is known to induce aromatase degradation (115), the effects of each cannabinoid on the expression of aromatase were investigated by Western-Blot (Figure 21). MCF-7aro cells were treated with each cannabinoid at 10 µM during 8 hours, whilst **Exe** (10 µM) was used as a reference AI. Of the three cannabinoids tested, **CBD** caused the largest decrease in aromatase expression levels (54%; $p < 0.001$), followed by **THC** (29%) and **AEA** (21%) ($p < 0.01$) (Figure 21). As expected, **Exe** caused a significant decrease (61%; $p < 0.001$) in aromatase levels.

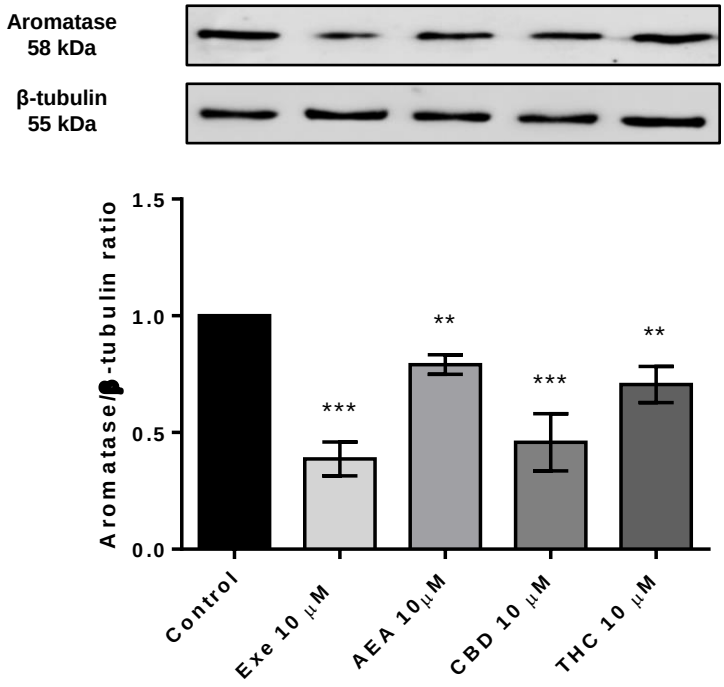

Figure 21: Aromatase expression levels in MCF-7aro cells treated with each cannabinoid. Cells were treated with **AEA**, **CBD** and **THC** at 10 µM for 8 hours. **Exe**, also at 10 µM, was used as a reference AI. Untreated cells were used as a control. β-tubulin was used as a loading control. Representative Western-blot of aromatase and β-tubulin, as well as densitometric analysis of aromatase expression levels after normalisation with β-tubulin levels, are shown. Western-blot is a representative of one example of at least three different experiments. Results are the mean ± SEM of at least three different experiments. Significant differences between the control and **Exe**- or cannabinoid-treated cells are shown by * ($p < 0.05$), ** ($p < 0.01$) and *** ($p < 0.001$).

3.6. The involvement of the oestrogen-receptor in the effects induced by cannabinoids in MCF-7aro cells

In order to determine whether the effects of each cannabinoid on MCF-7aro cell viability were due to a deregulation of oestrogen receptor (ER), an MTT assay was carried out, with the cells being treated with cannabinoids in combination with ICI 182 780 (**ICI**). **ICI** is a selective oestrogen receptor down-regulator (SERD) that binds irreversibly to the ER, destabilising it and leading to its degradation (117). For this reason, cells were incubated with **ICI** in combination with each cannabinoid, in order to see whether their effects on cell viability were dependent on ER. MCF-7aro cells stimulated with T (1 nM) were treated with each cannabinoid at 1, 5 and 10 µM plus **ICI** at 100 nM, during 6 days. Results were then compared with those of the cells treated only with cannabinoids and T (1 nM). As presented in Figure 22, **AEA** and **THC** caused almost no effects on cell viability when added in combination with **ICI** (reduction in cell viability of 3% and 12% at 10 µM, respectively), with significant ($p < 0.01$) differences being observed between cells treated with **AEA** or **THC** with and without **ICI**. On

the contrary, **CBD**, when combined with **ICI**, still caused a large reduction in cell viability (reduction of 63% at 10 µM), albeit less than when added alone (92% at 10 µM). Moreover, significant ($p < 0.01$) differences between cells treated with **CBD** and with or without **ICI** were observed.

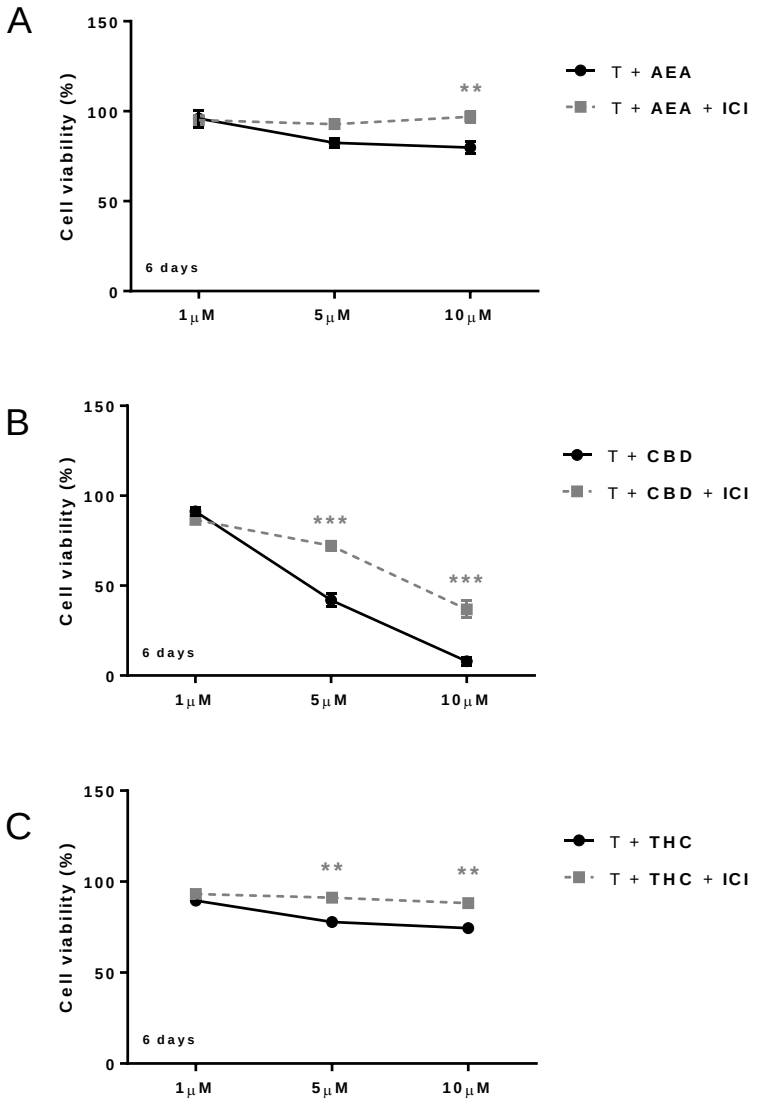

Figure 22: Effects of cannabinoids in combination with ICI on viability of MCF-7aro cells. Cells stimulated with T (1 nM) were treated with **AEA** (A), **CBD** (B) and **THC** (C) at 1, 5 and 10 µM and with **ICI** at 100 nM, during six days. Cells treated only with T and **ICI** were used as control (100% cell viability), and results were compared with those of previous assays under the same conditions but without **ICI**. Results are the mean ± SEM of at least three independent experiments, each performed in triplicate. Significant differences between cells treated with cannabinoid and with or without **ICI** are shown by ** ($p < 0.01$) and *** ($p < 0.001$).

As previous results suggested that the effects of cannabinoids on MCF-7aro cells may be dependent on the ER, their effects on the expression levels of ERα and ERβ were also

investigated, using a Western-blot analysis. It must be noted that, in ER^+ breast cancer cells, ERα is associated with cell survival, whereas ERβ is associated with cell death (36, 37). In this assay, cells were treated with each cannabinoid at 10 μM plus T for three days, and cells receiving no cannabinoid treatment were used as a control. As presented in Figure 23, **AEA**, **CBD** and **THC** significantly ($p < 0.001$) decreased the expression levels of ERα, by 39%, 37% and 42%, respectively. **AEA** and **CBD** also significantly ($p < 0.01$ and $p < 0.05$, respectively) increased the expression levels of ERβ, by 38% and 33%, respectively. **THC** did consistently increase the expression of ERβ (by an average of 9%), however the results were not significant, suggesting that **THC** caused no effect on ERβ expression levels.

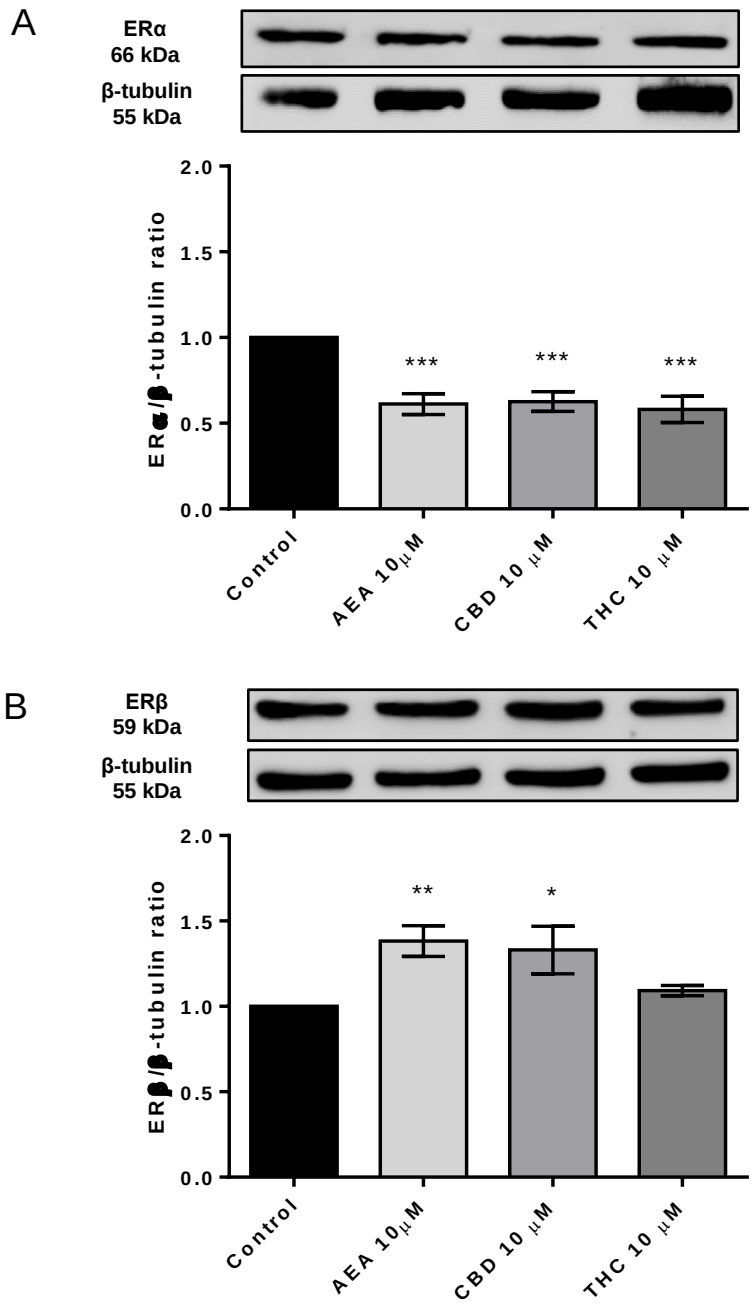

Figure 23: Western-blot analysis of ERα and ERβ expression. MCF-7aro cells stimulated with T (1 nM) were treated with **AEA**, **CBD** and **THC** at 10 μM for three days. Cells treated only with T were used as control. β-tubulin was used as a loading control. (A) Representative Western-blot for ERα and β-tubulin followed by densitometric analysis of ERα expression levels after normalisation with β-tubulin levels. (B) Representative Western-blot for ERβ and β-tubulin followed by densitometric analysis of ERβ expression levels after normalisation with β-tubulin levels. Western-blot is a representative of one example from at least three independent experiments. Results for both receptors are the mean ± SEM of at least three different experiments. Significant differences between the control and cannabinoid-treated cells are shown by * ($p < 0.05$), ** ($p < 0.01$) and *** ($p < 0.001$).

3.7. Effects of cannabinoids on MCF-7aro cell cycle progression

Cell cycle analysis by flow cytometry was performed, in order to understand if a disruption in cell cycle progression was a possible cause for the reduction in viability of MCF-7aro cells induced by cannabinoids. Cells stimulated with T (1 nM) were treated with each cannabinoid, at 5 and 10 µM, during three days. Cells only stimulated with T were used as a control. After fixation, cells were stained with propidium iodide (PI), a fluorescent intercalating dye that binds to DNA, allowing for the evaluation of DNA content, and thus at which stage/phase the cells are in the cell cycle. As the results for each cannabinoid were highly similar between both concentrations, only the results at 10 µM were selected to be presented. As shown in Table 2 and by comparing with control, all three cannabinoids caused a clear and significant ($p < 0.001$) increase in the number of cells in the G_0/G_1 phase, as well as a significant ($p < 0.001$) decrease in the number of cells in the S phase. Furthermore, **CBD** also caused a significant ($p < 0.01$) decrease in the number of cells in the G_2/M phase.

Table 2: Effects of cannabinoids on MCF-7aro cell cycle progression.

	G_0/G_1	S	G_2/M
Testosterone	75.668 ± 0.591	8.379 ± 0.3	14.622 ± 0.507
T + AEA 10 µM	82.743 ± 0.582 ***	3.453 ± 0.133 ***	13.785 ± 0.614
T + CBD 10 µM	84.6 ± 0.750 ***	3.469 ± 0.258 ***	12.032 ± 0.519 **
T + THC 10 µM	82.338 ± 0.335 ***	3.416 ± 0.169 ***	13.905 ± 0.386

Cells were treated with **AEA**, **CBD** and **THC** at 10 µM plus T (1 nM) for three days. Cells were stained with PI (1 µg/mL) and analysed by flow cytometry. Values are expressed as a percentage of single cell events in each stage of the cell cycle and are the mean ± SEM of at least three independent experiments, all performed in triplicate. Significant differences between the control and cannabinoid-treated cells are shown by ** ($p < 0.01$) and *** ($p < 0.001$).

3.8. Effects of cannabinoids on MCF-7aro cell morphology

To examine any potential modifications in cell morphology imposed by cannabinoids on MCF-7aro cells, Giemsa and Hoechst staining was carried out, before observing the cells under bright-field and fluorescence microscopes, respectively. As observed in Figure 24, all three cannabinoids caused chromatin condensation, a typical morphological feature of cells undergoing apoptosis. In comparison to the control, **THC** seems to be the cannabinoid that induced the most chromatin condensation, while **CBD** caused the most pronounced decrease in cell density. Phase contrast microscopy also showed that cells treated with **CBD** present cytoplasm vacuolisation (data not shown).

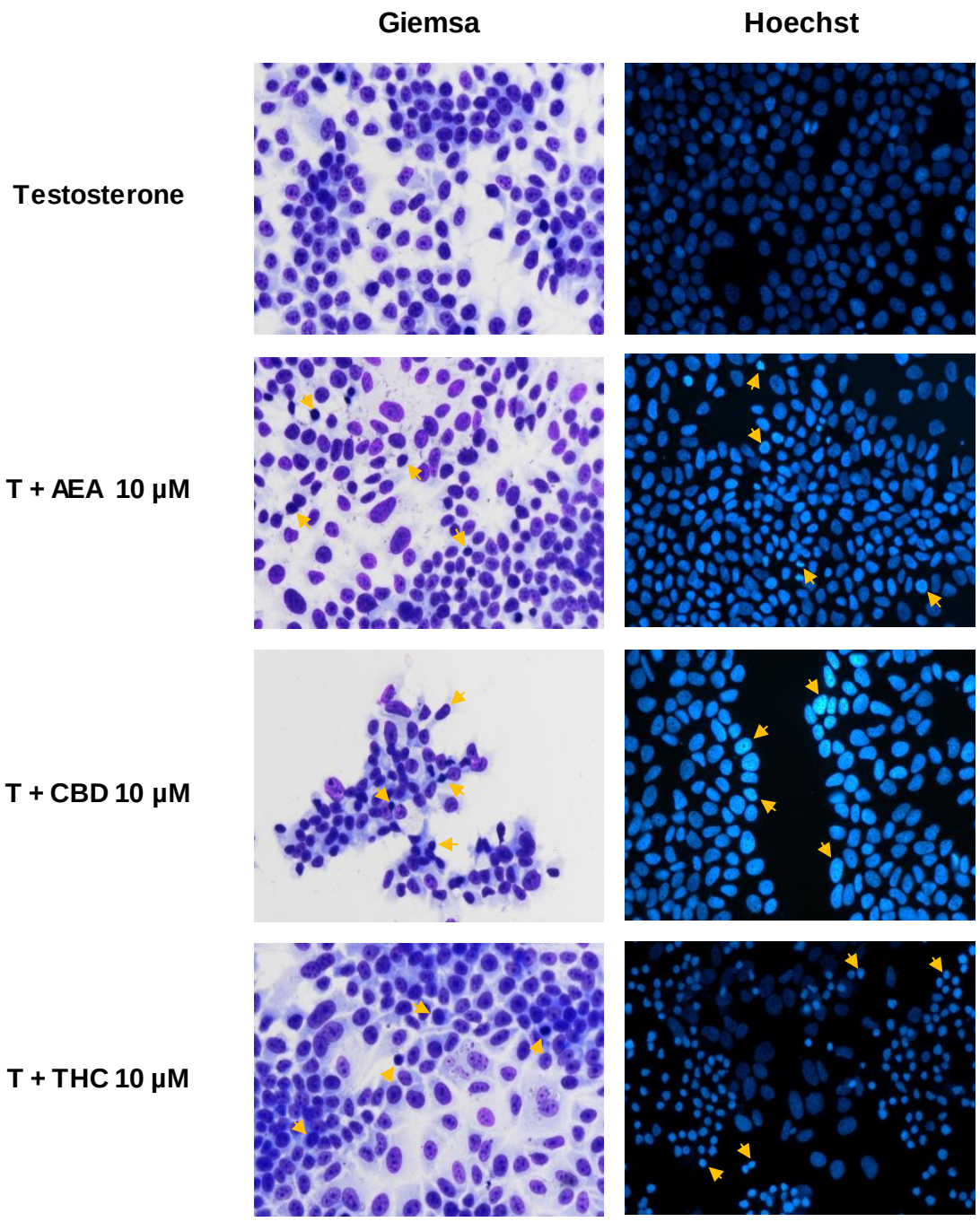

Figure 24: Effects of each cannabinoid on MCF-7aro cell morphology. Cells were treated with **AEA**, **CBD** and **THC** at 10 µM plus T (1 nM), for three days. Cells treated only with T were used as control. After fixation, cells were stained with either Giemsa or Hoechst, and viewed under bright-field and fluorescence microscopes, respectively. Results are a single interpretation of at least three independent experiments. Chromatin condensation is shown using orange arrows. Original magnification 400x.

3.9. Analysis of MCF-7aro cell death

A reduction in cell viability can be a result of various different mechanisms of cell death. As Giemsa and Hoechst staining demonstrated the presence of chromatin condensation, which

suggests the involvement of apoptosis as a potential cause for cell death, further studies were carried out in order to investigate whether the effects induced by **AEA**, **CBD** and **THC** were due to the occurrence of this particular mechanism. Thus, in MCF-7aro cells treated with T (1 nM) and with 5 and 10 μM of **AEA**, **CBD** and **THC** during two and three days, intracellular reactive oxygen species (ROS) levels, mitochondrial membrane potential (ΔΨm), and activation of caspases -7 and -9 were measured. An increase in intracellular ROS is a sign of oxidative stress, which, along with the activation of caspases and a decrease in ΔΨm, is an indicator that apoptosis is occurring inside the cell (112, 118).

The production of ROS in MCF-7aro cells following treatment with each cannabinoid was measured by a fluorescence assay, using $DCFH_2$-DA as a probe. $DCFH_2$-DA is a permeable, non-fluorescent dye that, after crossing the cell membrane is oxidised into the fluorescent compound DCF (111). Results demonstrate that, of the three cannabinoids tested, **AEA** at 5 and 10 μM and after three days, was the only one to cause a significant ($p < 0.01$) increase in intracellular ROS production (Figure 25A). **CBD** appeared to reduce the amount of intracellular ROS, although this could be due to the pronounced decrease in the number of viable cells. **THC** did not appear to affect the amount of intracellular ROS. Initially, this assay was carried out after only three days but, as the overall outcome may be affected by a reduction in cell viability, the assay was repeated and results were read after 30 minutes, one hour, two hours, six hours, one day and two days. Curiously, there was no significant increase in ROS production for any cannabinoid until three days.

As ROS production may lead to mitochondrial dysfunction (112), changes in ΔΨm were also measured by a fluorescence assay, using $DiOC_6(3)$ as a probe. $DiOC_6(3)$ is a fluorescent lipophilic dye that, when applied at low concentrations, will selectively stain viable mitochondria (112). Results presented in Figure 25B show that all three cannabinoids caused a significant ($p < 0.001$) loss of ΔΨm.

Loss of ΔΨm can be associated with the release of cytochrome *c* in the cytosol and the formation of the apoptosome, leading to activation of caspase-9 and, consequently, the activation of the effector caspases in order for the cells to undergo apoptosis (112). To confirm the occurrence of apoptosis, Caspase-7 and -9 activation assays, using Caspase-Glo® 3/7 and Caspase-Glo® 9 kits, were carried out. It must be pointed out, that caspase-3 is not present in this cell line (105). The results showed that, whilst all three tested cannabinoids caused a significant ($p < 0.001$) increase in the activity of caspase-9 (Figure 25C), only **AEA** and **THC** induced a significant ($p < 0.05$, $p < 0.01$, respectively) activation of caspase-7. The pan-caspase inhibitor Z-VAD-FMK, used to confirm the activation of caspases, reverted significantly the activation of capase-7 induced by both **AEA** and **THC** ($p < 0.001$ and $p < 0.01$, respectively) (Figure 25D).

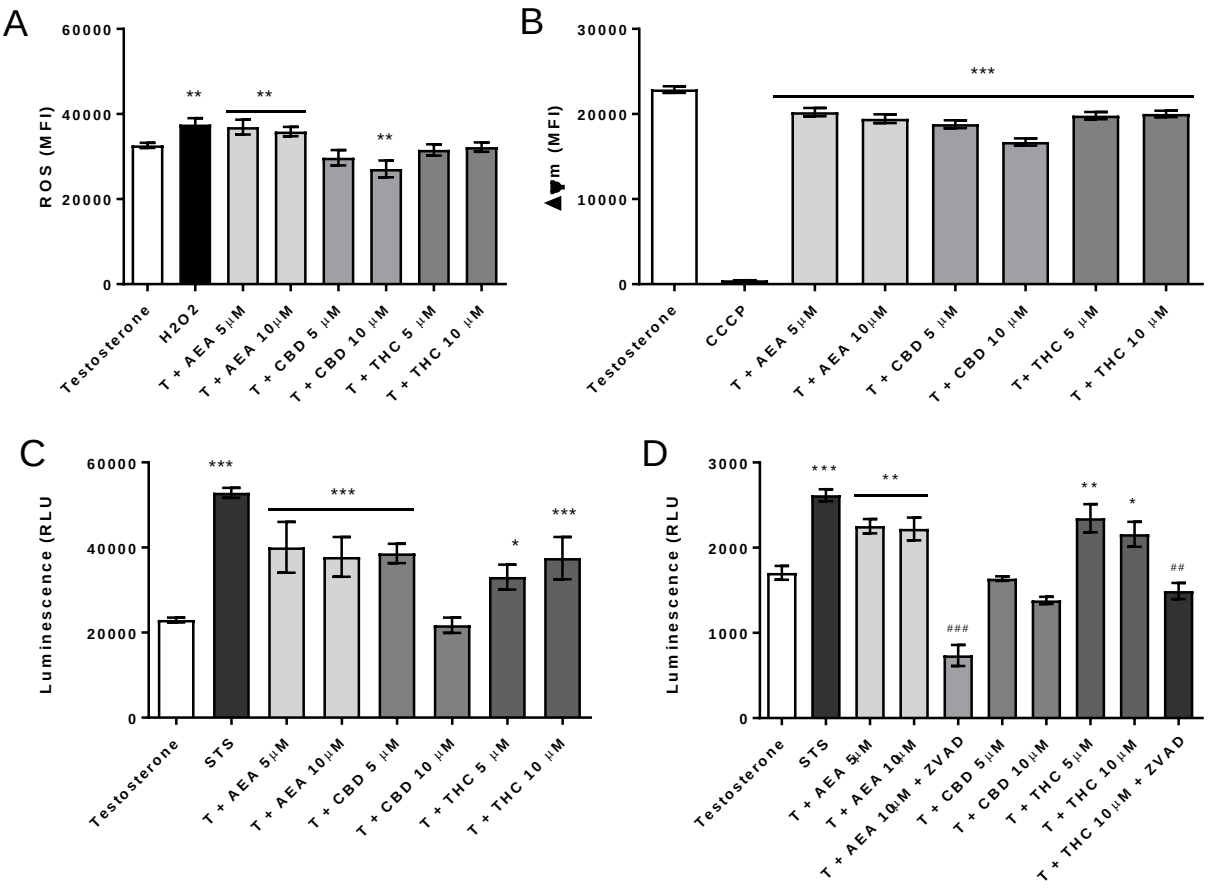

Figure 25: Analysis of cell death parameters in MCF-7aro cells following treatment with cannabinoids. Cells stimulated with T (1 nM) were treated with **AEA**, **CBD** and **THC**, at 5 and 10 µM, during two or three days. Intracellular ROS production (A) was measured after three days, whereas ΔΨm (B), caspase-9 activation (C) and caspase-7 activation (D) were measured after two days. Cells treated only with T were used as a control. H_2O_2 and CCCP were used as positive controls for ROS and ΔΨm assays, respectively, and results are expressed as a mean fluorescence intensity (MFI). For caspase activation assays, STS was used as a positive control, and results are expressed in relative luminescence units (RLU). Z-VAD-FMK was used as a pan-caspase inhibitor in caspase-7 activation assays. Results for all assays are the mean ± SEM of at least three independent experiments, each performed in triplicate. Significant differences between the control and cannabinoid-treated cells are shown by * ($p < 0.05$), ** ($p < 0.01$) and *** ($p < 0.001$). Significant differences between cannabinoid and with and without Z-VAD-FMK are indicated by ## ($p < 0.01$) and ### ($p < 0.001$).

As **CBD** does not appear to induce caspase-7 activation, and in order to confirm the occurrence of apoptosis, PARP cleavage was evaluated by Western-blot. Cleavage of PARP is another typical process that occurs in cells undergoing apoptosis (118, 119). As presented in Figure 26, **AEA** and **THC** increased significantly ($p < 0.01$, $p < 0.001$, respectively) c-PARP levels by more than two-fold, whereas **CBD** increased by three-fold ($p < 0.001$).

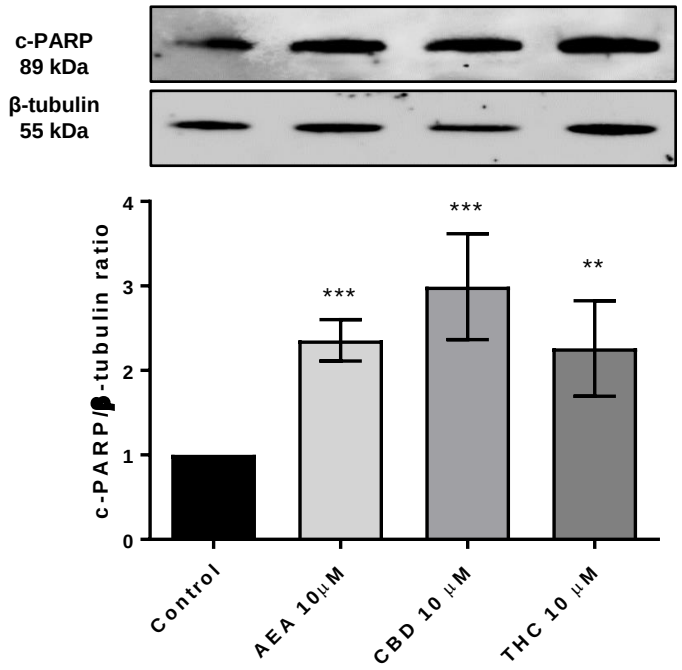

Figure 26: Expression of c-PARP protein in MCF-7aro cells following cannabinoid treatment. Cells stimulated with T (1 nM) were treated with **AEA**, **CBD** and **THC** at 10 μM, during three days. Cells treated only with T were used as control. β-tubulin was used as a loading control. Representative Western-blot for c-PARP and β-tubulin, as well as densitometric analysis of c-PARP expression levels after normalisation with β-tubulin levels, are shown. Western-blot is a representative of one example from at least three independent experiments. Results are the mean ± SEM of at least three different experiments. Significant differences between the control and cannabinoid-treated cells are shown by ** ($p < 0.01$) and *** ($p < 0.001$).

3.10. The involvement of autophagy in MCF-7aro cells treated with CBD

In phase contrast microscopy, after one and two days of **CBD** treatment, the presence of vacuoles in cytoplasm of MCF-7aro cells were observed (data not shown). To confirm this, the formation of acid vesicular organelles (AVOs) was investigated, using acridine orange (AO) staining and fluorescence microscopy. As can be seen in Figure 27, cells treated with **CBD**, during one and two days, presented a shift from green to yellow/orange/red fluorescence when compared to control (green fluorescence), suggesting the presence of AVOs, a typical feature of autophagy. Further assays were therefore carried out, using 3-Methyladenine (3-MA) as an inhibitor of autophagy, in order to determine whether autophagy was taking place. Cells treated with both **CBD** and 3-MA have a decrease in yellow/orange/red fluorescence, when compared with cells treated only with **CBD**, with the DNA and cytoplasm being stained green (Figure 27).

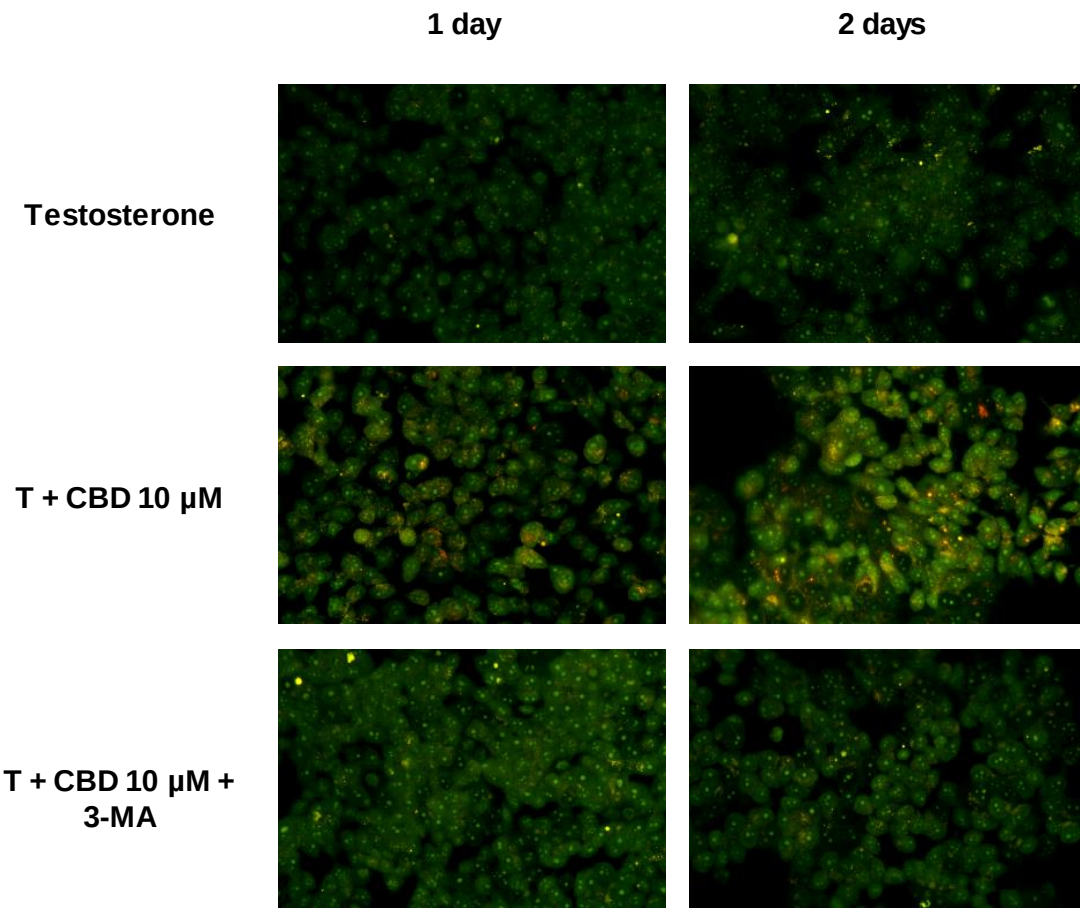

Figure 27: Formation of AVOs in MCF-7aro cells following treatment with CBD. Cells stimulated with T (1 nM) were treated with **CBD** at 10 µM, with and without 3-MA (1 mM), during one and two days. Cells treated only with T were used as control. Results are a single representative experiment of at least three independent experiments. Original magnification 400x.

In order to confirm that autophagy was occurring following **CBD** treatment, a Western-blot analysis was carried out, in order to determine the levels of LC3 II. LC3 is a soluble protein that is present in mammalian tissue. In cells undergoing autophagy, LC3 I binds to phosphatidylethanolamine, which can be found in the membrane of autophagosomes, and is converted into LC3 II. The turnover of this protein is therefore a widely used biomarker of autophagy. An increase in the amount of LC3 II will thus suggest an increase in the rate of autophagy (113). Comparing to control, results show that **CBD** significantly ($p < 0.001$) increased almost three-fold the amount of LC3 II present in cells and that its combination with 3-MA reverted significantly ($p < 0.01$) this effect (Figure 28).

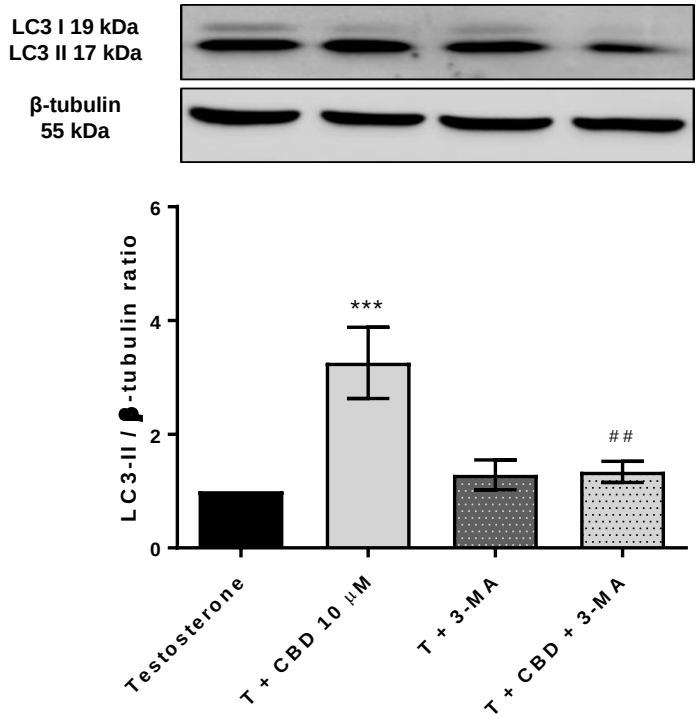

Figure 28: Expression of LC3 II levels in MCF-7aro cells following treatment with CBD. Cells stimulated with T (1 nM) were treated with **CBD** at 10 µM, with and without 3-MA (1 mM), during three days. Cells treated only with T were used as control. β-tubulin was used as a loading control. Representative western blots for LC3 II and β-tubulin, as well as densitometric analysis of LC3 II expression after normalisation with β-tubulin levels, are shown. Western-blot is a representative of one example of at least three independent experiments. Results are the mean ± SEM of at least three different experiments. Significant differences between the control and cannabinoid-treated cells are shown by *** ($p < 0.001$). Significant differences between **CBD**-treated cells with and without 3-MA are denoted by ## ($p < 0.01$).

As 3-MA appeared to completely revert the production of AVOs and the expression of LC3 II in MCF-7aro cells treated with **CBD**, MTT and LDH-release assays were performed, in order to investigate the role of autophagy. Assays were carried out under the same conditions as previously described, during one, two and three days. Results showed that, after one day, 3-MA significantly ($p < 0.01$) reduced the decrease in cell viability caused by **CBD** at 20 µM (Figure 29). After two days, significant ($p < 0.001$) differences were observed with **CBD**, at both 10 and 20 µM, whereas after three days, these significant ($p < 0.001$) differences could be seen at 5, 10 and 20 µM.

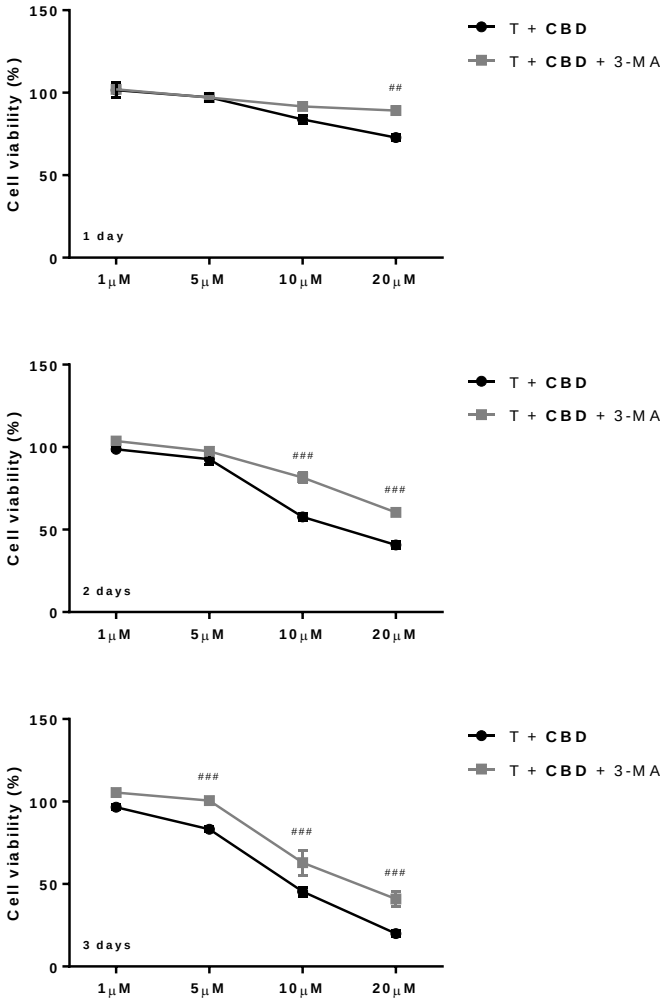

Figure 29: Cell viability of MCF-7aro cells after CBD treatment with and without 3-MA. Cells stimulated with T (1 nM) were treated with **CBD** at 1, 5, 10 and 20 μM, with and without 3-MA (1 mM), during one (A), two (B) and three (C) days. Cells without **CBD** treatment were used as control. Results are shown as the mean ± SEM of at least three independent experiments, each performed in triplicate. Significant differences between cells treated with and without 3-MA are shown by ## ($p < 0.01$) and ### ($p < 0.001$).

An LDH assay was also performed in order to determine if, by preventing autophagy through the use of 3-MA, the cells lose cell membrane integrity. An LDH-release assay was performed under the same conditions as previously mentioned, during one, two and three days. As presented in Figure 30, after three days, **CBD** at 10 and 20 μM caused significant LDH release ($p < 0.01$). This may suggest the loss of cell membrane integrity, which may be linked to necrosis, in MCF-7aro cells, when autophagy has been inhibited with 3-MA. Further studies must be performed to confirm this observation.

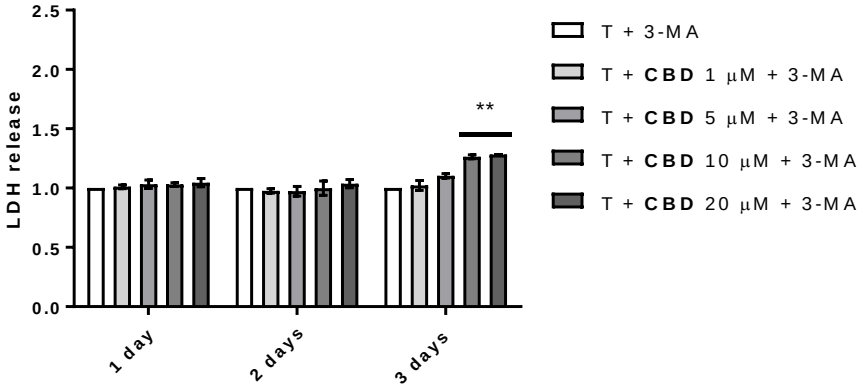

Figure 30: LDH release from MCF-7aro cells treated with CBD in combination with 3-MA. Cells stimulated with T (1 nM) were treated with **CBD** at 1, 5, 10 and 20 µM, and 3-MA (1 mM), during one, two and three days. Cells treated only with T and 3-MA were used as control. Results are expressed as a mean ± SEM of at least three independent experiments, each performed in triplicate. Significant differences are indicated by ** ($p < 0.01$).

Autophagy and apoptosis can occur at the same time in order to promote an efficient cell death, or to prevent it (96, 120, 121). In order to understand the link between both processes in MCF-7aro cells treated with **CBD**, a caspase-9 activation assay was carried out. Assays were carried out under the same conditions as previously described, during one and two days. Results demonstrate that 3-MA was able to revert the activation of caspase-9 caused by **CBD** ($p < 0.001$) after one (data not shown) and two days (Figure 31).

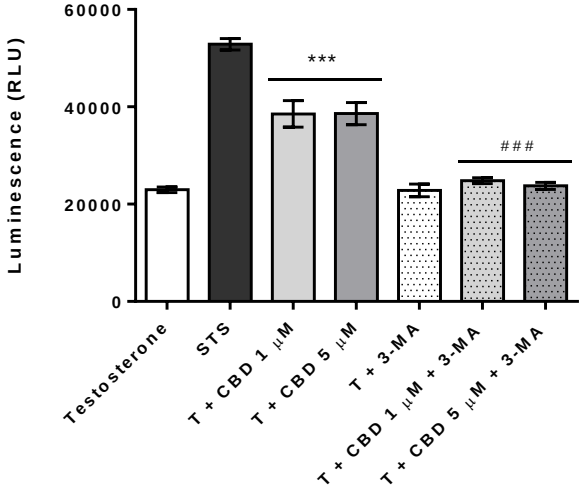

Figure 31: Caspase-9 activation in MCF-7aro cells following CBD treatment with and without 3-MA. Cells stimulated with T (1 nM) were treated with **CBD** at 1 and 5 µM, with and without 3-MA (1mM), during two days. Cells receiving no **CBD** treatment were used as control. Results are expressed in relative luminescence units (RLU) and are the mean ± SEM of at least three different experiments, each performed in triplicate. Significant differences between the control and cells treated with **CBD** are shown by *** ($p < 0.001$), whilst significant differences between cells treated with **CBD** with and without 3-MA are indicated by ### ($p < 0.001$).

3.11. Cell viability in resistant LTEDaro cell line

One of the major concerns in breast cancer therapy is the occurrence of acquired resistance to the AIs currently being used in the clinic (7). In order to test whether **AEA**, **CBD** and **THC** had the ability to revert this type of resistance, MTT and LDH assays were carried out using an AI-resistant ER^+ breast cancer cell line, LTEDaro. Cell viability assays were performed under the same conditions as the assays with MCF-7aro cells, only without T, during three and six days for MTT assays and three days for LDH-release assays.

As presented in Figure 32, all three cannabinoids caused approximately the same reduction in LTEDaro cell viability as they did in MCF-7aro cells. **AEA** significantly ($p < 0.01$, $p < 0.001$) reduced cell viability in a dose-dependent manner, whereas **CBD** and **THC** acted in a dose- and time-dependent manner ($p < 0.05$, $p < 0.001$). As with the MCF-7aro cells, **CBD** in particular caused a pronounced decrease in LTEDaro cell viability, of around 62% after three days of treatment at 20 µM.

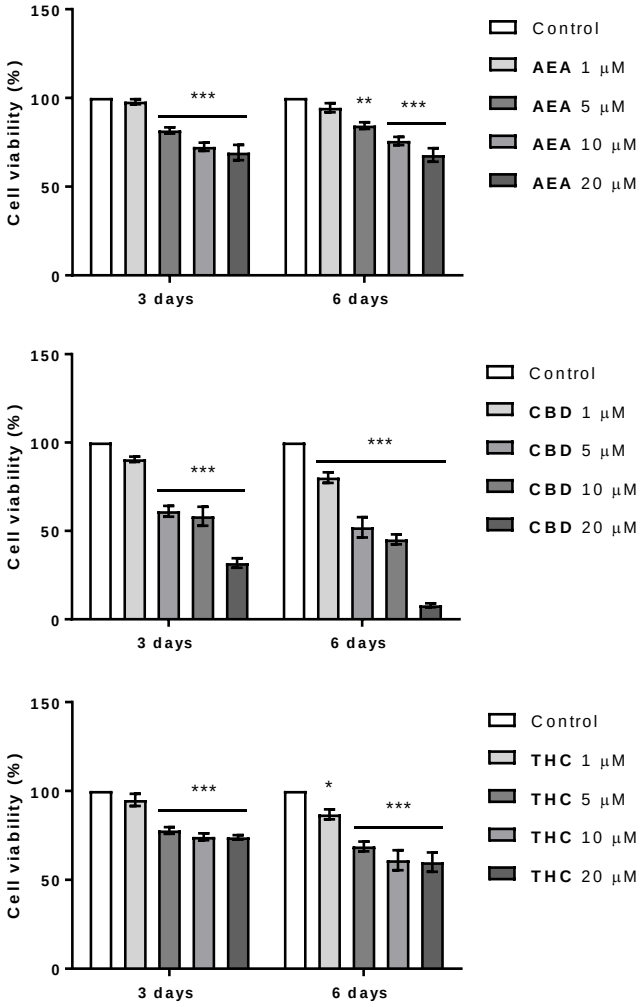

Figure 32: Effects of cannabinoids on viability of resistant LTEDaro cells. Cells were treated with **AEA** (A), **CBD** (B) and **THC** (C) at 1, 5, 10 and 20 µM, during three and six days. Cells with no cannabinoid treatment were used as control (100% cell viability). Results are expressed as a mean ± SEM of at least three independent experiments, each performed in triplicate. Significant differences between cannabinoid-treated cells and the control were shown by * ($p < 0.05$), ** ($p < 0.01$) and *** ($p < 0.001$).

LDH release was also measured following LTEDaro cells exposure to cannabinoid treatment, and results demonstrate that only **CBD** at 20 µM appeared to cause significant ($p < 0.05$) (Figure 33) increase in LDH release.

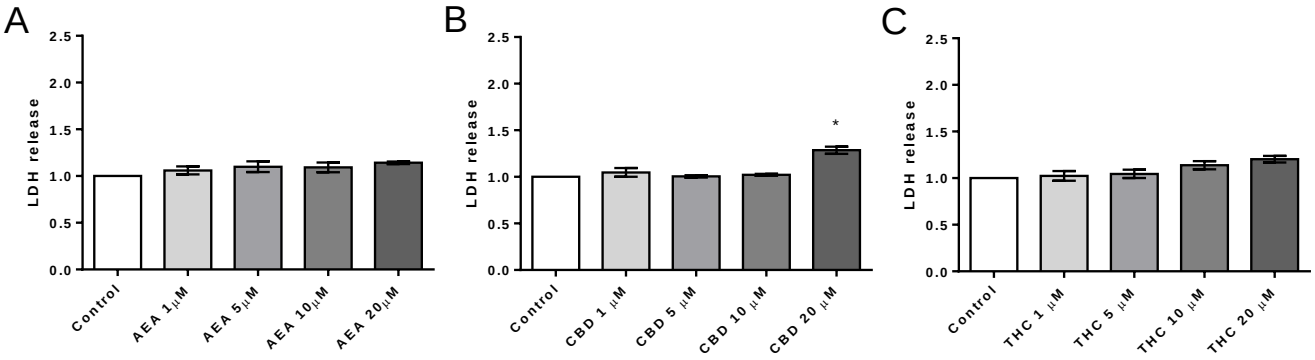

Figure 33: LDH release from LTEDaro cells after cannabinoid treatment. Cells were treated with **AEA** (A), **CBD** (B) and **THC** (C) at 1, 5, 10 and 20 µM, during three days. Cells receiving no cannabinoid treatment were used as control. Results are expressed as a mean ± SEM of at least three independent experiments, each performed in triplicate. Significant differences between cannabinoid-treated cells and the control were shown using * ($p < 0.05$).

4. Discussion

AIs are the current first-line treatment approach for postmenopausal women with ER^+ breast cancer (54). They inhibit the enzyme aromatase, thus preventing it from converting androgens into oestrogens (6, 7, 12, 26). Oestrogens bind to the ER, which is overexpressed in ER^+ breast cancer cells, in order to stimulate cell growth, and thus tumour progression (7, 20). Although AIs have proven to be a successful form of therapy, acquired resistance can occur, leading to tumour relapse (7, 58, 59, 66), this being considered the major concern in breast cancer therapy. Therefore, the need to find novel therapies is important and research into new anticancer drugs is constantly ongoing. The anticancer properties of cannabinoids have already been reported in various different cancer cell lines, including breast, suggesting that these compounds may be suitable for the treatment of ER^+ breast cancer (76, 88, 122). Furthermore, cannabinoids have been shown to cause fewer side effects than many of the currently used treatments, often improving their results when administered in combination and alleviating unwanted symptoms caused by disease and other medications (94, 122).

Taking this into consideration, the main aim of this study was to evaluate the *in vitro* effects and the mechanisms behind the two principal phytocannabinoids found in plants of the *Cannabis* genus, cannabidiol (**CBD**) and Δ^9-tetrahydrocannabinol (**THC**), as well as the major endocannabinoid anandamide (**AEA**), on ER^+ breast cancer cells (MCF-7aro and LTEDaro). MCF-7aro cells are considered the best *in vitro* cell model to study this type of cancer and AIs, because they overexpress aromatase, thus causing an increase in oestrogen levels and mimicking the ER^+ breast cancer tumour microenvironment. LTEDaro cells, on the other hand, are resistant ER^+ breast cancer cells that have adapted to oestrogen deprivation in order to grow, mimicking, *in vitro*, the late-stage of acquired resistance. Furthermore, as LTEDaro cells are resistant to the AIs currently used in the clinic, as well as to Tamoxifen, they are considered the best *in vitro* cell model for the study of endocrine resistance (106, 114, 123).

As cannabinoids are known to act through mechanisms both dependent and independent of cannabinoid receptors (principally CB_1 and CB_2) or the vanilloid receptor (TRPV1) (89, 93, 95, 107), it was important to determine whether these receptors were expressed in the cell models used in this work. Results demonstrate that CB_1 and CB_2 were detected in both cell lines under our conditions, although TRPV1 was not. This suggests that the TRPV1 receptor may not be present, or that it may be expressed in trace amounts, being difficult to be detected by a Western-blot under our conditions. Thus, further studies must be performed, like a PCR analysis, in order to confirm the presence of this receptor in both cell models. Furthermore, results demonstrated that **AEA**, **CBD** and **THC** are non-toxic towards HFF-1 cells, a non-cancerous cell line. This is important for any compound with the potential to be used as an anticancer agent in the clinic, as non-cancerous cells should remain unaffected. Following these results, all three cannabinoids were investigated on MCF-7aro and LTEDaro cells. As

already reported in various studies on other breast cancer cell lines (95, 124-127), in this study, **AEA**, **CBD** and **THC** caused a significant dose- and time-dependent reduction in MCF-7aro cell viability, but without affecting cell membrane integrity.

In order to determine whether the effects on MCF-7aro cell viability for each cannabinoid were dependent on cannabinoid or vanilloid receptors, the effects of cannabinoids in cells pre-treated with antagonists for each receptor were explored. Contrary to **CBD**, the reduction in MCF-7aro cell viability induced by **AEA** was CB_2-dependent, whereas for **THC** it was dependent on both CB_1 and CB_2. The results obtained for **THC** were in accordance with what has been reported in the literature (75, 95, 100, 125, 128). Interestingly, **CBD** appears not to work through cannabinoid or vanilloid receptors, which is in agreement with the study of Murase *et al*., where the *in vitro* effects of **CBD** on breast cancer cell viability were not affected by the presence of a CB_2 antagonist (125), and with the study of Shrivastava *et al*., where **CBD** caused cell death in a triple-negative breast cancer cell line (MDA-MB-231), independently of cannabinoid or vanilloid receptor binding (96). It has, however, been reported that **CBD** does in fact bind to TRPV1 in different cancer cell models (91, 95, 107, 129). Nevertheless, it must be pointed out, that Capsaicin (CAPS), the antagonist for the TRPV1 receptor, did not alter the effects induced by the three cannabinoids, indicating that either none of these cannabinoids work through this receptor, or that it may not be present in this cell line.

As it has been described that cannabinoids inhibit various enzymes from the cytochrome P450 (CYP450) family (130), of which aromatase is a member, further assays were conducted in order to determine if the effects of cannabinoids on MCF-7aro cells were dependent on aromatase. Firstly, as aromatase converts androgens (such as T) into oestrogens (such as E_2), which are important for ER^+ breast cancer cell growth (106), the effects of cannabinoids on the viability of cells stimulated with T or with E_2 were compared. In the case of **AEA** and **THC**, the results suggest that the effects on cell viability are independent of aromatase, however, the effects of **CBD** seem to be due to a mechanism that may be partially dependent on aromatase activity since, in the presence of the substrate of aromatase, the reduction in cell viability induced by **CBD** was higher than in the presence of its product. Nevertheless, it must be pointed out that other mechanisms may be occurring simultaneously. Taking into account these results, the anti-aromatase activity of each cannabinoid in these cells was explored. As AIs are currently the first-line treatment approach for postmenopausal women with ER^+ breast cancer (54), the inhibition of aromatase would therefore be an interesting mechanism through which cannabinoids could act, in order to prevent the proliferation of cancer cells. Results demonstrate that **THC** presented low anti-aromatase activity, which is in accordance with a study by Lewysohn *et al*. (131). On the contrary, and for the first time, it was shown that **AEA** and **CBD** presented reasonable levels of anti-aromatase activity. This was interesting, because the reduction in MCF-7aro cell viability was only aromatase-

dependent for **CBD**, and not for **AEA**. In addition, as **Exe** is an AI that also has the ability to degrade aromatase through the proteasome (115), and in order to determine if the cannabinoids can also affect the expression levels of this enzyme, a Western-blot analysis was carried out. **CBD** caused the largest decrease in aromatase levels, reducing its expression by 54.2% when compared to the control. Furthermore, **AEA** and **THC** also reduced the expression of aromatase, by 21% and 29.4%, respectively, when compared to the control. Nevertheless, a PCR analysis should be performed in order to explore whether these reductions were due to a decrease in the synthesis of aromatase, or, like **Exe**, these molecules have the ability to induce aromatase degradation.

As these cancerous cells overexpress ERα, which has a pivotal role in breast cancer cell growth (36), it was also investigated whether the effects of cannabinoids on MCF-7aro cells were dependent on ER. In order to do so, an MTT assay was carried out with the cannabinoids in combination with **ICI**, a selective oestrogen receptor down-regulator (SERD), that causes ER degradation (117). In the presence of **ICI**, **AEA** and **THC** were both unable to reduce MCF-7aro cell viability, contrary to what is observed when cells are treated with each compound on its own. This suggests that the mechanism of action for these cannabinoids may be dependent on ER. This is an interesting observation considering the fact that cannabinoids also cause cell death in triple-negative breast cancer cells, that do not express the ER (95, 96, 103). On the other hand, **CBD** in combination with **ICI** continued to cause a reduction in cell viability, although this reduction was in fact less pronounced than in the case of **CBD** alone. This suggests that the mechanism of action of **CBD** may be only partially dependent on the ER. Following these results, a Western-blot analysis was further performed in order to investigate whether these compounds affected the expression levels of ERα and ERβ. In breast cancer cells, ERα transduction pathway is linked to cell survival, whereas activation of ERβ is linked to breast cancer cell death (36, 37). Curiously, results demonstrated that **AEA**, **CBD** and **THC** caused a similar decrease in the expression of ERα, whilst an increase in ERβ expression levels was also observed for **AEA** and **CBD**. Contrary to what has been reported in MCF-7 and MDA-MB-231 cells (101), in our conditions, **THC** did not cause any significant increase in ERβ expression. This suggests that, for **AEA** and **CBD**, both ERα and ERβ are involved in the mechanism behind the reduction in MCF-7aro cell viability. For **THC**, however, it is more likely that only ERα is involved. Even so, these results are very interesting, since several reports (132, 133) suggest that the next generation of drugs for this type of cancer should target both aromatase and ER, especially ERβ, to obtain an efficient inhibition of tumour growth.

Many studies on various cancer cell models have demonstrated that cannabinoids have the ability to cause cell cycle arrest (99, 100, 134-136). Taking this into account, flow cytometry was carried out, to investigate the effects of **AEA**, **CBD** and **THC** on cell cycle progression in MCF-7aro cells. All three cannabinoids arrested cell cycle in the G_0/G_1 phase, and as a result,

reduced the number of cells in the S phase. Moreover, the results obtained for **AEA** and **CBD** are in accordance with the studies by De Petrocellis *et al*. (135), and Ligresti *et al*. (136), and suggest that the reduction in MCF-7aro cell viability induced by cannabinoids could also be explained by a disruption in cell cycle progression, which may be due to the anti-aromatase activity and/or the effects of cannabinoids on the expression levels of aromatase and ER.

In addition, as cell cycle arrest is linked to apoptosis (137), the involvement of apoptosis was also investigated. Cell morphology studies on MCF-7aro cells demonstrated that the cannabinoids appeared to cause chromatin condensation, a typical feature of apoptotic cells (138). In order to confirm the involvement of this process as a mechanism of cell death induced by cannabinoids, their effects on intracellular ROS production, on ΔΨm, and on the activation of caspases -7 and -9, as well as PARP cleavage, were analysed. It is known that an increase in intracellular ROS levels can cause oxidative stress and thus damage to vital components of the cell (112, 139). Contrary to **CBD** and **THC**, only **AEA** after three days caused an increase in intracellular ROS production. The results obtained for the two phytocannabinoids were surprising and contrary to several existing studies (95-97, 140-142). Treatment with any of the three cannabinoids did, however, lead to a reduction in ΔΨm, with **CBD** causing the most pronounced effect. Along with other mechanisms, the loss of ΔΨm may occur as a result of an increase in ROS production leading to mitochondrial membrane permeabilisation, which is associated with mitochondrial dysfunction and thus cell death (112). In addition, as a decrease in ΔΨm can eventually lead to caspase activation (112), further studies involving the activation of caspases -9 and -7 were performed, in order to confirm the occurrence of apoptosis. The activation of initiator caspases, such as caspase-9, leads to the activation of downstream effector caspases, such as caspase-7 (118, 119). Results demonstrated that all three cannabinoids caused caspase-9 activation, whereas only **AEA** and **THC** caused activation of caspase-7. Curiously, despite causing a reduction in ΔΨm, **CBD** did not lead to significant caspase-7 activation. A study by Marcu *et al*. also found that **CBD** did not cause caspase-7 activation, whilst **THC** only induced a light increase in caspase activity. Interestingly, however, these authors also showed that, when combined, **CBD** and **THC** caused higher activation of caspase-7 than when alone (143). Nevertheless, to confirm the occurrence of apoptosis, especially in the case of **CBD**, the expression levels of cleaved PARP in MCF-7aro cells treated with cannabinoids were also investigated. The nuclear protein PARP, which is cleaved and inactivated by effector caspases, performs a range of functions inside the cell, including DNA repair. Cleavage of PARP will lead to cell death, therefore being another indicator that apoptosis may be occurring in a cell (144, 145). Treatment with any of the three cannabinoids increased the levels of cleaved PARP in MCF-7aro cells, confirming that these cells will eventually undergo apoptosis, through the involvement of mitochondria.

This is in accordance with various other studies, that have also demonstrated that cannabinoids induce apoptosis, in both ER^+ and ER^- breast cancer cells (96, 100, 103, 136).

After observation using phase contrast microscopy, vacuoles were clearly visible in the cytoplasm of MCF-7aro cells treated with **CBD**. The formation of vacuoles is a typical feature of cells undergoing autophagy, which can be a mechanism of cell survival - which has already been noted in various cancer cases (66, 105, 146) - or a promoter of the process of programmed cell death (114, 121). Curiously, these vacuoles were almost non-existent in **CBD**-treated cells after three days, so all assays involving the role of autophagy in **CBD**-treated cells were performed over one or two days. In order to detect the presence of AVOs, which is a typical feature of autophagic cells (66, 105, 113), acridine orange (AO) staining was carried out and the cells were observed under a fluorescence microscope. Results showed that **CBD** caused a clear increase in AVOs inside the cells. Furthermore, this effect was reverted when the cells were treated with **CBD** in combination with 3-MA, an inhibitor of autophagy. These results suggest the occurrence of autophagy in these cells following treatment with **CBD**, though to confirm and clarify this, the conversion of LC3 protein was investigated. The conversion of LC3 I into LC3 II is a process that occurs in cells undergoing autophagy, due to the role of LC3 II in the formation of the autophagosome (96, 113). Results showed that **CBD**-treatment increased the levels of LC3 II, whilst this increase was completely reverted when the cells were treated with **CBD** plus 3-MA. Therefore, it can be proposed that, besides apoptosis, **CBD** also causes the occurrence of autophagy in MCF-7aro cells, as has already been suggested in other reports on different cancer cell lines (76, 90, 95, 96).

Taking into account the results obtained, the relationship between these two processes after treatment with **CBD** was investigated, as it is already known that apoptosis and autophagy may act together in order to induce an efficient cell death. On the other hand, however, autophagy may also act as an antagonist to block apoptotic cell death, by promoting cell survival (120, 121). In order to determine if the inhibition of autophagy would decrease the reduction in cell viability caused by this cannabinoid, an MTT assay was carried out during one, two and three days, with **CBD** in combination with 3-MA. An LDH-release assay was also performed in order to investigate the possible occurrence of membrane rupturing as an alternative mechanism of cell death to autophagy. Treatment with **CBD** and 3-MA still caused a reduction in cell viability, however this reduction was lower when compared with cells treated only with **CBD**, meaning that the inhibition of autophagy via the use of 3-MA impaired the reduction in cell viability induced by **CBD**. No LDH release occurred after one or two days of **CBD** treatment with 3-MA, however, after three days, an increase in LDH release was detected. This suggests that a more drastic process of cell death occurs when autophagy is inhibited, perhaps due to the occurrence of necrosis, although further studies must be performed in order to confirm this.

Based on the fact that a reduction in cell viability was still observed, albeit reduced, even after autophagy had been inhibited, and the fact that autophagy and apoptosis can occur simultaneously in order to lead to an efficient cell death (120, 121), as has been reported in triple-negative breast cancer cells after treatment with **CBD** (96), in this study, the effects of **CBD** and 3-MA on the activation of caspase-9 were also investigated. Results demonstrated that the activation of caspase-9 caused by **CBD** was completely reverted by 3-MA, thus suggesting that autophagy and apoptosis may both be linked, and that by inhibiting autophagy, the occurrence of apoptosis may be at least partially prevented. The fact that, after treatment with **CBD** and 3-MA, a smaller reduction in cell viability was observed, and that autophagic vacuoles were no longer visible after three days of **CBD** treatment, but that a large reduction in cell viability still occurred, suggest that autophagy may precede and contribute to the occurrence of apoptosis, for an efficient ER^+ breast cancer cell death. The fact that it was already reported that autophagy occurs simultaneously with apoptosis in triple-negative breast cancer cells after treatment with **CBD** (96), reinforces our findings for the process of cell death caused by **CBD** in MCF-7aro cells.

From the results of this study, it is therefore possible to deduce that, although **AEA**, **CBD** and **THC** belong to the same family of compounds, and all cause cell cycle arrest at the same phase in MCF-7aro cells, each one acts through different mechanisms in order to cause ER^+ breast cancer cell death. **AEA** appears to act through the CB_2 receptor to induce apoptosis, whereas **CBD** works independently of cannabinoid receptors in order to trigger autophagy, which then leads to apoptosis, an effect that seems to be, at least in part, dependent on aromatase. **THC**, on the other hand, seems to induce apoptotic cell death by binding both CB_1 and CB_2 receptors. Curiously, all three cannabinoids have the ability to decrease ERα levels, whilst **AEA** and **CBD** also up-regulate ERβ expression in MCF-7aro cells.

In addition, as resistance to current therapies is the principal concern with ER^+ breast cancer treatment (7, 66, 108), the *in vitro* effects of cannabinoids on an AI-resistant ER^+ breast cancer cell line (LTEDaro) were also investigated. According to our results, **AEA**, **CBD** and **THC** caused similar reductions in LTEDaro cell viability as in MCF-7aro cells, suggesting that LTEDaro cells are sensitive to all the three cannabinoids. Nevertheless, further studies will be required in order to determine the exact mechanism underlining the reduction in viable LTEDaro cells following treatment with cannabinoids. These preliminary results do, however, offer a promising hope into future treatments for ER^+ breast cancer patients who have developed resistance to AIs.

5. Conclusions

In summary, the results from this study suggest that all three cannabinoids induce a reduction in MCF-7aro cell viability and in the late-stage AI-resistant LTEDaro cells, whilst not affecting the non-tumoural HFF-1 cells. Furthermore, in ER^+ breast cancer cells, all three cannabinoids presented anti-aromatase activity, whilst also reducing the levels of aromatase and ERα. Interestingly, **AEA** and **CBD** also induced an up-regulation of ERβ, which along with aromatase inhibition is a therapeutic advantage for this type of cancer. Moreover, cannabinoids also disrupted cell cycle progression and induced apoptosis in MCF-7aro cells, via the mitochondrial pathway. In addition to this, there was clear evidence that **CBD** induced autophagy in MCF-7aro cells, and that this process may precede and cooperate with apoptosis in order to obtain an efficient ER^+ breast cancer cell death. It must be pointed out, that the phytocannabinoid **CBD** was the most effective at inducing cancer cell death. Therefore, with this study, it was proven that these cannabinoids have promising anti-tumour properties regarding ER^+ breast cancer treatment, and even for late-stage resistant cases. Nonetheless, an investigation into the effects of a combination of phytocannabinoids on ER^+ breast cancer cells could also yield interesting results, as these compounds are found together in nature, and have been reported to be more effective *in vitro* when combined than when alone (143, 147, 148).

In conclusion, this study will contribute to the growing mass of evidence that cannabinoids present relevant anti-tumour properties in cancerous cells, thus highlighting them as new potential anti-cancer drugs for this type of cancer, which in the near future could proceed to preclinical and even clinical studies.

6. Bibliography

1. Hassanpour SH, Dehgani M. Review of cancer from perspective of molecular. Journal of Cancer Research and Practice. 2017;4(4):127-9.
2. Benjamin EJ, Blaha MJ, Chiuve SE, Cushman M, Das SR, Deo R, et al. Heart Disease and Stroke Statistics-2017 Update: A Report From the American Heart Association. Circulation. 2017;135(10):e146-e603.
3. Silvestri V, Barrowdale D, Mulligan AM, Neuhausen SL, Fox S, Karlan BY, et al. Male breast cancer in BRCA1 and BRCA2 mutation carriers: pathology data from the Consortium of Investigators of Modifiers of BRCA1/2. Breast Cancer Res. 2016;18(1):15.
4. Ferlay J, Soerjomataram I, Dikshit R, Eser S, Mathers C, Rebelo M, et al. Cancer incidence and mortality worldwide: sources, methods and major patterns in GLOBOCAN 2012. Int J Cancer. 2015;136(5):E359-86.
5. Viale G. The current state of breast cancer classification. Ann Oncol. 2012;23 Suppl 10:x207-10.
6. Chen S. An "omics" approach to determine the mechanisms of acquired aromatase inhibitor resistance. OMICS. 2011;15(6):347-52.
7. Augusto TV, Correia-da-Silva G, Rodrigues CMP, Teixeira N, Amaral C. Acquired resistance to aromatase inhibitors: where we stand! Endocr Relat Cancer. 2018;25(5):R283-R301.
8. Gray JM, Rasanayagam S, Engel C, Rizzo J. State of the evidence 2017: an update on the connection between breast cancer and the environment. Environ Health. 2017;16(1):94.
9. Howell A, Anderson AS, Clarke RB, Duffy SW, Evans DG, Garcia-Closas M, et al. Risk determination and prevention of breast cancer. Breast Cancer Res. 2014;16(5):446.
10. Teegarden D, Romieu I, Lelievre SA. Redefining the impact of nutrition on breast cancer incidence: is epigenetics involved? Nutr Res Rev. 2012;25(1):68-95.
11. Caldon CE. Estrogen signaling and the DNA damage response in hormone dependent breast cancers. Front Oncol. 2014;4:106.
12. Nabholtz JM. Long-term safety of aromatase inhibitors in the treatment of breast cancer. Ther Clin Risk Manag. 2008;4(1):189-204.
13. Jerry DJ, Shull JD, Hadsell DL, Rijnkels M, Dunphy KA, Schneider SS, et al. Genetic variation in sensitivity to estrogens and breast cancer risk. Mamm Genome. 2018;29(1-2):24-37.
14. World Health Organisation. Cancer Country Profiles 2014 [cited 2018 28 Aug]. Available from: http://www.who.int/cancer/country-profiles/en/.
15. Bjornstrom L, Sjoberg M. Mechanisms of estrogen receptor signaling: convergence of genomic and nongenomic actions on target genes. Mol Endocrinol. 2005;19(4):833-42.
16. Marino M, Galluzzo P, Ascenzi P. Estrogen signaling multiple pathways to impact gene transcription. Curr Genomics. 2006;7(8):497-508.
17. Vrtacnik P, Ostanek B, Mencej-Bedrac S, Marc J. The many faces of estrogen signaling. Biochem Med (Zagreb). 2014;24(3):329-42.
18. Lee HR, Kim TH, Choi KC. Functions and physiological roles of two types of estrogen receptors, ERalpha and ERbeta, identified by estrogen receptor knockout mouse. Lab Anim Res. 2012;28(2):71-6.
19. Leu YW, Yan PS, Fan M, Jin VX, Liu JC, Curran EM, et al. Loss of estrogen receptor signaling triggers epigenetic silencing of downstream targets in breast cancer. Cancer Res. 2004;64(22):8184-92.
20. Lipovka Y, Konhilas JP. The complex nature of oestrogen signalling in breast cancer: enemy or ally? Biosci Rep. 2016;36(3).
21. Yasuda MT, Sakakibara H, Shimoi K. Estrogen- and stress-induced DNA damage in breast cancer and chemoprevention with dietary flavonoid. Genes Environ. 2017;39:10.
22. Di Sante G, Di Rocco A, Pupo C, Casimiro MC, Pestell RG. Hormone-induced DNA damage response and repair mediated by cyclin D1 in breast and prostate cancer. Oncotarget. 2017;8(47):81803-12.

23. Miller WR, Bartlett J, Brodie AM, Brueggemeier RW, di Salle E, Lonning PE, et al. Aromatase inhibitors: are there differences between steroidal and nonsteroidal aromatase inhibitors and do they matter? Oncologist. 2008;13(8):829-37.
24. Hamilton A, Volm M. Nonsteroidal and steroidal aromatase inhibitors in breast cancer. Oncology (Williston Park). 2001;15(8):965-72; discussion 72, 77-9.
25. Hong Y, Li H, Yuan YC, Chen S. Molecular characterization of aromatase. Ann N Y Acad Sci. 2009;1155:112-20.
26. Chan HJ, Petrossian K, Chen S. Structural and functional characterization of aromatase, estrogen receptor, and their genes in endocrine-responsive and -resistant breast cancer cells. J Steroid Biochem Mol Biol. 2016;161:73-83.
27. Zhao H, Zhou L, Shangguan AJ, Bulun SE. Aromatase expression and regulation in breast and endometrial cancer. J Mol Endocrinol. 2016;57(1):R19-33.
28. Ghosh D, Griswold J, Erman M, Pangborn W. Structural basis for androgen specificity and oestrogen synthesis in human aromatase. Nature. 2009;457(7226):219-23.
29. Hanukoglu I. Steroidogenic enzymes: structure, function, and role in regulation of steroid hormone biosynthesis. J Steroid Biochem Mol Biol. 1992;43(8):779-804.
30. Pasqualini JR, Gelly C, Nguyen BL, Vella C. Importance of estrogen sulfates in breast cancer. J Steroid Biochem. 1989;34(1-6):155-63.
31. Levin ER. Integration of the extranuclear and nuclear actions of estrogen. Mol Endocrinol. 2005;19(8):1951-9.
32. Yasar P, Ayaz G, User SD, Gupur G, Muyan M. Molecular mechanism of estrogen-estrogen receptor signaling. Reprod Med Biol. 2017;16(1):4-20.
33. Zilli M, Grassadonia A, Tinari N, Di Giacobbe A, Gildetti S, Giampietro J, et al. Molecular mechanisms of endocrine resistance and their implication in the therapy of breast cancer. Biochim Biophys Acta. 2009;1795(1):62-81.
34. Lannigan DA. Estrogen receptor phosphorylation. Steroids. 2003;68(1):1-9.
35. Kumar R, Zakharov MN, Khan SH, Miki R, Jang H, Toraldo G, et al. The dynamic structure of the estrogen receptor. J Amino Acids. 2011;2011:812540.
36. Anbalagan M, Rowan BG. Estrogen receptor alpha phosphorylation and its functional impact in human breast cancer. Mol Cell Endocrinol. 2015;418 Pt 3:264-72.
37. Paruthiyil S, Parmar H, Kerekatte V, Cunha GR, Firestone GL, Leitman DC. Estrogen receptor beta inhibits human breast cancer cell proliferation and tumor formation by causing a G2 cell cycle arrest. Cancer Res. 2004;64(1):423-8.
38. Park BW, Kim KS, Heo MK, Ko SS, Hong SW, Yang WI, et al. Expression of estrogen receptor-beta in normal mammary and tumor tissues: is it protective in breast carcinogenesis? Breast Cancer Res Treat. 2003;80(1):79-85.
39. Shaw JA, Udokang K, Mosquera JM, Chauhan H, Jones JL, Walker RA. Oestrogen receptors alpha and beta differ in normal human breast and breast carcinomas. J Pathol. 2002;198(4):450-7.
40. Acconcia F, Kumar R. Signaling regulation of genomic and nongenomic functions of estrogen receptors. Cancer Lett. 2006;238(1):1-14.
41. McDevitt MA, Glidewell-Kenney C, Weiss J, Chambon P, Jameson JL, Levine JE. Estrogen response element-independent estrogen receptor (ER)-alpha signaling does not rescue sexual behavior but restores normal testosterone secretion in male ERalpha knockout mice. Endocrinology. 2007;148(11):5288-94.
42. Glidewell-Kenney C, Weiss J, Lee EJ, Pillai S, Ishikawa T, Ariazi EA, et al. ERE-independent ERalpha target genes differentially expressed in human breast tumors. Mol Cell Endocrinol. 2005;245(1-2):53-9.
43. Fiorito E, Katika MR, Hurtado A. Cooperating transcription factors mediate the function of estrogen receptor. Chromosoma. 2013;122(1-2):1-12.
44. Cheng SB, Graeber CT, Quinn JA, Filardo EJ. Retrograde transport of the transmembrane estrogen receptor, G-protein-coupled-receptor-30 (GPR30/GPER) from the plasma membrane towards the nucleus. Steroids. 2011;76(9):892-6.

45. Filardo EJ, Quinn JA, Sabo E. Association of the membrane estrogen receptor, GPR30, with breast tumor metastasis and transactivation of the epidermal growth factor receptor. Steroids. 2008;73(9-10):870-3.
46. Pedram A, Razandi M, Aitkenhead M, Hughes CC, Levin ER. Integration of the non-genomic and genomic actions of estrogen. Membrane-initiated signaling by steroid to transcription and cell biology. J Biol Chem. 2002;277(52):50768-75.
47. Pistelli M, Mora AD, Ballatore Z, Berardi R. Aromatase inhibitors in premenopausal women with breast cancer: the state of the art and future prospects. Curr Oncol. 2018;25(2):e168-e75.
48. Fabian CJ. The what, why and how of aromatase inhibitors: hormonal agents for treatment and prevention of breast cancer. Int J Clin Pract. 2007;61(12):2051-63.
49. Benson JR, Pitsinis V. Update on clinical role of tamoxifen. Curr Opin Obstet Gynecol. 2003;15(1):13-23.
50. Xiong R, Zhao J, Gutgesell LM, Wang Y, Lee S, Karumudi B, et al. Novel Selective Estrogen Receptor Downregulators (SERDs) Developed against Treatment-Resistant Breast Cancer. J Med Chem. 2017;60(4):1325-42.
51. Waters EA, McNeel TS, Stevens WM, Freedman AN. Use of tamoxifen and raloxifene for breast cancer chemoprevention in 2010. Breast Cancer Res Treat. 2012;134(2):875-80.
52. Lumachi F, Luisetto G, Basso SM, Basso U, Brunello A, Camozzi V. Endocrine therapy of breast cancer. Curr Med Chem. 2011;18(4):513-22.
53. Tremont A, Lu J, Cole JT. Endocrine Therapy for Early Breast Cancer: Updated Review. Ochsner J. 2017;17(4):405-11.
54. Cardoso F, Costa A, Senkus E, Aapro M, Andre F, Barrios CH, et al. 3rd ESO-ESMO International Consensus Guidelines for Advanced Breast Cancer (ABC 3). Ann Oncol. 2017;28(1):16-33.
55. Sobral AF, Amaral C, Correia-da-Silva G, Teixeira N. Unravelling exemestane: From biology to clinical prospects. J Steroid Biochem Mol Biol. 2016;163:1-11.
56. Seber S, Solmaz D, Yetisyigit T. Antihormonal treatment associated musculoskeletal pain in women with breast cancer in the adjuvant setting. Onco Targets Ther. 2016;9:4929-35.
57. Satija A, Ahmed SM, Gupta R, Ahmed A, Rana SP, Singh SP, et al. Breast cancer pain management - a review of current & novel therapies. Indian J Med Res. 2014;139(2):216-25.
58. Daldorff S, Mathiesen RM, Yri OE, Odegard HP, Geisler J. Cotargeting of CYP-19 (aromatase) and emerging, pivotal signalling pathways in metastatic breast cancer. Br J Cancer. 2017;116(1):10-20.
59. Ma CX, Reinert T, Chmielewska I, Ellis MJ. Mechanisms of aromatase inhibitor resistance. Nat Rev Cancer. 2015;15(5):261-75.
60. Giuliano M, Schifp R, Osborne CK, Trivedi MV. Biological mechanisms and clinical implications of endocrine resistance in breast cancer. Breast. 2011;20 Suppl 3:S42-9.
61. Huang D, Yang F, Wang Y, Guan X. Mechanisms of resistance to selective estrogen receptor down-regulator in metastatic breast cancer. Biochim Biophys Acta. 2017;1868(1):148-56.
62. Zhang X, Wang ZY. Estrogen receptor-alpha variant, ER-alpha36, is involved in tamoxifen resistance and estrogen hypersensitivity. Endocrinology. 2013;154(6):1990-8.
63. de Leeuw R, Neefjes J, Michalides R. A role for estrogen receptor phosphorylation in the resistance to tamoxifen. Int J Breast Cancer. 2011;2011:232435.
64. Cook KL, Shajahan AN, Clarke R. Autophagy and endocrine resistance in breast cancer. Expert Rev Anticancer Ther. 2011;11(8):1283-94.
65. Musgrove EA, Sutherland RL. Biological determinants of endocrine resistance in breast cancer. Nat Rev Cancer. 2009;9(9):631-43.
66. Amaral C, Augusto TV, Tavares-da-Silva E, Roleira FMF, Correia-da-Silva G, Teixeira N. Hormone-dependent breast cancer: Targeting autophagy and PI3K overcomes Exemestane-acquired resistance. J Steroid Biochem Mol Biol. 2018.
67. Gertsch J, Pertwee RG, Di Marzo V. Phytocannabinoids beyond the Cannabis plant - do they exist? Br J Pharmacol. 2010;160(3):523-9.

68. Fonseca BM, Costa MA, Almada M, Correia-da-Silva G, Teixeira NA. Endogenous cannabinoids revisited: a biochemistry perspective. Prostaglandins Other Lipid Mediat. 2013;102-103:13-30.
69. Pertwee RG. The pharmacology of cannabinoid receptors and their ligands: an overview. Int J Obes (Lond). 2006;30 Suppl 1:S13-8.
70. Lu HC, Mackie K. An Introduction to the Endogenous Cannabinoid System. Biol Psychiatry. 2016;79(7):516-25.
71. Mackie K. Cannabinoid receptors: where they are and what they do. J Neuroendocrinol. 2008;20 Suppl 1:10-4.
72. Morales P, Hurst DP, Reggio PH. Molecular Targets of the Phytocannabinoids: A Complex Picture. Prog Chem Org Nat Prod. 2017;103:103-31.
73. Zou S, Kumar U. Cannabinoid Receptors and the Endocannabinoid System: Signaling and Function in the Central Nervous System. Int J Mol Sci. 2018;19(3).
74. Pertwee RG. Cannabinoid pharmacology: the first 66 years. Br J Pharmacol. 2006;147 Suppl 1:S163-71.
75. Guindon J, Hohmann AG. The endocannabinoid system and cancer: therapeutic implication. Br J Pharmacol. 2011;163(7):1447-63.
76. Chakravarti B, Ravi J, Ganju RK. Cannabinoids as therapeutic agents in cancer: current status and future implications. Oncotarget. 2014;5(15):5852-72.
77. Hanus LO. Discovery and isolation of anandamide and other endocannabinoids. Chem Biodivers. 2007;4(8):1828-41.
78. Murataeva N, Straiker A, Mackie K. Parsing the players: 2-arachidonoylglycerol synthesis and degradation in the CNS. Br J Pharmacol. 2014;171(6):1379-91.
79. Astarita G, Ahmed F, Piomelli D. Identification of biosynthetic precursors for the endocannabinoid anandamide in the rat brain. J Lipid Res. 2008;49(1):48-57.
80. Lee HC, Simon GM, Cravatt BF. ABHD4 regulates multiple classes of N-acyl phospholipids in the mammalian central nervous system. Biochemistry. 2015;54(15):2539-49.
81. Simon GM, Cravatt BF. Anandamide biosynthesis catalyzed by the phosphodiesterase GDE1 and detection of glycerophospho-N-acyl ethanolamine precursors in mouse brain. J Biol Chem. 2008;283(14):9341-9.
82. Liu J, Wang L, Harvey-White J, Huang BX, Kim HY, Luquet S, et al. Multiple pathways involved in the biosynthesis of anandamide. Neuropharmacology. 2008;54(1):1-7.
83. Hermanson DJ, Hartley ND, Gamble-George J, Brown N, Shonesy BC, Kingsley PJ, et al. Substrate-selective COX-2 inhibition decreases anxiety via endocannabinoid activation. Nat Neurosci. 2013;16(9):1291-8.
84. Basavarajappa BS. Critical enzymes involved in endocannabinoid metabolism. Protein Pept Lett. 2007;14(3):237-46.
85. Long JZ, Nomura DK, Cravatt BF. Characterization of monoacylglycerol lipase inhibition reveals differences in central and peripheral endocannabinoid metabolism. Chem Biol. 2009;16(7):744-53.
86. McAllister SD, Christian RT, Horowitz MP, Garcia A, Desprez PY. Cannabidiol as a novel inhibitor of Id-1 gene expression in aggressive breast cancer cells. Mol Cancer Ther. 2007;6(11):2921-7.
87. Hanus LO, Meyer SM, Munoz E, Taglialatela-Scafati O, Appendino G. Phytocannabinoids: a unified critical inventory. Nat Prod Rep. 2016;33(12):1357-92.
88. Pyszniak M, Tabarkiewicz J, Luszczki JJ. Endocannabinoid system as a regulator of tumor cell malignancy - biological pathways and clinical significance. Onco Targets Ther. 2016;9:4323-36.
89. Fonseca BM, Teixeira NA, Correia-da-Silva G. Cannabinoids as Modulators of Cell Death: Clinical Applications and Future Directions. Rev Physiol Biochem Pharmacol. 2017;173:63-88.
90. Velasco G, Sanchez C, Guzman M. Towards the use of cannabinoids as antitumour agents. Nat Rev Cancer. 2012;12(6):436-44.

91. De Petrocellis L, Ligresti A, Schiano Moriello A, Iappelli M, Verde R, Stott CG, et al. Non-THC cannabinoids inhibit prostate carcinoma growth in vitro and in vivo: pro-apoptotic effects and underlying mechanisms. Br J Pharmacol. 2013;168(1):79-102.
92. McAllister SD, Soroceanu L, Desprez PY. The Antitumor Activity of Plant-Derived Non-Psychoactive Cannabinoids. J Neuroimmune Pharmacol. 2015;10(2):255-67.
93. Cridge BJ, Rosengren RJ. Critical appraisal of the potential use of cannabinoids in cancer management. Cancer Manag Res. 2013;5:301-13.
94. Ladin DA, Soliman E, Griffin L, Van Dross R. Preclinical and Clinical Assessment of Cannabinoids as Anti-Cancer Agents. Front Pharmacol. 2016;7:361.
95. Fraguas-Sanchez AI, Fernandez-Carballido A, Torres-Suarez AI. Phyto-, endo- and synthetic cannabinoids: promising chemotherapeutic agents in the treatment of breast and prostate carcinomas. Expert Opin Investig Drugs. 2016;25(11):1311-23.
96. Shrivastava A, Kuzontkoski PM, Groopman JE, Prasad A. Cannabidiol induces programmed cell death in breast cancer cells by coordinating the cross-talk between apoptosis and autophagy. Mol Cancer Ther. 2011;10(7):1161-72.
97. Pisanti S, Malfitano AM, Ciaglia E, Lamberti A, Ranieri R, Cuomo G, et al. Cannabidiol: State of the art and new challenges for therapeutic applications. Pharmacol Ther. 2017;175:133-50.
98. Hermanson DJ, Marnett LJ. Cannabinoids, endocannabinoids, and cancer. Cancer Metastasis Rev. 2011;30(3-4):599-612.
99. Laezza C, Pisanti S, Crescenzi E, Bifulco M. Anandamide inhibits Cdk2 and activates Chk1 leading to cell cycle arrest in human breast cancer cells. FEBS Lett. 2006;580(26):6076-82.
100. Caffarel MM, Sarrio D, Palacios J, Guzman M, Sanchez C. Delta9-tetrahydrocannabinol inhibits cell cycle progression in human breast cancer cells through Cdc2 regulation. Cancer Res. 2006;66(13):6615-21.
101. Takeda S, Yoshida K, Nishimura H, Harada M, Okajima S, Miyoshi H, et al. Delta(9)-Tetrahydrocannabinol disrupts estrogen-signaling through up-regulation of estrogen receptor beta (ERbeta). Chem Res Toxicol. 2013;26(7):1073-9.
102. Solinas M, Massi P, Cantelmo AR, Cattaneo MG, Cammarota R, Bartolini D, et al. Cannabidiol inhibits angiogenesis by multiple mechanisms. Br J Pharmacol. 2012;167(6):1218-31.
103. Blasco-Benito S, Seijo-Vila M, Caro-Villalobos M, Tundidor I, Andradas C, Garcia-Taboada E, et al. Appraising the "entourage effect": Antitumor action of a pure cannabinoid versus a botanical drug preparation in preclinical models of breast cancer. Biochem Pharmacol. 2018.
104. Zhou DJ, Pompon D, Chen SA. Stable expression of human aromatase complementary DNA in mammalian cells: a useful system for aromatase inhibitor screening. Cancer Res. 1990;50(21):6949-54.
105. Amaral C, Borges M, Melo S, da Silva ET, Correia-da-Silva G, Teixeira N. Apoptosis and autophagy in breast cancer cells following exemestane treatment. PLoS One. 2012;7(8):e42398.
106. Amaral C, Varela CL, Mauricio J, Sobral AF, Costa SC, Roleira FMF, et al. Anti-tumor efficacy of new 7alpha-substituted androstanes as aromatase inhibitors in hormone-sensitive and resistant breast cancer cells. J Steroid Biochem Mol Biol. 2017;171:218-28.
107. Fonseca BM, Correia-da-Silva G, Teixeira NA. Cannabinoid-induced cell death in endometrial cancer cells: involvement of TRPV1 receptors in apoptosis. J Physiol Biochem. 2018;74(2):261-72.
108. Masri S, Phung S, Wang X, Wu X, Yuan YC, Wagman L, et al. Genome-wide analysis of aromatase inhibitor-resistant, tamoxifen-resistant, and long-term estrogen-deprived cells reveals a role for estrogen receptor. Cancer Res. 2008;68(12):4910-8.
109. Chan FK, Moriwaki K, De Rosa MJ. Detection of necrosis by release of lactate dehydrogenase activity. Methods Mol Biol. 2013;979:65-70.

110. Thompson EA, Jr., Siiteri PK. Utilization of oxygen and reduced nicotinamide adenine dinucleotide phosphate by human placental microsomes during aromatization of androstenedione. J Biol Chem. 1974;249(17):5364-72.
111. Chen X, Zhong Z, Xu Z, Chen L, Wang Y. 2',7'-Dichlorodihydrofluorescein as a fluorescent probe for reactive oxygen species measurement: Forty years of application and controversy. Free Radic Res. 2010;44(6):587-604.
112. Kroemer G, Galluzzi L, Brenner C. Mitochondrial membrane permeabilization in cell death. Physiol Rev. 2007;87(1):99-163.
113. Klionsky DJ, Abdelmohsen K, Abe A, Abedin MJ, Abeliovich H, Acevedo Arozena A, et al. Guidelines for the use and interpretation of assays for monitoring autophagy (3rd edition). Autophagy. 2016;12(1):1-222.
114. Amaral C, Lopes A, Varela CL, da Silva ET, Roleira FM, Correia-da-Silva G, et al. Exemestane metabolites suppress growth of estrogen receptor-positive breast cancer cells by inducing apoptosis and autophagy: A comparative study with Exemestane. Int J Biochem Cell Biol. 2015;69:183-95.
115. Wang X, Chen S. Aromatase destabilizer: novel action of exemestane, a food and drug administration-approved aromatase inhibitor. Cancer Res. 2006;66(21):10281-6.
116. Varela CL, Amaral C, Tavares da Silva E, Lopes A, Correia-da-Silva G, Carvalho RA, et al. Exemestane metabolites: Synthesis, stereochemical elucidation, biochemical activity and anti-proliferative effects in a hormone-dependent breast cancer cell line. Eur J Med Chem. 2014;87:336-45.
117. Carlson RW. The history and mechanism of action of fulvestrant. Clin Breast Cancer. 2005;6 Suppl 1:S5-8.
118. Ghobrial IM, Witzig TE, Adjei AA. Targeting apoptosis pathways in cancer therapy. CA Cancer J Clin. 2005;55(3):178-94.
119. Debatin KM. Apoptosis pathways in cancer and cancer therapy. Cancer Immunol Immunother. 2004;53(3):153-9.
120. Eisenberg-Lerner A, Bialik S, Simon HU, Kimchi A. Life and death partners: apoptosis, autophagy and the cross-talk between them. Cell Death Differ. 2009;16(7):966-75.
121. Song S, Tan J, Miao Y, Li M, Zhang Q. Crosstalk of autophagy and apoptosis: Involvement of the dual role of autophagy under ER stress. J Cell Physiol. 2017;232(11):2977-84.
122. Velasco G, Sanchez C, Guzman M. Anticancer mechanisms of cannabinoids. Curr Oncol. 2016;23(2):S23-32.
123. Masri S, Phung S, Wang X, Chen S. Molecular characterization of aromatase inhibitor-resistant, tamoxifen-resistant and LTEDaro cell lines. J Steroid Biochem Mol Biol. 2010;118(4-5):277-82.
124. Elbaz M, Nasser MW, Ravi J, Wani NA, Ahirwar DK, Zhao H, et al. Modulation of the tumor microenvironment and inhibition of EGF/EGFR pathway: novel anti-tumor mechanisms of Cannabidiol in breast cancer. Mol Oncol. 2015;9(4):906-19.
125. Murase R, Kawamura R, Singer E, Pakdel A, Sarma P, Judkins J, et al. Targeting multiple cannabinoid anti-tumour pathways with a resorcinol derivative leads to inhibition of advanced stages of breast cancer. Br J Pharmacol. 2014;171(19):4464-77.
126. Emery SM, Alotaibi MR, Tao Q, Selley DE, Lichtman AH, Gewirtz DA. Combined antiproliferative effects of the aminoalkylindole WIN55,212-2 and radiation in breast cancer cells. J Pharmacol Exp Ther. 2014;348(2):293-302.
127. Grimaldi C, Pisanti S, Laezza C, Malfitano AM, Santoro A, Vitale M, et al. Anandamide inhibits adhesion and migration of breast cancer cells. Exp Cell Res. 2006;312(4):363-73.
128. Reggio PH. Endocannabinoid binding to the cannabinoid receptors: what is known and what remains unknown. Curr Med Chem. 2010;17(14):1468-86.
129. Iffland K, Grotenhermen F. An Update on Safety and Side Effects of Cannabidiol: A Review of Clinical Data and Relevant Animal Studies. Cannabis Cannabinoid Res. 2017;2(1):139-54.
130. Zendulka O, Dovrtelova G, Noskova K, Turjap M, Sulcova A, Hanus L, et al. Cannabinoids and Cytochrome P450 Interactions. Curr Drug Metab. 2016;17(3):206-26.

131. Lewysohn O, Cordova T, Nimrod A, Ayalon D. The suppressive effect of delta-1-tetrahydrocannabinol on the steroidogenic activity of rat granulosa cells in culture. Horm Res. 1984;19(1):43-51.
132. Gallo D, De Stefano I, Grazia Prisco M, Scambia G, Ferrandina G. Estrogen receptor beta in cancer: an attractive target for therapy. Curr Pharm Des. 2012;18(19):2734-57.
133. Warner M, Huang B, Gustafsson JA. Estrogen Receptor beta as a Pharmaceutical Target. Trends Pharmacol Sci. 2017;38(1):92-9.
134. Galanti G, Fisher T, Kventsel I, Shoham J, Gallily R, Mechoulam R, et al. Delta 9-tetrahydrocannabinol inhibits cell cycle progression by downregulation of E2F1 in human glioblastoma multiforme cells. Acta Oncol. 2008;47(6):1062-70.
135. De Petrocellis L, Melck D, Palmisano A, Bisogno T, Laezza C, Bifulco M, et al. The endogenous cannabinoid anandamide inhibits human breast cancer cell proliferation. Proc Natl Acad Sci U S A. 1998;95(14):8375-80.
136. Ligresti A, Moriello AS, Starowicz K, Matias I, Pisanti S, De Petrocellis L, et al. Antitumor activity of plant cannabinoids with emphasis on the effect of cannabidiol on human breast carcinoma. J Pharmacol Exp Ther. 2006;318(3):1375-87.
137. Linke SP, Clarkin KC, Di Leonardo A, Tsou A, Wahl GM. A reversible, p53-dependent G0/G1 cell cycle arrest induced by ribonucleotide depletion in the absence of detectable DNA damage. Genes Dev. 1996;10(8):934-47.
138. Widlak P, Palyvoda O, Kumala S, Garrard WT. Modeling apoptotic chromatin condensation in normal cell nuclei. Requirement for intranuclear mobility and actin involvement. J Biol Chem. 2002;277(24):21683-90.
139. Redza-Dutordoir M, Averill-Bates DA. Activation of apoptosis signalling pathways by reactive oxygen species. Biochim Biophys Acta. 2016;1863(12):2977-92.
140. Rajesh M, Mukhopadhyay P, Batkai S, Patel V, Saito K, Matsumoto S, et al. Cannabidiol attenuates cardiac dysfunction, oxidative stress, fibrosis, and inflammatory and cell death signaling pathways in diabetic cardiomyopathy. J Am Coll Cardiol. 2010;56(25):2115-25.
141. Massi P, Solinas M, Cinquina V, Parolaro D. Cannabidiol as potential anticancer drug. Br J Clin Pharmacol. 2013;75(2):303-12.
142. Donadelli M, Dando I, Zaniboni T, Costanzo C, Dalla Pozza E, Scupoli MT, et al. Gemcitabine/cannabinoid combination triggers autophagy in pancreatic cancer cells through a ROS-mediated mechanism. Cell Death Dis. 2011;2:e152.
143. Marcu JP, Christian RT, Lau D, Zielinski AJ, Horowitz MP, Lee J, et al. Cannabidiol enhances the inhibitory effects of delta9-tetrahydrocannabinol on human glioblastoma cell proliferation and survival. Mol Cancer Ther. 2010;9(1):180-9.
144. Chaitanya GV, Steven AJ, Babu PP. PARP-1 cleavage fragments: signatures of cell-death proteases in neurodegeneration. Cell Commun Signal. 2010;8:31.
145. Mullen P. PARP cleavage as a means of assessing apoptosis. Methods Mol Med. 2004;88:171-81.
146. White E, DiPaola RS. The double-edged sword of autophagy modulation in cancer. Clin Cancer Res. 2009;15(17):5308-16.
147. Torres S, Lorente M, Rodriguez-Fornes F, Hernandez-Tiedra S, Salazar M, Garcia-Taboada E, et al. A combined preclinical therapy of cannabinoids and temozolomide against glioma. Mol Cancer Ther. 2011;10(1):90-103.
148. Scott KA, Dalgleish AG, Liu WM. The combination of cannabidiol and Delta9-tetrahydrocannabinol enhances the anticancer effects of radiation in an orthotopic murine glioma model. Mol Cancer Ther. 2014;13(12):2955-67.